

Deep Learning to Predict Glaucoma Progression using Structural Changes in the Eye

by

Sayan Mandal

Department of Electrical and Computer Engineering
Duke University

Date: December 08, 2023

Approved:

Felipe A. Medeiros, Co-Supervisor

Vahid Tarokh, Co-Supervisor

Leslie Collins

Ricardo Henao

Yiran Chen

Dissertation submitted in partial fulfillment of the requirements for the degree of
Doctor of Philosophy in the Department of Electrical and Computer Engineering
in the Graduate School of Duke University

2024

ABSTRACT

Deep Learning to Predict Glaucoma Progression using Structural Changes in the Eye

by

Sayan Mandal

Department of Electrical and Computer Engineering
Duke University

Date: December 08, 2023

Approved:

Felipe A. Medeiros, Co-Supervisor

Vahid Tarokh, Co-Supervisor

Leslie Collins

Ricardo Henao

Yiran Chen

An abstract of a dissertation submitted in partial fulfillment of the requirements for
the degree of Doctor of Philosophy in the Department of Electrical and Computer
Engineering
in the Graduate School of Duke University
2024

Copyright © 2024 by Sayan Mandal
All rights reserved except the rights granted by the
Creative Commons Attribution-Noncommercial Licence

Abstract

Glaucoma is a group of chronic eye diseases characterized by optic neuropathy, which causes irreversible vision loss. It is caused by progressive degeneration of the optic nerve, leading to gradual loss of the visual field from the periphery to the center, resulting in blindness if left untreated. Since the changes are gradual and the damage progresses generally slowly, glaucoma development is insidious and often diagnosed until it reaches an advanced stage. Early detection of glaucoma progression is necessary to monitor the atrophy and formulate treatment strategies to halt progressive functional vision impairments. The availability of data centric methods have made it possible for researchers to develop computer-aided algorithms for the clinical diagnosis of glaucoma and capture accurate disease characteristics. In this research, we use deep learning models, one such forefront, to identify complex disease characteristics and progression criteria, enabling the detection of subtle changes indicative of glaucoma progression.

To this end, we investigate the structure-function relationship of glaucoma progression and explore the possibility of predicting functional impairment from structural eye deterioration. We also analyze various statistical and machine-learning methods that have aided previous attempts to estimate progression, including emerging deep-learning techniques that use structural features like optical coherence tomography (OCT) scans to predict glaucoma progression accurately. We show through our investigations that these methods are still prone to confounding risk factors, especially variability due to age, data imbalances, potential noisy labels, lack of gold standard criteria, etc. We developed novel semi-supervised time-series algorithms to overcome these multifaceted challenges using unique data-driven approaches:

Weakly-Supervised Time-Series Learning: We develop a convolutional neural network-long short-term memory (CNN-LSTM) base model to encode the spa-

tiotemporal features from the OCT scan sequence taken over a fixed follow-up. We model the rest of the deep learning architecture on the fact that original OCT sequences exhibit age-related progression, and reshuffling the sequence order, along with the knowledge of healthy eyes from a positive-unlabeled dataset, can establish robust pseudo-progression criteria for glaucoma. This circumvents the need for gold standard labels for disease progression.

Semi-supervised Time-Series Learning: We extend the above notion to a labeled case where labels are obtained from Guided Progression Analysis (GPA), a well-known, stable, and accurate functional assessment for glaucoma progression, but might be prone to noisy labels due to nuances in data acquisition. We model the structural progression as a pseudo-identifier for functional glaucoma deficits. We use this knowledge in a contrastive learning scheme where the CNN-LSTM base architecture learns accurate spatiotemporal characteristics from potentially mislabeled data and improves predictions.

Finally, we compare and show that these methods outperform conventional and state-of-the-art techniques.

Dedication

In the loving memory of my father, a source of strength and inspiration throughout my life.

Contents

Abstract	iv
List of Tables	xi
List of Figures	xii
List of Abbreviations and Symbols	xiv
Acknowledgements	xx
1 Introduction	1
1.1 Background	1
1.1.1 Brief History of Glaucoma	1
1.1.2 Current Understanding	3
1.2 A Clinical Overview of Glaucoma	3
1.2.1 Pathophysiology	3
1.2.2 Types of Glaucoma	4
1.2.3 Common Risk Factors	5
1.2.4 Glaucoma Progression: An Unique Prelude	6
1.3 Methods for Glaucoma Diagnosis	7
1.3.1 Structural Tests for Glaucoma	8
1.3.2 Functional Assessments for Glaucoma	10
1.3.3 Structure-Function Relationship	11
1.3.4 Assessment of Glaucoma Progression	11
1.3.5 Progression Criteria	13
1.3.6 Challenges in Glaucoma Progression Analysis	13
1.4 Problem Statements and Motivations	16
1.4.1 Research Objectives	18

1.4.2	Research Contributions	19
1.5	Thesis Structure	20
2	Literature Review	22
2.1	Background	22
2.2	Review	23
2.3	Landmark Glaucoma Studies	25
2.4	Glaucoma Progression Detection using Assessments of Visual Fields .	31
2.4.1	Clinical Assessments and Event-Based Methods	31
2.4.2	Linear Regression and Trend-Based Methods	32
2.4.3	Probabilistic Methods	33
2.4.4	Machine Learning Methods	34
2.4.5	Deep Learning Methods	35
2.4.6	Time Series Analysis and Forecasting Methods	36
2.5	Detection of Structural Progression	45
2.5.1	Clinical and Conventional Methods	46
2.5.2	Probabilistic Methods	47
2.5.3	Machine Learning Techniques	49
2.5.4	Deep Learning Approaches	50
2.5.5	Time Series Approaches in Structural Assessment	51
2.6	Structure-Function Relationship in Glaucoma Progression Detection .	58
2.6.1	Clinical Methods for the Assessment of Glaucoma Progression Using Structure and Function	58
2.6.2	Sophisticated Methods to Detect Glaucoma Progression Using Combined Structure and Function	58
2.6.3	Artificial Intelligence Utilising Combined Structure and Func- tion Relationship to Evaluate Glaucoma Progression	60
2.7	Glaucoma Progression Detection with EHR and Clinical Data	69

2.8	Conclusion	70
3	Methodology	71
3.1	Dataset Overview	71
3.1.1	Duke Ophthalmic Registry	71
3.1.2	Population Characteristics	72
3.2	Experiment Design and Setup	74
3.2.1	Input Features for the Model: Longitudinal SDOCT Scans . .	75
3.2.2	Reference Standard: Guided Progression Analysis	76
3.2.3	Baseline Comparison: Ordinary Least Squares Regression Method	79
3.2.4	Evaluation Metrics	79
3.2.5	Post-Hoc Statistical Analysis	83
3.3	The Time-Series Deep Learning Model	84
3.3.1	Pre-trained CNN Networks: 3DCNN + ResNet50	85
3.3.2	Sequence Learning: LSTM Networks	86
3.3.3	Spatio-temporal Learning: Combining CNN and LSTM	88
3.3.4	Classification Head	88
3.4	Modelling with Healthy Patient Data: Modified Positive Unlabeled Learning	89
3.4.1	Hypothesis and Mathematical Formulation	91
3.4.2	Objective Rationale	93
3.5	Modelling DL with External Labels: A Contrastive Learning Approach	93
3.5.1	Hypothesis and Mathematical Formulation	95
3.5.2	Objective Rationale	99
4	Weakly Supervised Time Series Learning to Detect Glaucoma Progression from Optical Coherence Tomography B-scans	100
4.1	Introduction	100

4.2	Methods	102
4.2.1	Weakly Supervised Time Series Learning	103
4.2.2	Training and Validation	105
4.2.3	Model Evaluation and Statistical Analysis	107
4.3	Results	108
4.4	Discussion	113
5	Regularized - Contrastive Learning to Predict Functional Glaucoma Progression Using Longitudinal OCT Scans.	120
5.1	Introduction	120
5.2	Methodology	123
5.2.1	Definition of Glaucoma Progression	124
5.2.2	DL Method	125
5.2.3	Training and Validation	128
5.2.4	Model Evaluation and Statistical Analysis	130
5.3	Results	131
5.4	Discussion	138
6	Conclusion and Future Work	145
	Bibliography	149
	Biography	173

List of Tables

2.1	A brief review of some landmark glaucoma studies	27
2.2	A Review of Methods for Detection and Prediction of Glaucoma Progression using Visual Field Tests	38
2.3	A Review of Methods for Detection and Prediction Glaucoma Progression using Structural Assessments	52
2.4	A Review of Methods for Detection and Prediction Glaucoma Progression using both Structure and Function	63
4.1	Baseline Demographics and Clinical Characteristics for glaucoma and healthy eyes for all subjects included in the study.	109
4.2	Comparison of Performance Metrics of various Machine Learning and Deep Learning methods with the Noise-PU model.	111
4.3	Baseline Demographics and Clinical Characteristics for the Deep Learning model Predictions of Glaucoma Eyes in the test set.	113
5.1	Baseline Demographics and Clinical Characteristics for Progressing and Non-progressing Subjects based on the GPA criteria.	131
5.2	Dataset distribution used by the DL model at eyes and observation levels for training, validation, and testing set.	132
5.3	Baseline Demographics and Clinical Characteristics of the Test Set based on GPA reference standard.	134
5.4	Comparison of Performance Metrics across conventional and different DL model configurations trained and evaluated on our dataset.	136
5.5	Baseline Demographics and Clinical Characteristics for eyes predicted as Progressing versus Non-Progressing by RegCon model.	138

List of Figures

1.1	Open-Angle and Angle-Closure Glaucoma (Texas (2007)).	5
1.2	Spectralis SDOCT scan report of an eye highlighting glaucomatous damage (Dong et al. (2016)).	9
1.3	A Visual Field Mapping obtained from Visual Field Test (Salim et al. (2022))	10
3.1	Demographic Characteristics of patients in the Duke Ophthalmic Registry.	73
3.2	Comparison of top three causes of irreversible blindness in the DOR database.	74
3.3	A comprehensive SDOCT report of a normal eye obtained from Spectralis (Zembarain et al. (2020)).	76
3.4	A longitudinal sequence of SDOCT B-scan images used as DL model input (resized to 224×224 pixels).	76
3.5	A GPA report representing different progression events (Diaz-Aleman et al. (2009)).	78
3.6	Classification Confusion Matrix based on items retrieved from all relevant examples (Walber (2014)).	81
3.7	Representative example of 34-layer Deep Residual Network architecture (He et al. (2016)).	87
3.8	A schematic of the Long Short-Term Memory cell explaining components of the Recurrent Neural Networks (Chevalier (2018)).	87
3.9	An overview of the combined CNN-LSTM Network with a Classification Head.	89
4.2	The Net Loss and Accuracy plots for predictions obtained from the Noise-PU Model.	109
4.3	Deep Learning Heatmaps of a glaucoma eye sequence predicted as progressing by the Noise-PU Model.	114
4.4	Deep Learning Heatmaps of a glaucoma eye sequence predicted as non-progressing by the Noise-PU Model.	115

5.1	An overview of the RegCon Semi-Supervised CNN-LSTM Network. . .	129
5.2	The Net Loss and Accuracy plots for predictions obtained from the RegCON Model training.	133
5.3	Receiver Operating Characteristic and Precision Recall Plots for various DL methods versus RegCon Model.	135
5.4	Representative example sequence of an eye predicted as glaucoma progressing by the RegCon Model.	137

List of Abbreviations and Symbols

Symbols

dB	Denotes Decibels, A Unit of Visual Field Measure.
μm	Denotes Micro-Meter, A Unit of RNFL Thickness Measure.
$ \cdot $	Denotes Absolute Value or Number of Items.
$\ \cdot\ _2$	Denotes Frobenius Norm of Matrix or Euclidean Norm of Vector.
$\mathbb{1}$	Denotes Indicator Function.
Δ	Denotes Difference between Values.
e	Residuals: Difference between Observed and Estimated Values.
P	Denotes Probability on Events or Distributions.
π	Denotes a Function for Random Number Generator.
α, β, γ	Denotes Factor Constants used in Objective Functions.
δ, ϵ	Denotes Small Positive Quantities.
T	Denotes OCT Follow Up Time.
$x^{(t)}$	Denotes Input (Image) at Time t .
X	Denotes Input (Image) Sequence.
y	Denotes Outcome (Observed) Measure.
\hat{y}	Denotes Estimated (Predicted) Value.
$z^{(t)}$	Denotes Time Series Encoding at Time t .
Z_n	Denotes Spatiotemporal Encoding from CNN-LSTM Network.
τ	Denotes No. of OCT Bscan Images (Inputs).
\mathcal{T}	Denotes Time at Endpoints for VF GPA.
κ	Denotes Cohen's Kappa, A Measure of Agreement Between Variables.
r	Denotes Correlation between Two Variables.
H	Denotes Entropy Function.

L	Denotes Non-Negative Real-Valued Loss Function.
$\mathcal{L}(\cdot)$	Denotes Likelihood Function.
$\mathbf{J}(\cdot)$	Denotes Objective Function.
Π	Denotes Randomizing Function with k Permutations.
\mathcal{X}	Denotes Input Space in Dataset.
\mathcal{Y}	Denotes Output Space in Dataset.
\mathbb{R}^n	Denotes Real-Valued n -Dimensional Space.
H, W	Denotes Image Height and Width.
F	Denotes 1D Feature Width.
\mathcal{A}	Denotes Augmentation Function.
θ	Denotes CNN-LSTM Model Parameters.
\mathbb{H}	Denotes Hypothesis Space for DL Models.
h	Denotes DL Model Candidate from Hypothesis Space.
\mathcal{H}	Denotes DL Model Function.
ϕ, ψ	Denotes Parameters for Projection Heads in the DL Model.
\mathcal{D}, \mathcal{S}	Denotes Dataset and Data Subset.
R	Denotes Risk Function.
\mathbb{P}	Denotes Theoretic Measure of Probability on Countable Sets.
τ	Denotes Temperature Parameter for Contrastive Learning.

Abbreviations

AA	African American
ACG	Angle-Closure Glaucoma
AGIS	Advanced Glaucoma Intervention Study
AI	Artificial Intelligence
AUC	Area Under [Receiver Operator Characteristic] Curve

BLUP	Best Linear Unbiased Predictors
BCE	Binary Cross Entropy
Bi-RM	Bidirectional Recurrent Model
CAM	Class Activation Maps
CAR	Conditional Auto-Regressive Models
CCE	Categorical Cross Entropy
CCT	Central Corneal Thickness
CDR	Cup-Disk Ratio
CIGTS	Collaborative Initial Glaucoma Treatment Study
CNN	Convolutional Neural Network
cpRNFL	Circumpapillary Retinal Nerve Fiber Layer
CPT	Current Procedural Terminology
CSLO	Confocal Scanning Laser Ophthalmoscopy
CTHMM	Continuous Time-Hidden Markov Model
DL	Deep Learning
DLS	Differential Light Sensitivity
DOR	Duke Ophthalmic Registry
DSF	Dynamic Structure-Function
EGPS	European Glaucoma Preventing Study
EHR	Electronic Health Records
EMGT	Early Manifest Glaucoma Trial
FC	Fully Connected
FBDS	Fuzzy Bayesian Detection Scheme
GAN	Generative Adversarial Network
GCC	Ganglion Cell Complex
GCIPL	Ganglion Cell-Inner Plexiform Layer

GDx-VCC	Glaucoma Detection with Variable Corneal Compensation
GEM	Gaussian Mixture Model Expectation Maximization
GLMM	Generalized Linear Mixed Models
GLT	Glaucoma Laser Trial
GMM	Gaussian Mixture Model
GON	Glaucomatous Optic Neuropathy
GPA	Guided Progression Analysis
GTN	Gated Transformer Network
HFA	Humphrey Field Analyzer
HRT	Heidelberg Retina Tomograph
ICD	International Classification of Diseases
ICA	Independent Component Analysis
IOP	Inter Ocular Pressure
IRB	Institutional Review Board
JLSM	Joint Longitudinal Survival Model
LMM	Linear Mixed Models
LSTM	Long Short-Term Memory
MAE	Mean Absolute Error
M2M	Machine to Machine
MD	Mean Deviation
MLE	Maximum Likelihood Estimation
ML	Machine Learning
MLP	Multi-Layer Perceptron
MCC	Matthew's Correlation Coefficient
NLP	Natural Language Processing
NTG	Normal Tension Glaucoma

OAG	Open-Angle Glaucoma
OCT	Optical Coherence Tomography
OCTA	Optical Coherence Tomography Angiography
OHTS	Ocular Hypertension Treatment Study
OLS	Ordinary Least Squares
OLSLR	Ordinary Least Square Linear Regression
ONH	Optic Nerve Head
PACG	Primary Angle-Closure Glaucoma
PCA	Principal Component Analysis
PLR	Pointwise Linear Regression
PoP	Permutation of Points
PoPLR	Permutation of Pointwise Linear Regression
POAG	Primary Open-Angle Glaucoma
POD	Proper Orthogonal Decomposition
PSD	Pattern Standard Deviation
PU	Positive-Unlabeled Learning
RGC	Retinal Ganglion Cells
RNFL	Retinal Nerve Fiber Layer
RA	Rim Area
ROC	Receiver Operator Characteristics
SAP	Standard Automated Perimetry
SDOCT	Spectral-Domain Optical Coherence Tomography
SGD	Stochastic Gradient Descent
SITA	Swedish Interactive Threshold Algorithm
SLP	Scanning Laser Polarimetry
SSOCT	Swept-Source Optical Coherence Tomography

SVM	Support Vector Machine
TDOCT	Time-Domain Optical Coherence Tomography
TPA	Trend-Based Progression Analysis
TSNIT	Temporal, Superior, Nasal, Inferior and Temporal Regions
UKGTS	United Kingdom Glaucoma Treatment Study
VA	Visual Acuity
VAE	Variational Auto Encoder
VCA-MA	Variational Change Analysis with Markovian A-Priori
VF	Visual Field
VFI	Visual Field Index
VIM	Variational Bayesian Independent Component Mixture Model

Acknowledgements

I would like to express my deepest gratitude to my advisor, Felipe Medeiros, whose invaluable feedback, consistent mentoring, and patience, even during my mistakes, have shaped this thesis. Your guidance has been instrumental, and I have learned so much from our discussions and your perspectives.

My mentor at the lab, Alessandro Jammal, has been a tremendous source of support, almost paralleling the guidance I received from my advisor. Your accessibility during various hours and your unwavering assistance were pivotal in my journey. I would also like to thank other lab members, Rizul Naithani, Davina Malek, Aasma Youssif, Vahid Ownagh, and Gary Gan, whose help, although varied, contributed significantly to my research.

To my defense committee members, your feedback during the preliminary exams enriched the final form of this work. Your expertise and insights were much appreciated. I would like to express my gratitude to my co-chair, Vahid Tarokh, for his invaluable support and guidance during my advisors transition.

I extend my heartfelt gratitude to the ECE department for their unwavering assistance throughout my academic journey. Their support in clarifying departmental intricacies, ensuring seamless scheduling, and handling administrative matters played a crucial role in allowing me to focus on my research. Their behind-the-scenes efforts are much appreciated.

To my friends at Duke University and Durham, Harsh Bandhey, Deniz Acil, Viswa Alaparthi, Tyler King, Lalit Yadav, Vidvat Ramachandran, Edward Hanson, Keerti Anand you have been my rock. The late-night hang-outs, study sessions, and moments of respite were possible because of you. Friends Chung Wang, Francesco Luzi, Catalena Le, Arjun Sridhar, Vani Yadav and Bhavna Gopal deserve special mention for enduring my rants and being there for me. I'm also profoundly grateful

to a special individual, Jayoshree Adhikari, who stood by me, providing mental and emotional strength. An exceptional thanks to Anurag Kashyap, who redefined the essence of true friendship for me.

My undergraduate and childhood friends, Sourav Agarwal, Utkarsh Tyagi, Sourav Kundu, Soumyadeep Dasgupta, Vinsea Singh, and Prateeksha Pamshetty, your fun conversations and cherished memories have been my solace, reminding me of simpler times and keeping me grounded.

The pillars of my life, my parents, have been my unwavering supporters even from 8,300 miles away. My late father, whose belief in me led me to pursue this PhD, supported me until his very last breath. My mother, with her boundless love and constant prayers, has been my anchor. She stood by me, talked to me whenever I needed, always providing words of encouragement. My sister, too, has been a beacon of strength, uplifting me during my lowest moments.

I would like to acknowledge the funding agency, Google Inc., whose support was integral to my research and PhD. I also recognize the National Institutes of Health/National Eye Institute grants EY029885 and EY031898 for their generous assistance.

Lastly, I know there are many who have crossed my path, provided support in various capacities, and have not been named here. Please know that I am genuinely grateful for every bit of support and kindness I've received. I am privileged to be surrounded by such incredible individuals, and I aspire to give back in any way I can for the support, no matter how small, that I've received.

Introduction

Vision is the ability of a person to see, interpret, and interact with the world. The eyes provide the sense of sight, capturing images from our surroundings. The brain interprets these images, allowing us to make sense of what we see. The sense of sight is one of the most vital sources of information we receive out of all five senses combined. Many of the movements and tasks we perform and our interactions with our environment rely heavily on vision. Thus, taking care of our vision is crucial, and protecting our sense of sight is fundamental to this care.

As such, eye diseases may cause vision impairments, often leading to partial or complete loss of sight. When individuals lose the ability to see, basic activities that were once taken for granted, such as reading, driving, or recognizing loved ones, become arduous or even impossible and significantly reduce the quality of life. Among these eye diseases, glaucoma stands out as uniquely insidious. Unlike most other conditions, glaucoma develops slowly and without noticeable symptoms, leading to vision loss before even a person realizes the problem. Thus, detecting the progression of glaucoma early on its inception is necessary. This research focuses on investigating the current state of research in glaucoma progression detection and finding novel methods to detect glaucoma progression accurately and efficiently.

1.1 Background

1.1.1 Brief History of Glaucoma

The term glaucoma was first used in Hippocrates' Aphorisms (Anderson et al. (2018)), originating from the Greek words 'Γλαύξ – Γλαύκος' (glaukos) and 'Γλαύσω'

(glausso; Tsatsos and Broadway (2007)). Glaukos is a noun which is a non-specific term that means diseased bluish-green or light-gray hue on healthy irrides. Glausso, on the other hand, is a verb that means "to glow" or "to shine." Both words have slightly different meanings but point to the same connotation, "some sort of opacification or hardening of the cornea or lens resulting in apparent discoloration of the eye, most commonly occurring in the elderly" (Fronimopoulos and Lascaratos (1991)). However in contemporary medicine the term glaucoma encompassed multiple eye diseases, including cataract (Leffler et al. (2015b)), definitions of multiple eye conditions involving glaucoma such as hardness of the eyeball, increased eye pressure, dilated pupil and reduced vision were reported (Leffler et al. (2015a)). It was not until the scientific advancements in ophthalmology during the 1700s and 1800s, that glaucoma and cataracts were recognized as distinct diseases with different pathological mechanisms. William MacKenzie observed and described the role of interocular pressure (IOP) in glaucoma (Mackenzie (1855)), which was followed by an illustration of the first glaucomatous understanding of the optic disc by Jaeger (Lazaridis (2022)). Graefe spearheaded some of the most notable developments in the modern knowledge of glaucoma, such as the structural understanding (deterioration of optic nerve fibers), functional understanding (difference in central and peripheral vision within stages of glaucoma) and different types of glaucoma based on clinical signs of inflammation: acute, chronic or secondary (v. Graefe (1856)). In the subsequent years, the development of modern scientific apparatus, assessment techniques, and advancements in medicine allowed researchers to define glaucoma more precisely, leading to the current understanding of its underlying pathophysiological mechanisms.

1.1.2 Current Understanding

Today, glaucoma is understood not just as a single disease but as a group of eye conditions with multiple etiologies leading to optic nerve damage. Elevated IOP is found to be a significant risk factor and not the whole cause as previously assumed (Frankfort et al. (2013)). It is found that different types of glaucoma have varying pathophysiologies and different treatments. Early detection, primarily through regular eye check-ups, is essential since vision loss due to glaucoma is reversible but can be slowed down with appropriate treatment. Advancements in treatment strategies and the advent of sophisticated diagnostic tools have enabled easy detection and monitoring of the disease's progression. The focus of treatment strategies has also expanded from eyedrops that decrease IOP to surgical interventions to reverse the damage to the optic nerve.

1.2 A Clinical Overview of Glaucoma

Glaucoma is a type of chronic optic neuropathy caused by the pathological degeneration of the retinal ganglion cells (RGC) resulting in progressive visual function loss. It is the leading cause of irreversible blindness worldwide, with an estimated 80 million affected by the disease and a projected 111.8 million people affected by 2040 (Pascolini and Mariotti (2012); Mariotti and Pascolini (2012)).

1.2.1 Pathophysiology

Retina has photoreceptors, which are highly specialized cells that receive light and transmit visual information to the brain through RGC and their axons. The axons from the RGC converge to the optic disc in bundles, forming the retinal nerve fiber layer (RNFL). Glaucoma results from progressive RGC loss and axon degeneration, for which elevated IOP is the most important risk factor. This progressive cell loss gives rise to gradual visual field loss which generally starts from the periphery,

but can advance to generalized visual field loss and blindness (Hood et al. (2013)). Although the vision loss from glaucoma can be catastrophic, its generally chronic, slow, and discreet onset, with no early symptoms, makes it difficult to be perceived by the patient, thus making methods to detect glaucoma progression paramount, to provide treatment early on and prevent irreversible blindness.

1.2.2 Types of Glaucoma

Multiple classifications for glaucoma exist, but glaucoma can be generally classified into two large groups: 1) those caused by underlying systemic or ocular disorders (i.e., secondary) and 2) those caused by intrinsic changes in the eye leading to IOP elevation (i.e., primary) and increased susceptibility to IOP damage. Since the former present a combination of multiple diseases with distinct pathophysiological mechanisms, this dissertation focus on primary causes of glaucoma, which can be further classified into two main types based on the anatomical characteristics of the angle between the iris and the peripheral surface of the cornea. The iridocorneal angle is the region where the trabecular meshwork is located and it is responsible to continuously drain most of the aqueous humour which maintains the pressure inside the eye and changes in this structure may increase the IOP and lead to glaucomatous damage (figure 1.1). Morrison and Pollack (2003).

Primary Angle-Closure Glaucoma

Primary Angle-Closure Glaucoma (PACG) is characterized by elevated IOP due to iridocorneal angle blockage, limiting or completely stopping the flow of aqueous humor through the trabecular meshwork Schuster et al. (2020). PACG accounts for most ACG cases and is categorized by temporary and sudden apposition of the iris over the angle. leading to a drastic increase in the IOP. Due to the nature of the onset of PACG, this type of Glaucoma may occur suddenly and lead to important

clinical manifestations such as ocular pain and redness Schuster et al. (2020).

Primary Open-Angle Glaucoma

The large majority of patients who develop glaucoma have Primary Open-Angle Glaucoma (POAG), which is a more silent and slowly-progressive disease. POAG typically affects the optic nerve causing damage followed by visual field loss. It is seen that about 50-60% of patients develop an initial IOP measurement above 21 mm Hg against the standard population average of 15.7 mm Hg, with some having optic nerve head (ONH) damage with even lower IOP values (Schuster et al. (2020); Dielemans et al. (1994); Prum et al. (2016)). Since this is the most common and important cause of glaucoma worldwide, we focus our efforts on detecting POAG.

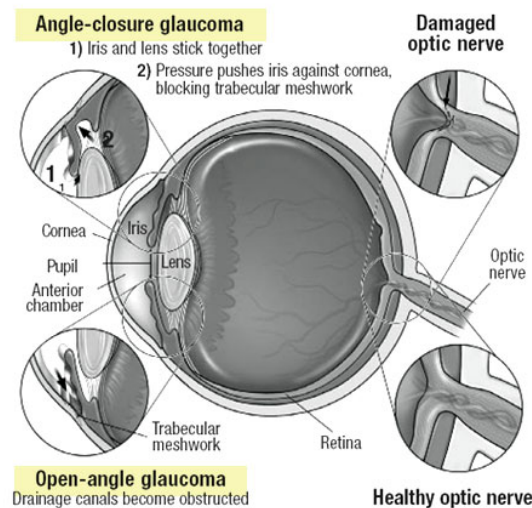


FIGURE 1.1: Open-Angle and Angle-Closure Glaucoma (Texas (2007)).

1.2.3 Common Risk Factors

Apart from elevated IOP, some other major risk factors for Glaucoma have been identified, such as age, and positive family history for glaucoma (Ramdas et al. (2011); Ekström (2012); Le et al. (2003); Czudowska et al. (2010)). Ethnicity has also been found to be a risk factor for Glaucoma, being more prevalent in people self

identified as Black or African American (AA) and Hispanics (Tham et al. (2014); Racette et al. (2005); Quigley and Broman (2006)). Studies focused on identifying risk factors for POAG indicated that advanced age (Leske et al. (2007)), elevated IOP (Nouri-Mahdavi et al. (2004b); Musch et al. (2009); Founti et al. (2020); Drance et al. (2001)), smoking (Founti et al. (2020)), bilateral diseases (Founti et al. (2020)), and disc hemorrhages (Le et al. (2003); Drance et al. (2001)) have been associated with faster disease progression. Apart from clinical factors, genome association research showed that genetics also plays a role in glaucoma development and progression (Gharahkhani et al. (2021)). More recently, degenerative neurological disorders such as Alzheimer’s disease, and Parkinson’s disease have been suggested as risk factors for Glaucoma (London et al. (2013); Koronyo-Hamaoui et al. (2011); Matlach et al. (2018)).

1.2.4 Glaucoma Progression: An Unique Prelude

Glaucoma is characterized by the loss of RGC, resulting in eye visual field defects. Glaucoma progression, on the other hand, refers to the worsening or advancement of the disease over time. While glaucoma indicates the presence of glaucomatous characteristics such as structural loss or functional impairments, its progression is characterized by active degradation in the RNFL layer, manifesting as an increase in optic nerve damage or a consistent visual field deterioration. Two primary factors differentiating glaucoma progression from glaucoma are the rate of deterioration and treatment strategies. Some patients may have glaucoma that remains stable for years, while others may progress rapidly with a faster vision loss rate. While detecting the disease itself is essential, regular follow-up and assessment are paramount to keep track of visual field deterioration over the patient’s lifespan. This allows clinicians to recommend appropriate treatment strategies early on so that it can halt or arrest glaucoma progression. Therefore, it is not only necessary to diagnose glaucoma for

appropriate disease intervention but also to monitor its progression to improve the ongoing visual quality of life for patients.

1.3 Methods for Glaucoma Diagnosis

Due to the nature of the disease, patients suffering from acute ACG generally experience pain in the eye, conjunctival hyperemia, nausea, and sudden visual impairment. Immediate treatment is required to prevent ocular damage. In contrast, POAG remains asymptomatic until it reaches an advanced stage and is only detected if the patient's vision deteriorates to a large extent (Crabb et al. (2013); Kim et al. (2016)). Since POAG (majority of glaucoma) remains asymptomatic for years, the American Academy of Ophthalmology (AAO) recommends regular eye exams for patients of age 40 onwards (Mowatt et al. (2008)). Due to the relatively low prevalence of glaucoma, low sensitivity and specificity, and high false positive rates, several tests are devised to diagnose glaucoma.

Eye exam for glaucoma evaluation usually involves Tonometry, Fundus Examination, Perimetry, Gonioscopy, and Pachymetry, each with a specific role in examining the eye.

- **Tonometry:** Since elevated IOP is the main risk factor for glaucoma and used to evaluate treatment strategies, a doctor or technician measures this pressure at a routine checkup by applying pressure to the cornea using a puff of air or the tip of the tonometer probe in contact with the cornea.
- **Fundus Examination:** Assessment of the retina and optic nerve head in glaucoma involves evaluating the presence of enlarged cup-to-disc ratio (CDR) and diffuse or localized loss of the peripapillary RNFL. A doctor might use a device that magnifies the posterior region of the retina and ONH, directly (ophthalmoscope), fundus photography for documentation and qualitative assessment,

and OCT for quantitative analysis.

- **Perimetry:** As patterns of vision loss, usually starting from the periphery, are characteristic of glaucoma, Computerized Perimetry or a visual field test is used to map the field of vision to determine the degree of vision loss associated to glaucoma.
- **Gonioscopy:** This test is used to evaluate changes in the anatomical features of the angle of the eye and subclassify the disease in different etiology groups, i.e., if the angle between the iris and cornea is closed and blocked (ACG) or wide and open (OAG).
- **Pachymetry:** In this test, a pachymeter is used to measure the thickness of the cornea, which has the potential to influence the IOP readings.

Regular check-ups for Glaucoma include a thorough eye exam and tonometry. Clinical evaluation is followed by the assessment using clinical devices, which falls under two large groups: structural evaluation (fundus photos and OCT) or functional evaluation (perimetry). These are currently the most effective tools for detecting Glaucoma and have been the mainstay for glaucoma detection.

1.3.1 Structural Tests for Glaucoma

Optic nerve imaging has been the staple for assessment of glaucomatous optic neuropathy (GON). A fundoscopic exam captures the morphological features of the optic disc and RNFL that are linked to glaucoma, such as enlargement of the optic disc cup, localized or diffuse thinning of the neuroretinal rim, and RNFL defects (Lucy and Wollstein (2016)). However, a fundoscopic exam provides only a subjective and qualitative overview of glaucoma more reproducible techniques for evaluation of the optic disc have been developed over the years. Today, OCT has become an

essential part of clinical routine eye exam, providing noninvasive objective and quantitative evaluation of the optic nerve head and measurement of the RNFL. There are three types of OCT based on the underlying technology in scanning the Optic Disc and neighboring structures. These are Time-Domain OCT, Spectral-Domain OCT (SDOCT), and more recently the Swept-Source OCT (SS-OCT), of which Spectral-Domain OCT is the most widely-available method that produces the most accurate and reproducible results to access glaucoma (Figure 1.2; Lazaridis (2022)).

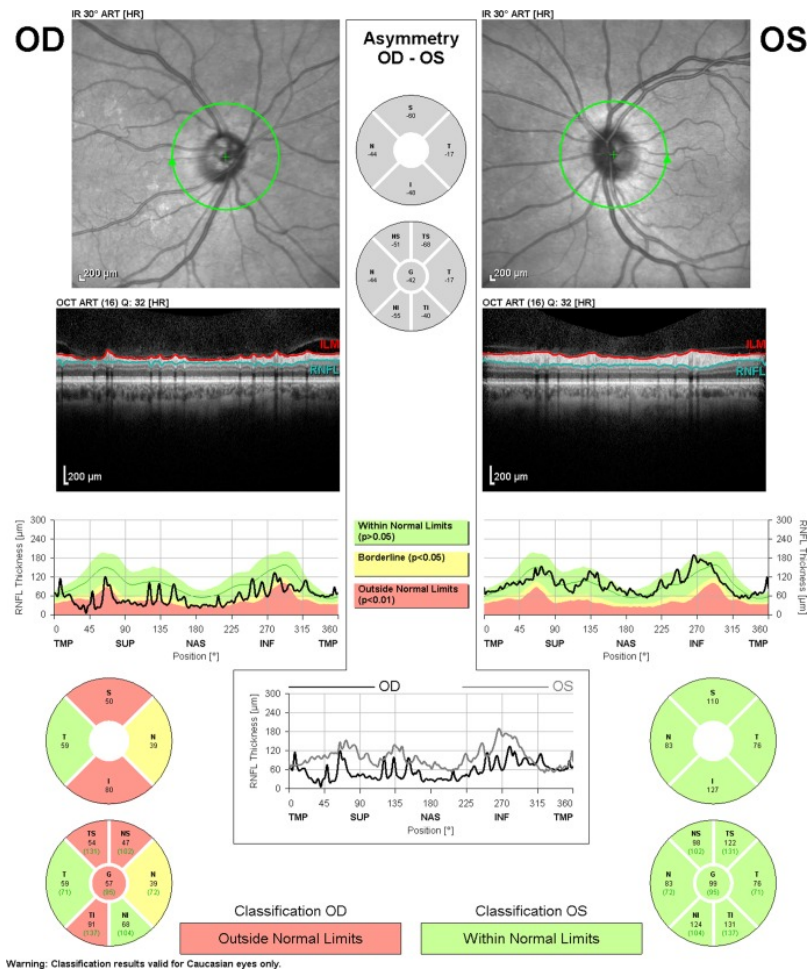


FIGURE 1.2: A scan report obtained from an eye exam from Spectralis-OCT (Heidelberg Engineering, Heidelberg, Germany) showing glaucomatous damage (Dong et al. (2016)).

1.3.2 Functional Assessments for Glaucoma

A Functional Diagnosis measures the visual field (VF) impairment due to the loss of optic nerve fibers. As discussed, VF Tests are done using standardized computerized algorithms (Standard Automated Perimetry; SAP), where stimuli are presented to the patient, and their responses are registered. White-on-white SAP is the reference standard to assess visual field loss in glaucoma and changes over time and is measured by mapping the patient's response to a contrast stimulus projected in the eye (Figure 1.3) (Lucy and Wollstein (2016)). The assessment is done by measuring the differential light sensitivity on a decibel scale. These values are measured for the entire field of view, mapped into a regular grid, and divided into four regions called quadrants. A major drawback of the VF test is the variability in the measurements due to cognitive function and cognitive load, such as fatigue, distraction, etc., the patient might experience during VF tests. Thus it is recommended that the VF test be done at regular intervals and that visual field defects should be confirmed with a subsequent exam.

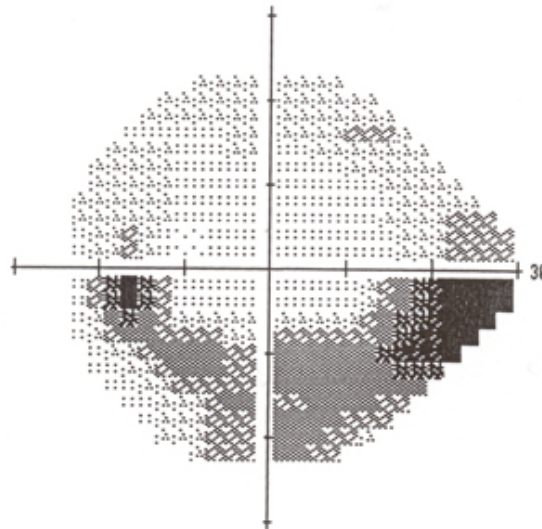


FIGURE 1.3: A Visual Field Mapping obtained from Visual Field Test (Salim et al. (2022))

1.3.3 Structure-Function Relationship

Studies have shown an association between larger neuroretinal rim area, RGC loss, and VF damage occurring in Glaucoma (Garway-Heath et al. (2002)). It was found that the relationship between Differential Light Sensitivity (DLS) (dB) and RGC count, and DLS (dB) and neuroretinal rim area follows a curvilinear relation (Garway-Heath et al. (1997); Harwerth et al. (1999)). In a study dated Oct 2012, Medeiros et al. showed that this relationship might not be linear nor curvilinear (Medeiros et al. (2009b)). They used a combination of RNFL assessment with OCT and SAP to show that the amount of neural damage perceived by the OCT and SAP highly depends on the stage of the disease. At early stages, a significant loss in RGC would amount to only a tiny change in Mean Deviation (MD) in SAP which increases as the disease advances. Thus progressive structural changes in the eye are useful indicators of VF loss, and combining VF and OCT would provide a more accurate assessment of rates of deterioration of eye sight early on.

1.3.4 Assessment of Glaucoma Progression

Although many efforts have been made in glaucoma diagnosis, detecting its progression is still challenging. Existing techniques for diagnosis find it hard to distinguish between glaucoma progression, normal age related loss and the variability due to other factors. No unified approach has been established for detecting or evaluating Glaucoma Progression in clinical practice. However, research is underway to develop techniques to assess glaucoma using extensive and complex data. These new techniques use different modalities to detect progression with high accuracy and fewer follow-up periods (Abu et al. (2020)).

Glaucoma Progression can be grouped into two types based on how tests have accumulated: a) Type of Analysis and b) Unit of Analysis. There are two categories for types of analysis: Trend-based and Event-based analysis and three types for unit

of analysis: Global, Sectoral or Pointwise Analysis.

Trend-based Analysis

Trend-based analysis for glaucoma determines whether progression is present in a series of functional or structural tests by evaluating longitudinal changes in test parameters over time. Most common methods to evaluate longitudinal changes are by linear regression or some of its variants (Hu et al. (2020)). It considers both the trajectory and magnitude of change in parameters than only relying on cross-sectional observations thereby providing information not only about the presence of glaucoma progression but also the rate of change over time. This allows clinicians to identify patients who are at a higher risk of rapid deterioration (fast progressors) and adjustment proactively. Trend analysis through linear regression can be done on global indices, cluster of indices are even individual points.

Event-based analysis

In event-based analysis, each new measurement is evaluated against two baseline test to determine whether progression (event) is present or not. Progression is identified if the new measurement exceeds the expected test-retest variability and this change persists over multiple tests. For glaucoma progression, search events might include a significant worsening in RNFL thickness, a certain degree of visual field loss, or a change in optic nerve appearance. Once one of these predefined event occurs, it indicates a potential stepwise progression or worsening of the disease.

Similar to trend-based analysis event-based methods rely on global, sectoral or pointwise deviations of multiple sensitivity measurements to define progression. In Global Analysis, all the individual measurements are averaged into a single examination (e.g., MD for SAP). This measurement provides a more concise metric for evaluation. Sectoral analysis, identifies a cluster of regions often dividing into prede-

finer zones (eg. superior, inferior, nasal, temporal etc) where changes are more likely to appear. Pointwise analysis, on the other hand, evaluates all pointwise sensitivity measurements separately to give an estimate of localized changes for a holistic analysis. All these methods have advantages and disadvantages during the examination and must be used carefully.

1.3.5 Progression Criteria

Doctors and Researchers use a set of rules called Progression Criteria to accurately estimate and classify glaucoma progression. Progression Criteria typically employs one or more statistical tests from the diagnostic tests mentioned above to obtain the likelihood and magnitude of glaucomatous change, assuming a null hypothesis of no evolution. Several Subjective and Objective criteria have been developed to identify eyes undergoing glaucoma progression. One such measure is to check for a minimum global RNFL thickness change of more than $0.5 \mu\text{m}/\text{year}$, with $p - \text{value} < 0.05$, confirmed with two consecutive tests. Similarly, different criteria have been developed for both Structural and Functional assessment of Glaucoma Progression, which uses both Subjective and Objective rules to classify progression in the eye (Thakur et al. (2023)).

1.3.6 Challenges in Glaucoma Progression Analysis

As mentioned earlier, there needs to be standardized criteria to identify glaucoma progression. Doctors and technicians rely on a combination of subjective and objective analysis to assess for progression using clinical, structural, and functional tests which introduces subtle biases in evaluations. Thus an objective standard is necessary to overcome this uncertainty. The most widespread objective standard to detect glaucoma progression has been the GPA used in HFA, which uses a series of functional tests, namely the 24-2 SAP test, to provide inference on progression

(Dixit et al. (2021); Nguyen et al. (2019); Vianna and Chauhan (2015)). GPA is a pointwise event-based analysis in which every point in the new VF test is compared with the values from two baseline tests. Points on the VF are flagged with (statistically) significant loss of sensitivity ($p < 0.05$) when the measured pointwise pattern deviation becomes more than the expected variability (already derived from a population of stable glaucoma patients). If changes occur at three or more points in two consecutive follow-up tests, the eye is labeled as "possible progression," If these points are repeated in three consecutive tests, the eye is said to be "likely progression" (Giraud et al. (2010)). Due to this, GPA becomes a qualitative measure that is relatively simple to implement and accounts for differences in variability associated with VF location, threshold sensitivity, and patient age (Rui et al. (2021); Vianna and Chauhan (2015)). Although GPA overcomes major challenges faced by subjective analysis, it has the same intrinsic limitations as the SAP test. More details on the GPA is provided in the later sections.

A question remains as to what might be a true objective criterion for Glaucoma Progression. Similar to VF GPA, some commercially available OCT devices provide a pointwise event-based change analysis of the RNFL thickness map and RNFL thickness profile for both global and sectoral RNFL averages (Nguyen et al. (2019)). Although OCT GPA is not susceptible to uncertainty due to cognitive stress during tests but significant changes in RNFL thickness do not always translate to true glaucoma progression, due to variability in the measurements and segmentation artifacts.

Age, another factor, significantly influences the rate at which visual fields and RNFL characteristics change. One of the pioneer studies on glaucoma, the Early Manifest Glaucoma Trial (EMGT), discovered that faster progression is linked with older age (Leske et al. (1999)). This finding is also observed in other research; studies by Vianna et al. (2015) and Leung et al. (2013) demonstrated that age is a crucial factor in the deterioration of neuroretinal parameters in healthy individuals.

Moreover, age-related changes have been found to skew the progression analysis in glaucoma patients. Subsequent research highlights these findings, indicating that healthy individuals do experience a significant age-related decrease in RNFL over time. Therefore, more accurate estimates of variability or thresholds are necessary to distinguish between age-related RNFL decline and progression from glaucoma (Nguyen et al. (2019); Vianna and Chauhan (2015)). In another tangent, the relationship between structure and function also found a similar effect. Zhang et al. (2017) showed that structural deterioration (RNFL) loss manifests in early stages, while visual field progression is more prevalent in advanced glaucoma. This discrepancy in the onset of glaucoma progression across various anatomical, functional, and clinical parameters underscores age as an important risk factor in progression analysis.

An ideal method for detecting glaucoma progression should indicate if the eye has glaucoma progression and estimate the rate of deterioration. Previous studies have shown that Joint Longitudinal Modeling can better characterize the relationship between structural and functional tests and improve glaucoma progression detection (Medeiros et al. (2011, 2012a,c, 2014)). Joint modeling allowed for a decrease in measurement error as longitudinal changes that would not have been significant in the VF test, might have shown significance in the OCT test (Medeiros et al. (2014); Strouthidis et al. (2011); Artes and Chauhan (2005)). Structural OCT tests have shown to detect glaucoma progression accurately in early stages while the sensitivity of functional VF tests increases in advanced glaucoma (Zhang et al. (2017)). The same study showed that although RNFL might not be able to detect progression, the ganglion cell complex (GCC) can be useful in all stages. This discrepancy between structure and function, coupled with the potential for combined modeling, highlights a research gap in progression detection. Thus in this research, we utilize the relationship between structural and functional deterioration in eyes to develop models

that can detect progression accurately.

1.4 Problem Statements and Motivations

As mentioned before in Section 1.2, glaucoma, often described as a silent thief of sight, is a group of optic neuropathies characterized by progressive optic nerve deterioration. Early detection and continuous monitoring of its progression are pivotal, not only in preventing irreversible blindness but also in managing the risk of functional impairment to improve the quality of life of affected individuals. While it is understood that functional progression of glaucoma directly impacts patient's vision-related quality of life, structural changes to the ONH and RGC often serve as precursors of these functional outcomes. However, a significant challenge in detecting glaucoma progression is the need for a standardized, unified metric for progression detection. This gap makes it difficult for researchers to track and predict the progressive characteristics across patients consistently. In light of the current advancements in the structural assessment of glaucoma, obtaining accurate and precise measurements of the ONH and RGC has become more accessible than before. But the need for a unified metric is still pressing. Coupled with the availability of functional outcomes of glaucoma progression through visual field tests, it would be valuable to develop algorithms that seamlessly integrate structural or functional data in detection process. Such advancements could not only help clinicians or researchers to pinpoint and predict progressive damage with ease but also reduce the reliance on clinical expertise. Hence, we lay in the following motivations for this research.

1. **Urgency of Early Detection:** Due to the insidious nature of glaucoma, a significant damage to the ONH can occur before any noticeable functional impairment symptoms arise. It is important to detect glaucoma progression early on to allow for timely interventions and treatment that can slow or halt

disease progression.

2. **Structure-Function Relationship:** Research has shown that structural deterioration in the eye due to glaucoma progression often precedes detectable functional changes in vision. Although the exact relationship between structure and function in glaucoma is not yet fully understood, identifying the association between them through modern methods and repeated assessments can help researchers accurately assess glaucoma progression.
3. **Precision of Structural Tests:** The Advent of modern imaging technologies for structural tests, particularly OCT, have not only proven to be reliable indicators of glaucomatous changes, but also provides repeated accurate and precise measurements. Analyzing the structural tests can help clinicians accurately identify functional progressive characteristics of glaucoma.
4. **Age-Related Progressive Characteristics:** The ONH in the eyes naturally undergoes structural deterioration as individuals age. Since the expected variability in glaucoma-induced changes increases with age, age-related changes can often be confused with the inherent test-retest variability observed in glaucoma progression. Identifying the distinction between progression due to age and progression due to glaucoma is challenging but, at the same time, holds potential for more accurate glaucoma progression insights.
5. **Unified Metric for Progression:** The lack of a universal reference standard for glaucoma progression makes consistent detection challenging. By leveraging surrogate methods such as age-related deterioration patterns, we aim to provide a basis for improved detection without the reliance on metrics for progression detection. This approach not only holds promise to achieve results comparable to some standardized methods like the GPA but also has the potential to refine

universal detection criteria.

6. **Advancements in Medical Image Analysis:** In pursuit to resolve some of the challenges in glaucoma progression detection, we would also confront fundamental challenges in medical image analysis, including imbalance data sets and noisy labels. By utilizing powerful and innovative deep learning methodologies and data driven methods, we aim to resolve these foundational challenges in data and provide holistic methods that can be transferable to other research.

In summary, our motivation for this research stems both from the clinical urgency of early and accurate glaucoma progression detection as well as the promise to resolve some fundamental challenges in medical image analysis and glaucoma research. In light of this, the research objectives can be summarized as follows

1.4.1 Research Objectives

- **Survey of Current Landscape:** Deep dive into the present state of glaucoma progression detection research and identifying the potential of deep learning methods for the same.
- **Data Driven Solution:** Develop, analyze and exploit Glaucoma Progression Data set, comprising of clinical characteristics from different modalities such as OCT scans and VF tests, to understand and predict glaucoma progression more holistically.
- **Deep Learning Technologies:** Develop a series of novel algorithms and models that leverage the spatiotemporal aspects of longitudinal structural assessments of the eye such as OCT scans and the underlying structure-function relationship to predict glaucoma progression.

1.4.2 *Research Contributions*

We will use the motivations drawn from the above research objectives to make the following contributions:

1. **State of the Art Survey:** I conducted an extensive survey of the current state of research in glaucoma progression detection using both traditional and machine learning methods. I cover a comprehensive review of both conventional and emerging technologies to understand glaucoma's structural and functional attributes. This allowed me to pinpoint the promising frontiers of glaucoma research and a potential paradigm shift towards using deep learning assisted imaging techniques for early detection of glaucoma progression.
2. **Duke Eye Dataset and Methodology:** I took a data driven approach to gain insights into the structure and function in glaucoma progression. This was achieved by developing, analyzing and utilizing the Duke Eye dataset. Specifically, I aggregated a data set comprising of longitudinal structural assessment of patient's eyes through sequences of OCT scans from the Duke Ophthalmology Registry. A rigorous analysis of the demographic and clinical attributes of this dataset was performed, to provide insights on structural deterioration using RNFL thickness slopes at the observation level. Additionally, a progression dataset was curated by integrating data obtained from the glaucoma registry. This was done by matching the longitudinal OCT scans with the corresponding GPA events derived from VF SAP tests, which served as the objective criteria for glaucoma progression in the subsequent deep learning analysis. All insights and glaucoma research were done on this dataset.
3. **Novel Deep Learning Algorithm:** I developed a novel deep-learning algorithm based on CNN-LSTM model. This model was specifically designed to

capture the spatiotemporal features from a sequence of longitudinal OCT scans to identify glaucoma progression. Identifying that eyes exhibit age-related structural deterioration naturally and that susceptibility to glaucoma increases with age, this algorithm captures a pseudo-progression criterion in longitudinal structural data. The approach uses reshuffling individual longitudinal OCT scan sequences of patients and the knowledge of healthy eyes from a separate standout data set to establish robust pseudo-progression criteria for glaucoma, eliminating the dependence on gold standard labels for disease progression prediction.

4. **Advanced Deep Learning Model with GPA:** Building upon the previous model, I incorporated labels obtained from GPA on the CNN-LSTM model to obtain an accurate detector of glaucoma progression. Given that GPA, although accurate, can have label noise due to its susceptibility to false positives. Owing to the nuances due to data acquisition, the deep learning (DL) model was designed to use age-related structural progression as a pseudo-identifier. A contrastive learning scheme was used to teach the base CNN-LSTM classifier accurate spatiotemporal characteristics of glaucoma progression from potentially noisy labels and highly imbalanced data to provide refined predictions.

1.5 Thesis Structure

Chapter 2 provides a literature review and an extensive survey of the current research in glaucoma progression detection. This also covers the recent developments in machine learning (ML) and DL approaches for glaucoma progression. In Chapter 3, we present the Duke Ophthalmic Registry dataset along with basic demographic and clinical characteristics analysis. We also introduce the basic methodology for DL analysis, input features, reference standard, baseline comparative methods and

post-hoc analysis. We present our novel weekly supervised deep learning algorithm to detect glaucoma progression using unlabeled longitudinal OCT scans in Chapter 4. This is followed by Chapter 5, in which we develop an advanced deep learning model assisted by noisy labels obtained from GPA to classify disease progression accurately. Finally, we provide the concluding remarks on the current research and discuss the future work in Chapter 6.

Literature Review

This chapter provides a comprehensive review of the current advancements in glaucoma progression detection. We begin with a meta-review of survey papers and an examination of some landmark studies. This is followed by an introduction to clinical, traditional, and machine-learning methods to detect disease progression, which covers the structural and functional aspects of evaluation techniques. Through this, we aim to learn the latest advancements and the challenges and pitfalls in tracking glaucoma. We then transition to the complex structure-function relationship and emphasize how it has improved the performance of various traditional and machine-learning detection methods. We will conclude the chapter by presenting an in-depth review of the current state of the art in deep learning approaches for detecting progression, which will form the basis of our research.

2.1 Background

Glaucoma, specifically glaucoma progression, has been a significant area of research in Ophthalmology. Recent advancements in artificial intelligence (AI) algorithms and the availability of large medical data sets have shown potential and a growing interest in its application for glaucoma progression detection and management. Numerous studies have tried to explore the effectiveness of AI in improving the diagnosis of glaucoma progression over standard clinical practice and traditional methods. These studies have relied on regular follow-up assessments of several clinical parameters such as demographics (age, sex), electronic health records (EHR; IOP, central corneal thickness - CCT, cup-disc ratio - CDR) data, structural properties (ONH

change, RNFL thickness) and functional characteristics (VF sensitivity) to identify glaucomatous change. While these features have improved the predictive accuracy, it still needs to be determined which set of data offers the best representation of glaucoma progression, balancing data acquisition, ease of access, and minimal expertise interpretation.

Modeling glaucoma progression has been challenging since combining spatial and temporal aspects with a single technique, even with AI, is difficult. Confounding risk factors, test-retest variability, and secondary diseases also make it hard to categorize glaucoma progression. Another contention amongst all studies is the inconsistent definition of progression and how it's measured. Although established methods exist, such as event-based GPA or trend-based point-wise linear regression (PLR), there are no universal criteria to define progression, which makes it difficult to develop AI algorithms for detection. Nonetheless, clinicians have overcome many challenges applying AI, especially deep learning techniques, to predict glaucoma progression using imaging and health records. We provide a brief review of such studies, discussing both the advantages and challenges of AI in glaucoma research shedding light on how AI overcomes limitations.

2.2 Review

Several surveys have reviewed primary studies focusing on methods used to detect glaucoma progression using either structure, function, or both. These papers present various perspectives on applying AI and deep learning in tracking glaucoma progression. For instance, an article by Thompson et al. (2020) lays a solid foundation, exploring how advances in computing technology and the availability of large datasets have enhanced glaucoma diagnosis. This paper reviewed 91 studies on traditional and machine learning methods, illustrating how the techniques can be integrated into clinical practice. The survey found that while evaluations have become more

accurate with imaging data, there remains a drawback in the inconsistent definitions of the reference standard. This underscores the importance of rigorous validations alongside expert opinions before AI techniques are deemed suitable for screening. Although the primary focus of this article is on glaucoma diagnosis, studies on tracking its progression have drawn similar conclusions. These techniques have yet to be incorporated into clinical decision-support systems and require thorough research before implementation.

A review by Mirzania et al. (2021) on AI for glaucoma detection has emphasized the influence of data quality for improving the DL algorithm’s performance. They imply that datasets with better demographic, clinical, structural, and functional representations obtain better performance. In a more specific case, Asaoka and Murata (2023) have reviewed 108 papers, and Hu et al. (2020) have reviewed 207 papers on the prediction of functional progression of glaucoma using visual fields. Both these surveys highlight that although VF is highly effective in predicting progression, the importance of model adjustment to specific nuances of experiment design (e.g., irregular testing) before applying AI is paramount. Both papers have outlined that none of the techniques can yet be incorporated in clinical settings due to a lack of validation with a universal ground truth. Similarly, a paper reviewing 30 papers by Bussell et al. (2014) demonstrating the importance of structural parameters like RNFL from OCT scans in detecting disease progression also fails to identify a common reference standard. Even though RNFL is a precise measure, providing AI methods with accurate estimates for structural progression, it faced challenges like limited reliable datasets, outliers, and the absence of long follow-up data. On the upside, these papers have prompted the use of combined structure and function index for improved glaucoma progression.

A more holistic view of DL approaches to detect and monitor glaucoma progression is provided in the works of Mayro et al. (2020), 71 papers and Thakur et al.

(2023), 108 papers. Both articles offer distinct but overlapping perspectives of DL methods using structure, function, and clinical data, highlighting innovative techniques for progression detection. The first paper demonstrates the transformative potential of DL methods to generate new image data, thereby forecasting disease trajectory. Various methods discussed in this paper underscore the utility of DL algorithms in efficiently processing information from multiple modalities, providing accurate predictions. It succeeds in pinpointing several limitations regarding data-centric modeling techniques, critiquing the algorithm’s inability to effectively analyze confounding factors, sensitivity to disease manifestations, and image quality. The second paper, on the other hand, adopts a broader approach to analysis, covering various ML and DL methods with multiple modalities (clinical, structure, function) for disease progression. It differs from the first in its ability to highlight variability in results, inconsistencies in datasets, lack of standard progression definitions, and the ability to provide a nuanced view of methods. This paper sets its narrative review specifically for glaucoma progression detection and provides evidence for the translational potential of current research in the field. Although all these papers offer critical reviews of the evolving AI field, laying down the groundwork for research, a more granular analysis that would help clinical understanding and provide a computational and data-centric perspective is necessary.

2.3 Landmark Glaucoma Studies

Several foundational glaucoma studies done over the years have highlighted the importance of early detection and intervention in glaucoma progression. Table 2.1 summarizes some landmark studies demonstrating the importance of timely intervention. The seminal work in The Early Manifest Glaucoma Trial (EMGT) showed that individuals are at a higher risk of progression if timely treatment is not provided (Leske et al. (1999)). It is one of the first studies that identified age as a significant

risk factor in VF deterioration. The Advanced Glaucoma Intervention Study (AGIS) emphasized the persistent risk of visual field loss throughout the follow-up, even after intervention (AGIS (1994)). The Ocular Hypertension Treatment Study (OHTS) proved that the risk of eyes evolving into POAG extended over 15 years, making glaucoma one of the most prolonged chronic progressive diseases (Gordon et al. (2002)). Both AGIS and the OHTS showed that lowering IOP can substantially delay the onset of POAG, underscoring the importance of preemptive care.

Further studies, like the Collaborative Initial Glaucoma Treatment Study (CIGTS), compared the efficacy of surgical and medical interventions in IOP management and their implications for vision-related quality of life (Musch et al. (1999)). On a tangential yet similar note, the Collaborative Normal-Tension Glaucoma Study (CNTGS) illustrated that IOP reduction is paramount for therapeutic impact on disease progression. The European Glaucoma Preventing Study (EGPS) supported the findings of other studies by recognizing the influence of IOP as a risk factor (Miglior et al. (2002)). The Glaucoma Laser Trial (GLT) by Glaucoma Laser Trial Research Group (1995) and the United Kingdom Glaucoma Treatment Study (UKGTS) by Garway-Heath et al. (2013) affirmed the above studies in determining the efficacy of IOP management through medical interventions. It showed that IOP management is an effective way to reduce the rate of visual field progression during the initial POAG stages. Collectively, these pioneering studies elucidated the relationship between structural nuances such as IOP fluctuations and their effects on functional components such as the visual field deterioration, thereby providing a holistic understanding of components in glaucoma progression. These studies also showed that early glaucoma progression detection and monitoring are pivotal for efficient and targeted therapeutic interventions.

Table 2.1: A brief review of some landmark glaucoma studies

Name	Study Type	Citation	Design	Dataset	Follow-up Period	Treatment	Outcome Measures	Findings
Early Manifest Glaucoma Trial (EMGT)	Leske et al. (1999)	Treatment vs No Treatment	Randomized, Clinical Trial.	255 Patients with mean age 68.1yrs; 66% women	>4 years	Laser Trabeculoplasty + Betaxolol	VF loss in 3 consecutive C30-2 Humphrey tests or Optic Disc Changes	Higher progression rate in controls group; High IOP frequently followed by progression; Old age was associated with faster progression.
Advanced Glaucoma Intervention Study (AGIS)	AGIS (1994)	Treatment vs Treatment	Randomized Clinical Trial	591 Patients (789 eyes) age 35-80yrs; 54.3% Female; 56.2% AA	7 years	Series of Laser Trabeculoplasty and Trabeculectomy	VF tests using 24-2 Humphrey Field Analyzer and Visual Acuity Tests	Over half the eyes showed VF progression throughout the follow-up after intervention.

Ocular Hypertension Treatment Study (OHTS)	Gordon et al. (2002)	Treatment vs No Treatment	Randomized Clinical Trial	1636 Patients age 40-80yrs; 57% Female; 25% AA	>5 years	Topical Ocular Hypotensive Medication	Reproducible 30-2 Humphrey VF deterioration and reproducible stereoscopic optic disc deterioration	Risk of developing POAG continues over at least 15 yrs of follow-up; High risk individuals more likely to respond to treatment.
Collaborative Initial Glaucoma Treatment Study (CIGTS)	Musch et al. (1999)	Treatment vs Treatment	Randomized, Controlled Clinical Trial	607 Patients age 25-75yrs; 45% Female; 38.1% AA	>5 years	Topical Ocular Hypotensive Medication vs Immediate Trabeculectomy	Sustained Progression in VF loss in 24-2 HFA.	Both treatments effective in slowing down POAG; Bpth group displayed similar rates of VF loss over time.
Collaborative Normal-Tension Glaucoma Study (CNTGS)	Anderson (2003)	Treatment vs No Treatment	Randomized, Controlled Clinical Trial.	145 Subjects age 20-90 yrs;	5 years	Topical Medication or Laser Trabeculectomy	VF Progression and Stereoscopic Optic Disc deterioration	Reducing IOP in patients with Normal-Tension Glaucoma significantly reduced progression in VF.

European Glaucoma Preventing Study (EGPS)	Miglior et al. (2002)	Treatment vs No Treatment	Randomized, Double-Blinded, Controlled Clinical Trial	1077 Subjects age \geq 30 years; 54.4% Female	5 years	Topical Ocular medication	IOP, VF Tests and Stereoscopic Optic Discs	Lower IOP associated with reduced risk of glaucoma onset; Similar clinical characteristics of POAG group with OHTS.
Glaucoma Laser Trial (GLT)	Glaucoma Laser Trial Research Group (1995)	Treatment vs Treatment	Randomized Clinical Trial.	271 Patients (542 eyes) age >35 yrs; 56% Female; 43% AA	>2 years (<9 years)	Topical Medication vs Laser Trabeculoplasty	IOP, VF Tests and Optic Disc Changes	Laser Trabeculoplasty had significant effect in lowering IOP than eyes with topical medication.

United Kingdom Glaucoma Treatment Study (UKGTS)	Garway-Heath et al. (2013)	Treatment vs No Treatment	Randomized, Controlled Multicenter Treatment Trial.	516 Subjects mean age 66 ±11 yrs; 47.1% Female	2 years	Topical Ocular Medication	VF 24-2 HFA II Testing, Confocal Scanning Laser Ophthalmoscopy, Scanning Laser Plarimetry, OCT, Monoscopic Optic Disc Photograph, Fundus Photographs, Tonometry	IOP treatment significantly reduced VF progression in early POAG; Pointwise Linear Regression helpful in detecting progression.
---	----------------------------	---------------------------	---	---	---------	---------------------------	---	---

2.4 Glaucoma Progression Detection using Assessments of Visual Fields

2.4.1 *Clinical Assessments and Event-Based Methods*

Visual field tests are usually used to assess the glaucoma progression leading to functional impairments. VF tests are obtained by measuring the patient’s response to contrast stimuli using various perimetric data as shown in Section 1.3.2. It is often measured as the intensity of light stimulus on a logarithmic scale (dB). VF has complex properties; therefore, assessment of progression requires additional analysis of the perimetric data such as clinical gradings, glaucoma change probability scores, event-based analysis, or trend-based analysis (Hu et al. (2020)). Clinical judgments are subjective and have been found to have moderate intraobserver agreement ($\kappa = 0.45 - 0.55$) (Aref and Budenz (2017)). Landmark studies have implemented some form of scoring system to detect progression. The most commonly used and explicit scoring criteria is the glaucoma change probability criteria developed by EMGT (Leske et al. (1999)), which detected early progression. AGIS and CIGTS have used similar methods, which have been repurposed for identifying progression by researchers (Katz (1999)). Studies have shown that all these methods have comparable statistics for detecting progression but have various tradeoffs between specificity and sensitivity (Hu et al. (2020); Katz et al. (1999)). The Glaucoma Change Probability (GCP) analysis and later the GPA were inspired by the EMGT and is now a commonly used event-based analysis. Research on the comprehensive analysis of the GPA found that there is a strong correlation between GPA and thorough, objective clinical criteria with 93% sensitivity and 95% specificity (Arnalich-Montiel et al. (2009)), which has shown to be a promising method for detecting VF loss. Some studies showed that GPA was conservative in declaring VF sequences progressing (Roberti et al. (2022); Tanna et al. (2012); Antón et al. (2013)). These papers showed that event-based GPA has a moderate agreement with expert clinical

judgments (Tanna et al. (2012)). In other studies, the GPA method was found to be susceptible to high false positive rates when predicting "possible progression" in patients with high test-retest variability (Artes et al. (2014); Wu and Medeiros (2018)). Future studies have tried to modify GPA, integrate sophisticated analysis, or add structural GPA to improve specificities (Tanna et al. (2012); Medeiros et al. (2012c); Leung et al. (2010)). Ubiquitously, all papers showed GPA could detect early signs of VF deterioration than other methods but are met with the same intrinsic limitations as SAP tests. Authors recommend using a sufficient number of VF tests, which can be time-consuming, require effort, or are prone to test-retest variability.

2.4.2 Linear Regression and Trend-Based Methods

Trend-based analysis has been widely used to detect glaucoma progression utilizing some form of linear regression on VF test parameters or indices. They predict progression by quantifying the VF deterioration as a rate of change over time. This not only helps detect progression but also identifies the onset of progression, rapid progressors, time to change, etc. An eye is classified as progressing using trend-based analysis if the rate of change is negative (usually $< 0dB/yr$) and is statistically significant (usually $p < 0.05$). Unlike GPA, which generally needs global context for analysis, trend-based methods can be applied to global (MD), sectoral, or individual points (pattern standard deviation - PSD or visual field index - VFI) (Hu et al. (2020)). Trend-based methods agreed with GPA and clinical judgments (Casas-Llera et al. (2009); Medeiros and Jammal (2023); Nouri-Mahdavi et al. (2004a)). Specialized analysis software using linear regression methods such as PROGRESSOR also showed similar sensitivities for detecting progression (De Moraes et al. (2012)). Adding mixed-effects, prior distribution, and clinical priors improved predictive accuracy (Zhang et al. (2015); Nouri-Mahdavi et al. (2004a); Swaminathan et al. (2022)). Trend analysis using different parameters of perimetric tests such as

VFI, MD, or PSD was also found to correlate well, identifying a similar proportion of eyes progressing. Still, they have intrinsic limitations (Cho et al. (2012); Fitzke et al. (1996)). The trend-based analysis detected progression accurately in patients with longer follow-ups, a common pattern observed in multiple studies (Casas-Llera et al. (2009)). When comparing how spatial information helps in detecting progression, generally, PLR or cluster trend analysis (CTA) performed better, but no consensus was observed (Viswanathan et al. (1997); Vesti et al. (2003); Mayama et al. (2004)). All these methods had limitations and trade-offs between experiment design, parameters to be used, and test results, often affected by confounding factors. Another study by Quigley et al. (1996) indicated that linear regression might not be sufficient to detect progression in the presence of bilateral disease. Adding statistical methods into linear regression has been shown to improve sensitivity in VF compared to linear regression and PLR alone. For example, the ANSWERS (Weibull Error Regression) method by Zhu et al. (2014) obtains 15% less prediction error than permutation of PLR (PoPLR). Overall, trend-based methods were moderately accurate, but more emphasis is needed on the experiment design and how to analyze trend data.

2.4.3 Probabilistic Methods

Table 2.2 summarizes complex modeling strategies used in glaucoma progression detection. Probabilistic methods provide a framework for modeling and understanding uncertainties in data. In the context of detecting glaucoma progression, these methods offer a robust and adaptive approach, taking into account the inherent variability and intricacies of ocular data.

Probabilistic methods, especially those based on Bayesian frameworks, have been extensively explored for detecting glaucoma progression using visual fields (VF). Medeiros et al. (2012a) showcased the Bayesian Hierarchical Model’s effectiveness, which integrates trend and event analyses. This approach significantly outperformed

ordinary least squares (OLS) regression, with a 98% detection rate at 96% specificity. Concurrently, studies like Warren et al. (2016) and Berchuck et al. (2019a) employed Conditional Autoregressive (CAR) models, each showing strong agreements with expert judgment on glaucoma progression. Betz-Stablein et al. (2013) further reinforced CAR’s utility, demonstrating it outperforms standard PLR methods. In another study, the Empirical Bayes Estimates of Best Linear Unbiased Predictors (BLUP) introduced by Medeiros et al. (2012b) significantly reduced mean squared error in predicting future VF impairments compared to traditional OLS. In the same domain, Montesano et al. (2021) proposed a Hierarchical Bayesian Analysis model that showed improved VF progression estimation for glaucoma progression.

Studies also demonstrated probabilistic methods can be repurposed for classification and unsupervised learning. For example, Yousefi et al. (2014, 2018) series of studies from 2014 to 2018 utilized Gaussian Mixture Models (GMM) and Variational Bayesian techniques for detecting progression. These models, especially GMM Expectation Maximization with Permutation of Points (GEM-PoP), were found to detect with high sensitivity and outperformed several baseline and clinical methods in predicting progression. Goldbaum et al. (2012) introduced a Variational Bayesian Independent Component Mixture Model (VIM), adding valuable clinical insights. Collectively, these probabilistic methods displayed superior performances against established reference standards and highlighted their potential to offer better interpretability and robustness in tracking glaucoma progression compared to conventional methods.

2.4.4 Machine Learning Methods

ML methods have gained significant traction in detecting glaucoma progression using visual fields (VF). O’Leary et al. (2012) introduced the Permutation Analysis PLR (PoPLR), which reordered permutations to yield a continuous estimate of deterio-

ration while maintaining control over specificity. Shuldiner et al. (2021) employed traditional classifiers such as Support Vector Machines (SVM) and Fully Connected (FC) networks to predict rapid progression using initial VF tests, achieving a notable AUC of 0.72. In another study, Jones et al. (2019) combined Principal Component Analysis (PCA) with a Soft Voting Classifier, using both longitudinal IOP and VF data, which enhanced accuracy in predicting rapid progression with an AUC of 0.83. Sample et al. (2005) applied Independent Component Analysis (ICA) in an unsupervised setting, outperforming traditional criteria like AGIS and EMGT. Unique methods such as Archetypal Analysis were also developed (Wang et al. (2019) to identify representative progression patterns, outperforming multiple established methods. Saeedi et al. (2021) used numerous ML classifiers, from Random Forests to CNNs, to distinguish progressing from non-progressing eyes, all of which achieved high sensitivity and specificity, outperforming conventional approaches.

When compared with probabilistic methods, ML techniques, especially when combined with unsupervised learning or ensemble classifiers, are adept at handling the intricacies of VF data for glaucoma progression. While probabilistic methods usually need prior knowledge to incorporate uncertainty, machine learning can learn the complex non-linear patterns directly from the datasets and produces superior performance in terms of accuracy and generalizability for detecting glaucoma progression using VF data.

2.4.5 Deep Learning Methods

DL methods have significantly advanced in detecting glaucoma progression using VFs, particularly by leveraging the data’s complex spatial, temporal, or spatiotemporal relationships. Several models, such as CascadeNet-5 utilized by Wen et al. (2019) and the generalized Variational Autoencoder (VAE) by Berchuck et al. (2019b), focus primarily on spatial patterns in VF, predicting future Humphrey VF (HVF) points

and trajectories of progression with commendable accuracy.

On the other hand, we saw that models that use both spatial and temporal aspects of VF data provided some of the most promising results. For instance, Dixit et al. (2021) developed a Convolutional Long Short-Term Memory (ConvLSTM) network, which captures spatiotemporal relationships in VF and demonstrated that combining VF data with clinical measures further improves predictive accuracy. Hosni Mahmoud and Alabdulkreem (2023) use of Bidirectional Recurrent Model (Bi-RM) and Sabharwal et al. (2023) implementation of ConvLSTM techniques further emphasized the efficacy of incorporating time-series data in defining VF progression patterns by producing state of the art results.

Unsupervised DL methods are another such technique that is shown to capture subtle characteristics of progression. For example, Berchuck et al. (2019b) developed a VAE latent space by reconstructing longitudinal VF data to effectively predict rates and trajectories of functional progression. The unsupervised Deep Archetypal Analysis by Yousefi et al. (2022) is another method that illustrates DL-based unsupervised methods can predict early signs of glaucoma and potential rapid progression accurately.

Compared to the previously discussed probabilistic and traditional ML techniques, DL models, especially those integrating spatiotemporal features, were found to be more holistic and produced a nuanced understanding of glaucoma progression, presenting an essential tool for glaucoma progression detection for researchers.

2.4.6 Time Series Analysis and Forecasting Methods

Time series and forecasting models emphasizing predicting future VF deterioration have also been researched in glaucoma progression. Specifically, models like the intrinsic CAR technique in studies by Warren et al. (2016) and Betz-Stablein et al. (2013) were inherently geared towards spatiotemporal data, making it proficient at

capturing the intricacies of VF changes over time. Berchuck et al. (2019a) extended the CAR framework and integrated it with Bayesian and Generalized Linear Mixed Models (GLMM) to improve the model’s predictive capability, especially highlighting the improvements made by spatiotemporal modeling over strictly spatial ones.

Outside the traditional probabilistic CAR domain, Garcia et al. (2019) employed traditional estimation techniques such as the Kalman Filter Estimator, a classical time-series forecasting approach. This model accounts for measurement uncertainties and inaccuracies, offering holistic forecasting results for disease trajectory, mainly seen with normal tension glaucoma (NTG).

A holistic comparison of all the above methods shows that DL methods provide adaptability and potential in handling large and complex datasets. Probabilistic schemes like CAR and Time-series models like the Kalman Filter provide a more structured, principled approach to predicting progression. Traditional models incorporate domain knowledge well, ensuring outcomes align with known clinical expectations and thus ensuring greater trustworthiness in clinical settings. DL model, on the other hand, although it provides better accuracies, needs to be carefully tuned to obtain desired outcomes.

Table 2.2: A Review of Methods for Detection and Prediction of Glaucoma Progression using Visual Field Tests

Citation	Setup	Algorithm/ Method	Dataset	Data Type	Follow-up Period	Reference Standard	Baseline Method	Model Output	Outcomes	Summary
Medeiros et al. (2012c)	Regression	Bayesian Hierarchical Model integrating trend and event	711 eyes - glaucoma and suspects; 55 eyes - stable	VFI from SAP with GPA prior	5 reliable tests, 5 years	2 consecutive VF test has PSD <0.05 from baseline and GPA	OLS regression slopes	Bayesian slopes of change for VFI	98% by Bayesian vs 50% OLS for 96% Specificity	Integrated Bayesian Model significantly better than OLS
∞ Warren et al. (2016)	Regression	Intrinsic Conditional Autoregressive Model	Train - 191 eyes, Test - 100 eyes	24-2 VF tests from HFA	5 follow-ups, 4.34 years	Clinicians Grading and GPA	Regression Models	Deviance Information Criterion, VF Progression Slopes	0.8 AUC, 92% Sensitivity, 95% Specificity	Model agrees with Progression by Experts

O'Leary et al. (2012)	Regression	Permutation Analysis PLR	944 eyes	24-2 HFA II SAP tests	10 exams, 8 years	Slopes <0 and <-1dB/y with p<0.05	PLR, MD Linear Regression	PoPLR slopes and p value	12%, 29%, 42% hit-rate at 5th, 8th and final exams	PoPLR uses permutation reordering to get continuous estimate of deterioration, allows for control over specificity
Medeiros et al. (2012b)	Regression	Empirical Bayes Estimates of BLUP	643 eyes	VFI from SAP Tests	10 tests, 6.5 years	significant negative slope (alpha = 0.05)	OLS Regression	Slopes of change with future VFI predictions	MSE 32.3 vs 13.9 for Bayesian vs OLS	BLUP is beneficial in predicting future impairment
Betz-Stablein et al. (2013)	Regression	Conditional Autoregressive (CAR) Model	194 eyes	Full SAP threshold, SITA exams	7.5 tests, 2.5 years	Clinical judgements on VF reports	PLR Slopes of change	Progression: Significant Slopes of change with varying alpha	68% sensitivity, 73% specificity	Model outperforms PLR method

Berchuck et al. (2019a)	Regression	Bayesian CAR with GLMM	191 eyes	VF SAP tests from HFA II	7.4 tests, 2.5 years	signifiant LR slope at all VF locations	PLR Method	Progression: Significant LR slopes	0.74 AUC for SpatioTemporal Method	Spatiotemporal method better than Spatial method in predicting progression
Montesano et al. (2021)	Regression	Hierarchical Bayesian Analysis	Modeling: 146 eyes, Analysis: 3352 eyes	24-2 SAP test from SITA HFA III	10 VFs, 4 years	P-score >0.5, significant negative slopes	OLSLR and PoPLR	Progression Score (one-sided p-value for slope)	57% Hit-rate at 95% Specificity	Bayesian Model better estimates VF progression
Bryan et al. (2017)	Regression	Bayesian Hierarchical Model	276 eyes	52 points from 24-2 SAP tests from HFA	10.5 years	-	-	VF Slopes, Posterior Predictive Checks, Deviance Information Control (DIC)	DIC=1075212, slope = -0.31dB/year for progressing	Two-stage modeling is beneficial to explore progression
Wen et al. (2019)	Regression	CascadeNet-5 and other DL models	8263 eyes (80% train, 10% test)	24-2 SAP tests from SITA HFA II	3.6 visits, 3.5 years	Mean and STD of rate of progression from EMGT	-	future HVF points, PMAE	2.47 dB PMAE, correlation with MD: 0.92	DL can predict future spatiotemporal HVF

Garcia et al. (2019)	Regression	Kalman Filter Estimator	263 eyes NTG, 601 eyes HTG	demo-graphics, IOP, VF MD, VF PSD	5.9 years NTG, 6.3 years HTG	-	Null Model, Linear Regression	future MD, PSD and IOP values	Predictive accuracy: 87.2% KF-NTG, 86% KF-HTG vs 86.4% Null Model, 72.7% LR	KF forecasts disease trajectory with NTG
Dixit et al. (2021)	Regression and Classification	Convolutional LSTM with VFI, MD, PLR slopes	11242 eyes	54 points 24-2 VF tests, IOP, CCT, CDR	4 follow-ups	statistical significant negative slopes	MD Slope, VFI Slope, PLR Slope	stable and progressing	0.89-0.93 AUC with VF and Clinical, 0.79-0.82 AUC with VF	ConvLSTM captures spatiotemporal relationships accurately, VF with clinical data more accurate than VF alone
Hosni Mahmoud and Alabdulkreem (2023)	Regression and Classification	Bidirectional Recurrent Model (Bi-RM)	Train: 5413 eyes, Test: 1272 eyes	54 points 12-2 HFA using ITT	6 tests, 3 years	-	Linear Regression, Term Memory	progressing vs non-progressing, VF points	92.6% AUC, 3.61 dB Prediction MAE	Bi-RM is predictive of VF progression

Hemelings et al. (2023)	Regression and Classification	ResNet50 with OLSR or Huber	Train: 1839, Valid: 272, Test: 271 eyes	24-2 VF HFA tests	8.5 tests, 5.37 years	significance - at different negative slope cut-offs		progression: significant negative slopes	AUC: 0.67 with OLS at 0.65 with Huber	DL predicts VF progression using baseline fundus
Goldbaum et al. (2012)	Classification	Variational Bayesian Independent Component Mixture Model (VIM)	2085 eyes	24-2 SAP test from HFA II, SITA	6.7 tests, 4 years	GPA outcomes, stereophotoclinical judgements	GPA outcomes	Progression: LR slopes from POP estimates	26.3% vs 14.5% accuracy for PGON eyes wrt GPA	POP adds information to clinicians to detect VF progression
Sabharwal et al. (2023)	Classification	Convolutional LSTM	8705 eyes (80% train, 10% valid, 10% test)	VF SAP tests	12 VF tests, 12 years	event (GPA) and trend-based (LR) methods	clinical assessment (EHR at final VF)	progressing vs non-progressing	0.78-0.94 AUC with all VF	DLM defines VF worsening successfully
Shuldiner et al. (2021)	Classification	SVM, FC Network, Random Forest	22925 eyes	24-2 VF tests	5 VF tests	significant negative MD slope <-1dB/y	Logistic Regression, naive Bayes	rapid and non-rapid progressors	AUC: 0.72 with SVM and FC Net	MLA predicts rapid progression with initial VF tests

Saeedi et al. (2021)	Classification	MLCs: Logistic Regression, RF, xgBoost, SVC, CNN, FCN	131156 eyes (80% train, 10% test), 161 eyes clinical test	24-2 VF SAP from SITA tests	6.9 follow-ups, 6.3 years	majority vote by MD slope, VFI slope, AGIS criteria, CIGTS score, PLR, PoPLR	-	progressing vs non-progressing	0.83-0.88 sensitivity, 0.92-0.96 specificity	MLC had better and balanced predictions than conventional methods
Yousefi et al. (2014)	Classification	GEM + longitudinal slopes	76 eyes progress, 91 eyes stable	52 points from 24-2 SITA SAP tests from HFA II	progressing: 5.5 follow-ups, 2.7 years, stable: 4.7 follow-ups, 4.2 weeks	expert grading of serial stereo photos	SAP GPA, VFI LR, MD LR	stable vs progressed	28.9% Sensitivity at 95% Specificity	Accuracy of GEM outperforms baseline and clinical methods
Jones et al. (2019)	Classification	PCA + Soft Voting Classifier	571 patients (80% train, 10% test)	IOP, MD, PSD data	6 years	statistical significant negative slopes < -1dB/y	-	rapid and non-rapid progressors	0.83 AUC for predicting rapid progression	IOP and VF data improves accuracy for Rapid Progression
Yousefi et al. (2018)	Unsupervised	Gaussian Mixture Model	2085 eyes - glaucoma	VF 24-2 SAP tests	5 follow-ups, 9 years	PSD < 0.05 in SAP tests wrt Baseline and reproducible at least once	Global, Regression, Point wise Linear Regression	Time to detect progression using ML slope and p-value	3.5 years vs 3.9 years to detect progression	ML outperformed other methods

Wang et al. (2019)	Unsupervised	Archetypal Analysis	method: 12217 eyes + validation: 400 eyes	24-2 VF SAP Tests	5 follow-ups, 5 years	Event-based and trend-based clinical assessment	MD Slope, AGIS score, CIGTS score, PoPLR	Rate of Archetype change ONL	51% accuracy and 77% correct rejection rate	Archetype significantly outperformed all methods
Sample et al. (2005)	Unsupervised	Independent Component Analysis (ICA)	191 eyes - glaucoma and suspect	24-2 and 30-2 VF SAP Tests	3 follow-ups, 6.24 years	Clinical assessment of Stereoscopic Photos + PGON	AGIS and EMGT scoring	Progressed vs Non-progressed	16.7% progressing, 31% PGON	vB-ICA outperforms AGIS and EMGT criteria
Berchuck et al. (2019b)	Unsupervised	generalized Variational Autoencoder	3832 eyes (80% train, 10% valid, 10% test)	24-2 SAP VF Test	7.61 visits, 4.95 years	significant negative rate of change (alpha = 0.05)	PW Linear Regression and OL-SLR slopes with MD	24-2 SAP VF points, rates of change using latent dimension	MAE: VAE vs PW 5.14dB vs 8.07dB	VAE can predict rates and trajectories of progression
Yousefi et al. (2022)	Unsupervised	Unsupervised Deep Archetypal Analysis	205 eyes from OHTS	30-2 VF from SITA HFA	16 years	OHTS expert-identified patterns	-	MD of 18 VF clusters, GEE LR slopes	-2.7 dB MD at glaucoma, -5.5dB MD at last visit	Automated ML system predicts early sign and rapid progression
Yousefi et al. (2016)	Unsupervised	GEM Progression of Patterns and VIM	2143 eyes	52 points in 24-2 SITA SAP tests	progress: 14 follow-ups, 9.1 years	expert grading of serial stereo photos	signifiacnt PoPLR, MD LR, VFI LR slopes	stable vs progressed	AUC: 0.86 for GEM-PoP, 0.82 VIM-Pop	GEM-PoP was significantly more sensitive to PGON

2.5 Detection of Structural Progression

Several methods have been developed for detecting structural progression in glaucoma by objectively and quantitatively measuring the anatomical changes in the eye, particularly the ONH and the RNFL. Comparison of advanced imaging techniques for glaucoma progression, such as OCT, scanning laser polarimetry (SLP), confocal scanning laser ophthalmoscopy (CSLO), etc., have been done previously in Miki (2012). The study found that although precision in the measurement of structure is generally good with imaging techniques, there was no uniform agreement regarding the most appropriate evaluation method. Several studies have shown and argued the usefulness of OCT in glaucoma progression detection due to its ability to visualize the retinal substructure (Geevarghese et al. (2021); Bussel et al. (2014); Abe et al. (2015); Tatham and Medeiros (2017)). This is because of the ability of OCT to focus on the circumpapillary RNFL (cpRNFL) thickness measurements, which are the most widely used parameters in clinical practice. Abe et al. (2015), Tatham and Medeiros (2017) and Kotowski et al. (2011) further reviewed different OCT assessment techniques and found that the SDOCT has more precision and reproducibility of RNFL measurements than other OCT methods, which is quintessential to evaluate glaucoma progression, with consistently high sensitivity in detection. Detection of glaucoma progression using different imaging techniques such as SLP from GDx-VCC software (Dada et al. (2014)), CSLO from Heidelberg Retina Tomograph (HRT) (Maslin et al. (2015)) exist. Still, again, agreement on the methods needed to be found. Although not widely researched, researchers have used fundus photos for glaucoma progression detection and found appreciative results (Medeiros et al. (2021)). These methods highlight various challenges in diagnosing glaucoma progression based on structural changes. These challenges include differentiating between age-related variations and actual glaucomatous changes, a decreased detection rate

in advanced glaucoma (floor effect), high costs of tests, and the need for specialized clinical expertise to operate the equipment. Nevertheless, structural diagnostic methods continue to be extensively researched because they provide detailed information about the RNFL in Optic Discs. In the subsequent sections, we will explore various methods and techniques researchers and clinicians have developed to identify structural changes in glaucoma progression.

2.5.1 Clinical and Conventional Methods

In clinical practice, experts identify glaucoma progression by analyzing changes in stereoscopic optic disc photographs. However, there's often only poor to moderate agreement in assessments between different experts (O'Leary et al. (2010)). Like event and trend-based analysis in visual fields, objective methods have also been used to evaluate glaucoma progression using structural parameters. Similar to VF, GPA can be translated to structural progression by measuring the RNFL test-retest variability with baseline measurements where progression means exceeding a predetermined criterion of this change. Research by Kaushik et al. (2015), which compared GPA using SAP parameters vs GPA using OCT measures, found that OCT detects progression in early glaucoma better but performs poorly in advanced stages with overall RNFL GPA obtaining lower sensitivity than SAP GPA. Because of these inconsistencies and the continuous advancements in OCT technologies, the application of GPA for structural evaluation is rare, and there is limited research in this area.

Trend analysis is another paradigm often explored for evaluating glaucoma progression due to its ease of implementation and ability to track both presence and rate of progression. A study by Lin et al. (2017) showed that cpRNFL rates of change using the PLR are informative of VF loss in glaucoma but not necessarily associated with VF defects. Several other research showed promise for ganglion cell-inner plexiform layer (GCIPL) thinning rates being applicable for objective assessment of

glaucoma progression (Lee et al. (2017); Wu et al. (2020)). Another research comparing trend-based progression analysis (TPA) with RNFL GPA found higher sensitivity for the TPA method - 48.8% vs 27.1% at 84.2% and 81.7% specificities respectively (Yu et al. (2016)). Using global and cluster-wise linear regression, Lee et al. (2011) showed that the localized OCT RNFL thinning rate also indicates progressive loss with high sensitivity (62% at 95% specificity). In other research by Thompson et al. (2021), a poor agreement was found between trend-based and qualitative assessment ($\kappa = 0.0135 - 0.1222$), so the performance of trend methods can be debated. Like functional progression, trend analysis using structure also has the same limitations, requiring longer follow-ups for accurate modeling (Miki (2012)) and is susceptible to age-related loss (Jammal et al. (2020); Leung et al. (2013)), etc.

2.5.2 Probabilistic Methods

Table 2.3 summarizes some methods to detect glaucoma progression using structural parameters using advanced techniques, specifically focusing on structural progression. In the following sections, we will discuss some of these sophisticated methods and draw insights into how structural assessments have shaped glaucoma progression detection.

Regression-based approaches have been studied in detail for predicting progression. A study by Nagesh et al. (2019) utilizing the Continuous Time-Hidden Markov Model (CT-HMM) on a dataset of 135 eyes with SDOCT images showed impressive results predicting future RNFL with a mean absolute error (MAE) of 3.48 vs 4.06 for VFI over 4.9 years follow-up. This method notably surpassed the performance of Linear Regression predictions. In Mohammadzadeh et al. (2021), a Hierarchical Longitudinal Bayesian Regression was applied on 112 eyes for predicting GCC thickness, resulting in a notable negative correlation between slope and baseline ranging from $r = -0.43$ to -0.50 over 2-4.2 year follow-up. In another study, Su et al.

(2023) incorporated spatially varying hierarchical random effects on 111 eyes to predict progression, emphasizing that including visit effects reduced estimation errors. This study demonstrated that the new model obtains an accuracy of 21.4% vs. 18% to detect significant negative slopes over the same follow-up duration with linear regression.

Belghith et al. explored several Bayesian methods to develop classification-based models for glaucoma progression. In a study, Belghith et al. (2014b) utilized the Fuzzy Bayesian Detection Scheme (FBDS) on a training set of 25 eyes and a test set of 117 eyes, achieving a 64% sensitivity at 94% specificity over three years. Belghith et al. (2014a), in another study, showed an improved 70% sensitivity at 94% specificity in its study over 2.2 years, indicating the Bayesian Fuzzy Detection Scheme performs better in shorter follow-ups. The Variational Change Analysis, as used in Belghith et al. (2013) on a dataset of 267 eyes, obtained a sensitivity of 86% at 96% specificity in the yet shorter follow-up of 0.5 years. In another research, Belghith et al. (2015) explored the Bayesian-Kernel Detection Scheme and demonstrated a 78% sensitivity at 94% specificity for non-progressing conditions in its 117-eye dataset over 1.7 years.

Some unsupervised models were also investigated for detecting progression. Yousefi et al. (2015) applied GEM on a large dataset of 2274 eyes with a short five-week follow-up and achieved a sensitivity of 78% at 95% specificity. Meanwhile, Huang et al. (2021) merged GEM with longitudinal slopes on another massive dataset (3485 eyes), reported a 38.6% accuracy, and showed that the ML model generally outperforms linear regression over numerous follow-ups.

The various probabilistic methods detailed in the studies for detecting structural glaucoma progression have demonstrated considerable promise. Many of these methods outperformed traditional linear regression models, showcasing advancements in prediction accuracy, sensitivity, and specificity. Regression and classification tech-

niques achieved impressive results on diverse datasets over varying follow-up durations. These structural assessments are crucial as they offer direct, quantitative insights into glaucoma progression, which can be complementary to functional assessments. While functional assessment remains the clinical gold standard for monitoring glaucoma progression, these probabilistic structural assessment techniques underscore the potential of providing an earlier and possibly more nuanced understanding of disease progression. Combining structural and functional assessments may offer the most comprehensive view of glaucoma progression as technology and algorithms advance.

2.5.3 Machine Learning Techniques

Machine Learning methods have shown significant potential in detecting glaucoma progression through structural assessments. A study by Balasubramanian et al. (2012) used Proper Orthogonal Decomposition (POD) for regression on topographic measurements of HRT II from 246 eyes. This approach could predict progression with high sensitivity and specificity, even for a smaller follow-up. Another study by Christopher et al. (2018), who applied unsupervised learning using PCA combined with Logistic Regression on swept-source OCT (SSOCT) images, showcased impressive AUC results, demonstrating its efficiency in identifying structural progression. Mohammadzadeh et al. (2022) similarly employed a multi-layer perceptron (MLP) classifier on macular OCT Angiography (OCTA) images and showed that it outperforms logistic regression, emphasizing machine learning’s capability in improving progression detection.

Comparatively, machine learning methods learn efficiently from intricate data patterns, allowing for potentially higher predictive accuracy than probabilistic methods. ML methods were found to be more proficient in handling complex datasets and generally required lower follow-up time. Unlike the previously discussed proba-

bilistic methods, which primarily depend on statistical models, ML techniques can easily extract meaningful features from the data. However, a potential limitation might be that they require larger datasets and computational power. While both probabilistic and ML methods offer valuable insights, integrating both could lead to more holistic and accurate detection of glaucomatous progression.

2.5.4 Deep Learning Approaches

Many Deep learning methods have been developed in glaucoma progression detection, particularly in structural assessments. These methods are more intricate than probabilistic and traditional ML models, and their results often exceed the latter in both learning from complex data and accuracy.

CNNs are among the most common choices for researchers to learn spatial representations from data. Mohammadzadeh et al. (2022) implemented a CNN classifier on macular OCTA images from 134 patients taken over four visits (2.4-5.5 years) and achieved an AUC of 0.81 vs 0.66 in logistic regression, a significant performance improvement. Similarly, Mariottoni et al. (2023) applied a CNN with an FC network on cpRNFL thickness from SDOCT from 816 eyes six visits (in 3.5 years) and obtained an impressive 87.3% sensitivity at 86.4% specificity. Mandal et al. (2023) developed a CNN-LSTM model based on SDOCT B-scans from 3253 eyes across five follow-ups, predicting progression with a 48% sensitivity at 95% specificity.

In a more specialized case, DL models have been modified to use structural information uniquely to draw insights and improve accuracy. Medeiros et al. (2021) developed a ResNet50 M2M model that predicted RNFL thickness from fundus photos trained on a dataset with 8831 eyes (6.2 visits in 5.5 years). The subsequent trend-based analysis using the RNFL thickness measure achieved an impressive AUC of 0.86. In another study, Hassan et al. (2020) used a Conditional Generative Adversarial Network (GAN) on macular OCT volume scans to predict future glaucoma

development in OCT scans in 109 eyes. Researchers found that the generative model could obtain better reconstruction on the 3rd visit than on the 2nd one. Hou et al. (2023) implemented a Gated Transformer Networks (GTN) that analyzed RNFL measurements from OCT scans of 4211 eyes and achieved an AUC of 0.97 with the Majority Voting scheme. In another research, Bowd et al. (2021) integrated Deep Learning Autoencoders with cpRNFL thickness map data from the OCT, which was able to identify progression with 90% sensitivity, demonstrating that focusing on specific regions of interest can notably improve predictive accuracy.

DL methods often exhibit superior performance and efficiency in processing large complex datasets compared to probabilistic and ML techniques. Their capacity to extract complex salient features from image datasets is a distinctive advantage. However, a limitation of this method is that it often requires large datasets to generalize and significant computational power to train. Nevertheless, with specialized models like M2M, Conditional GAN, GTN, etc., DL methods can replace conventional glaucoma progression detection practices, potentially minimizing the need for frequent expert evaluations.

2.5.5 Time Series Approaches in Structural Assessment

Advanced algorithms and models are rapidly becoming essential in glaucoma progression detection. For instance, the Gated Transformer Networks (GTN) from Hou et al. (2023) utilizes OCT scans to offer holistic insight into progression, signifying the growing importance of transformer architectures in medical applications. The LSTM approach in Mandal et al. (2023) also stands out by predicting progression using SD-OCT B-scans, highlighting the recurrent model's ability to capture temporal dependencies in ophthalmic data. These sophisticated models underscore the potential of modern DL architectures to provide both timely and accurate glaucoma progression assessments by efficiently processing time-series information.

Table 2.3: A Review of Methods for Detection and Prediction Glaucoma Progression using Structural Assessments

Citation	Setup	Algorithm/ Method	Dataset	Data Type	Follow-up Period	Reference Standard	Baseline Method	Model Output	Outcomes	Summary
Nagesh et al. (2019)	Regression	Cont. Time - Hidden Markov Model	135 eyes	SDOCT Images and Avg RNFL Thickness	7.9 visits, 4.9 years	VFI Progression	Linear Regression Predictions	Change in RNFL Thickness Maps and VFI State	3.48 MAE RNFL and 4.06 MAE VFI	OCT CT-HMM significantly outperforms LR and Avg RNFL CT-HMM
Asaoka et al. (2021)	Regression	Latent Space LR - Deep Learning	Cross-Sectional: 746 eyes, Longitudinal: Train 998 eyes, Test 148 eyes	OCT Image data: GCC thickness, macular RNFL, OS+RPE	8 VF tests, 5.6 OCT tests, 5.9 years	RMSE and Significant Slopes in LMM	MLR, SVM, DL, CNN-TR, PLR, DLLR	68 points in HFA 10-2 test, 52 points in HFA 24-2 test	RMSE cross-section 6.4dB, longitudinal 4.4dB and 3.7dB	LSLR-DL predicts both cross-sectional and longitudinal VF

Medeiros et al. (2021)	Regression	ResNet50 (M2M model)	8831 eyes (Test: 1147 eyes)	Color Fundus, SDOCT RNFL thickness	6.2 visits, 5.5 years	statistical significant negative slopes	-	SDOCT global RNFL measurements, rate of change in RNFL thickness	AUROC 0.86 for predicting progressors	M2M predicts RNFL thickness and can monitor progression
Balasubramanian et al. (2012)	Regression	Proper Orthogonal Decomposition	246 eyes	Topographic measurements of HRT II	4 follow-ups, 4.1 years	SAP GPA or stereophoto assessment	Topographic Component Analysis significant change	Progression: follow-ups observed positive rate greater than OPR	100%, 78%, 78% sensitivity, 0%, 86%, 86% specificity	POD with k-family-wise error rate reduces number of follow-ups to predict progression
Mohammadzadeh et al. (2021)	Regression	Hierarchical Longitudinal Bayesian Regression	112 eyes	GCC thickness from Macular OCT Scans	4 tests, 2-4.2 years	significant negative slope at Bayesian $p < 0.025$	-	GCC thickness estimates, macular slopes	Negative correlation between slope and baseline: -0.43 to -0.50	Bayesian method is efficient method for estimating macular rates
Su et al. (2023)	Regression	Spatially Varying Hierarchical Random Effects	111 eyes	GCC thickness from Macular OCT Scans	4 tests, 2-4.2 years	significant slope when 95% CI is less or greater than 0	Simple Linear Regression	GCC thickness estimates, macular slopes	21.4% vs 18% significance negative slopes	Including visit effects reduces estimation errors

Belghith et al. (2014b)	Classification	Fuzzy Bayesian Detection Scheme	Train - 25 eyes, Test - 117 eyes	3D SD-OCT Images	3 tests, 3 years	stereo photograph grading and VF GPA	RNFL-SVM and RNFL-ANN	Progressing vs Non-progressing	64% Sensitivity at 94% Specificity	FBDS using image features outperforms ANN and SVM using RNFL classifiers
Belghith et al. (2014a)	Classification	Bayesian Fuzzy Detection Scheme	117 eyes	3D SDOCT voxel images	2 follow-ups, 2.2 years	EMGT Criteria and Progression in stereophoto	RNFL-SVM, RNFL-ANN, MRF	progressor or non-progressor	70% sensitivity at 94% specificity	BFDS has higher diagnostic accuracy
Belghith et al. (2013)	Classification	Variational Change Analysis with Markovian-a-priori	267 eyes	Heidelberg Retina Tomograph (HRT II)	4 follow-ups, 0.5 years	progressing by stereophoto or VF change	Topographic CA, VCA	progressing vs non-progressing	86% sensitivity, 96% specificity	Detection formulated as missing data problem. VCA-MA outperforms other methods
Li et al. (2022a)	Classification	DiagnoseNet and PredictNet	3003 train, 422 valid, 337 test for progression	Color Fundus Photographs	34.8-41.7 months	3 VF points worse than 5% baseline in 2 consecutive test	-	progressing vs non-progressing	82% Sensitivity at 59% Specificity	DL model useful in early detection of glaucoma progression

Belghith et al. (2015)	Classification	Bayesian-Kernel Detection Scheme (BFDS)	117 eyes	3D SDOCT volume scans	2.21 tests, 1.7 years	Longitudinal VF testing, stereophoto assessment	RNFL-SVM, RNFL-ANN, KDS, GBKDS, RBF-BKDS	progressing vs non-progressing	78% Sensitivity, 94% Specificity for non-progressing	BKDS outperforms other methods, Only healthy and non-progressing eyes can produce high accuracy
Mariotoni et al. (2023)	Classification	CNN and FC Model	692 stable, 124 progressing eyes	RNFL thickness peripapillary SDOCT	16.2 tests, 6 visits, 3.5 years	Clinical judgements on longitudinal SDOCT reports	trend-based analysis	progressing vs non-progressing	87.3% sensitivity, 86.4% specificity	DL model agreed with experts, provided likely location of change
Mohammadzadeh et al. (2022)	Classification	CNN and MLP classifiers	134 patients	macular OCTA images	4 visits, 2.4-5.5 years	significant negative MD slope	Logistic Regression	progressing vs non-progressing	AUC: 0.81 DL vs 0.66 with LR	DL could extract and enhance progression detection

Hou et al. (2023)	Classification	Gated Transformer Networks (GTN)	4211 eyes (2666 patients)	OCT scans	5 tests, 1.2 - 4.7 years	significant negative slopes in SAP trend-based methods, SAP GPA	LMM, naive Bayes Classifiers	progressing vs non-progressing	AUC: 0.97 with Majority Voting (M6)	GTN outperforms conventional methods; Ensemble methods improve performance
Mandal et al. (2023)	Classification	CNN-LSTM Classifier	3253 eyes	SD-OCT B-scans	5 follow-ups, 3.1 years	-	OLSLR on global mean RNFL thickness	progressing vs non-progressing	48% sensitivity at 95% specificity	DL model identifies structural progression from age-related changes without reference standard
Hassan et al. (2020)	Generative	Conditional GAN: 3DCNN, UNet, PatchGAN	109 eyes	macular OCT volume scan	4 tests, 6 months apart	-	-	OCT Macular Volume Scan, SSIM, PSNR	0.8325 SSIM with 3 visits, 0.8336 with 2	GAN can predict future glaucoma development in OCT scans

Bowd et al. (2021)	Unsupervised	DL Autoencoders	44 progressing, 303 non-progressing, 109 healthy eyes	cpRNFL thickness maps from OCT	4 visits, 2.9 years	significant LMM slope for Region of Interest cpRNFL	global slopes from LMM	Progressing: significant LMM slopes	90% sensitivity, progression slope -1.28 $\mu\text{m}/\text{y}$	ROI from DL-AE can boost progression accuracy
Christopher et al. (2018)	Unsupervised	Principle Component Analysis with Logistic Regression	179 eyes	SSOCT images	7-8.7 tests, 1.7-2.2 years	significant negative slope	LR with cpRNFL, SAP MD, FDT MD	progressing vs non-progressing	AUC: 0.95 for RNFL PCA	Computational method can identify structural progression
Yousefi et al. (2015)	Unsupervised	Gaussian Mixture Model (GEM)	2274 eyes	RNFL Thickness from SD-OCT	5 tests, 5 weeks	event-based SAP GPA	Linear regression	progressing vs non-progressing	78% sensitivity, 95% specificity	GEM predicts RNFL patterns for glaucoma progression
Huang et al. (2021)	Unsupervised	GEM + Longitudinal Slopes	3485 eyes	RNFL thickness maps from OCT scans	9 follow-ups	statistical significant negative slopes	Linear Regression	stable vs progressed	38.6% accuracy with ML model	ML model predicts progression better than LR

2.6 Structure-Function Relationship in Glaucoma Progression Detection

2.6.1 *Clinical Methods for the Assessment of Glaucoma Progression Using Structure and Function*

As discussed previously, several studies indicated that OCT is more sensitive than VF in the early stages of glaucoma progression detection, but this sensitivity decreases as progression advances (Zhang et al. (2017); Abe et al. (2016)). Some research (Swaminathan et al. (2021); Gracitelli et al. (2015a)) exploring the effect of progressive RNFL loss found an association with loss in visual fields. Similar conclusions were drawn from studies where changes in macular thickness were used to find an association with central visual field loss (Mohammadzadeh et al. (2020)). Another research by Suda et al. (2018) found an appreciative correlation ($R=0.589$) between SAP and OCT results for glaucoma progression. In a more novel approach, both the structure and function were used to obtain rates of change of RGC count as indicators for neural damage in glaucoma progression, paving the way for combined structure-function index (Medeiros et al. (2012d); Hirooka et al. (2016); Wu and Medeiros (2021)). A survey by Lisboa et al. (2013), which analyzed several studies in the same field, found that a combined approach is more effective in detecting glaucoma progression even though there can be disagreements between detection using structural or functional measures alone. Gardiner et al. (2012) further found that even though the structure-function is still affected by inter-test variability, it is still feasible to combine them for progression assessment.

2.6.2 *Sophisticated Methods to Detect Glaucoma Progression Using Combined Structure and Function*

Studies in probabilistic methods for glaucoma progression detection using combined structure-function demonstrated improved predictive accuracy in general (Table 2.4).

Medeiros et al. (2011), showed in their research using the Bayesian Hierarchical Model on 434 glaucoma-suspected eyes that probabilistic methods obtain higher sensitivity with VFI and temporal, superior, nasal, inferior, and temporal (TSNIT) RNFL averages than traditional OLS regression standards. Similar results were also seen in Medeiros et al. (2012a), which used the Bayesian Joint Regression Model and applied to 242 eyes, which outperformed the OLS linear regression in predicting MD and rim area (RA) from SAP and CSLO data. In another study, Russell et al. (2012) implemented Bayesian Linear Regression on 179 eyes, which indicated higher performance for short time series, but traditional OLSLR was more accurate for longer follow-ups when analyzing VF. Overall, Bayesian methods have shown superior performance, though the input data type and follow-up time might influence detection accuracy for progression.

Following the studies on probabilistic methods, researchers have focused on developing innovative statistical methods for detecting glaucoma progression, leveraging both structural and functional indicators. In research by Bilonick et al. (2008), Latent Class Regression was developed, which was able to identify accurately baseline RNFL characteristics that indicate progression. Meanwhile, the study by Hu et al. (2014) employed a Dynamic Structure-Function (DSF) model, which demonstrated an improved performance over the conventional OLS regression, especially in shorter follow-ups. Drawing insights from glaucoma suspects, a study by Meira-Freitas et al. (2013) showed the advantages of the Joint Longitudinal Survival Model (JLSM) with RGC Estimation, which outperformed estimation with structure or function measurements alone. Medeiros et al. (2014), analyzing 492 eyes, reiterated this by linking progressive RA loss conclusively to VF loss, combining JLSM with RA and VF to predict progression. Further, Zhalechian et al. (2022) in their study with a Kalman Filter Estimator for estimating future MD with RNFL measures indicated that global RNFL just marginally enhanced MD predictions as compared to utilizing

MD by itself, showing confounding results.

These statistical methods illustrate that a holistic, combined structural and functional analysis is paramount for accurate detection of glaucoma progression. Time-series forecasting methods, such as the DSF model, showed the importance of shorter follow-up for detection and were helpful in frequent monitoring. However, when compared with the probabilistic Bayesian approaches, these methods, while promising, do show that the Bayesian techniques often have better sensitivity. Thus, it is essential to choose an appropriate model in clinical settings to detect progression based on the type of data and how long the patient has been monitored.

2.6.3 Artificial Intelligence Utilising Combined Structure and Function Relationship to Evaluate Glaucoma Progression

Machine learning techniques, especially when they combine both structural and functional data, have shown better results in identifying glaucoma progression. In classification methods, Nouri-Mahdavi et al. (2021) research used an Elastic net logistic regression and ML classifier to achieve AUCs between 0.79 and 0.81, suggesting an improvement of predictive power using baseline and longitudinal structural data on visual field (VF) progression. This was reflected by multiple studies notably Bowd et al. (2012) using Relevance Vector Machine, Yousefi et al. (2013) implementing a multitude of classifiers (including Bayesian Net and Lazy K Star), and Lee et al. (2020) employing Random Forest and Extra Trees, where all emphasized the significant role of RNFL measurements and baseline parameters for detecting progression. Notably, the study by Kamalipour et al. (2023) showed an impressive AUC of 0.89 by integrating OCT and OCTA features via a Gradient Boosting Classifier, demonstrating its efficacy in forecasting clinical VF progression.

On the other hand, regression methods by Lee et al. (2022) using Random Forest to measure the rate of change in RNFL thickness against baseline emphasized how

such models improve the predictive accuracy of baseline ONH characteristics. While the outcomes are varied, Random Forest, Gradient Boosting, and Elastic Net methods tend to produce superior performance, often surpassing traditional regression and decision trees. It is crucial to note that these studies used diverse data types, from cpRNFL and GCIPL thickness to OCT scans and VF parameters, allowing for nuanced analysis. While these methods were shown to be great at identifying complex patterns in the data, there's still a worry that they might overfit smaller datasets. Therefore, while ML methods provide a holistic view, a balance between model complexity and data characteristics is essential for optimal results.

Deep Learning techniques, being able to learn from complex data, provide advanced modeling capacity, especially when leveraging both structure and function. A study by Sedai et al. (2020) used a 3DCNN with traditional ML forecasting techniques, primarily utilizing cpRNFL from OCT, age, and 24-2 VF tests as input, which obtained the lowest MAE across healthy, suspect, and glaucoma subjects, showcasing the method's reliability in real-world applications. Lee et al. (2021) in their research introduced an innovative Machine to Machine (M2M) method paired with JLSM, which used Color Fundus and SDOCT RNFL thickness data to detect longitudinal changes, showed this method can distinguish between converter and non-converter groups in glaucoma. In a notable multimodal approach, Pham et al. (2023) combined ResNET50 and LSTM to forecast future VF points using the 30-2 VF HFA SITA and RNFL thickness map to demonstrate its predictive accuracy in noisy data environments. Among these, the incorporation of time-series data, as seen in LSTMs, highlights a paradigm shift towards capturing sequential data and temporal dependencies, improving prediction accuracy. However, while DL methods have shown superior predictive capabilities, the need for larger datasets for generalization and computational power for training is a significant drawback. Moreover, DL, being a black-box model, cannot provide interpretable results, especially in clinical settings

where understanding model decisions is crucial.

Elaborating on the DL methods, techniques like 3DCNNs, M2M methods, and complex architectures like ResNET50 with LSTM have been adopted efficiently to detect glaucoma progression. These models utilize large datasets to extract intricate patterns from both structural and functional data to produce improved performance. In comparison, traditional ML models, like Random Forest and Gradient Boosting, although sophisticated, often require a certain degree of manual feature extraction and may not capture intricacies as effectively as DL models. When compared with probabilistic and purely statistical models, such as PLR methods or linear regressions, both machine and deep learning offer superior predictive capabilities than the former. However, probabilistic and statistical methods provide interpretable results and a clear insight into data dynamics, often making them preferred choices for direct interpretability and better understanding of the data.

Table 2.4: A Review of Methods for Detection and Prediction Glaucoma Progression using both Structure and Function

Citation	Setup	Algorithm/ Method	Dataset	Data Type	Follow-up Period	Reference Standard	Baseline Method	Model Output	Outcomes	Summary
Bilonick et al. (2008)	Regression	Latent Class Regression	106 eyes	MD, PSD, AGIS score, VFI, RNFL	5 tests, 5 years	significant negative slope ($p < 0.05$)	-	LCR Model slope, AIC	2494.8 AIC	Baseline RNFL was indicative of progression
Medeiros et al. (2011)	Regression	Bayesian Hierarchical Model	434 eyes - glaucoma and suspect	VFI from SAP, GDx TSNIT average from Optic Disc Stereophotographs, Scanning Laser Polarimetry	3 reliable tests, 4.2 years	OLS regression slope of VFI, observer disagreement of stereophotograph change	OLS regression slopes on VFI and TSNIT with $p < 0.05$	Bayesian slopes of change for VFI and TSNIT	22.7% vs 12.8% using VFI, 74% vs 37% with optic disc at 100% specificity	Bayesian method obtains significantly higher sensitivity for progression with VFI and TSNIT 100% specificity

Hu et al. (2014)	Regression	Dynamic Structure-Function Model	220 eyes from DIGS and ADAGES	MS from 24-2 SAP Tests and Rim Area from scanning laser ophthalmoscopy	3 follow-ups, 8.4 years	Glaucoma Criteria based on ADAGES	OLS regression slopes	Prediction in future visits and MSE	Lower MSE 70% eyes at visit 4 and 60% for 5,6,7	DSF outperforms OLS in shorter intervals
Medeiros et al. (2012a)	Regression	Bayesian Joint Regression Model	242 eyes - glaucoma	MD from SAP Test, RA from CSLO	4 follow-ups, 6.4 years	PSD <0.05 in SAP tests wrt Baseline and reproducible at least once	OLS linear regression slopes with MD and RA	Bayesian regression slopes of change with MD and RA	5.13 vs 11.2 MSE predicting MD and 0.016 vs 0.027 MSE predicting RA	Bayesian method outperforms OLS
Meira-Freitas et al. (2013)	Regression	Joint Longitudinal Survival Model (JLSM) with RGC Estimation	288 glaucoma suspect eyes	Avg RNFL from OCT and MD from SAP	4 follow-up, 3.8 years	Significant Slopes from JLSM	Isolated Structure or Function Measurements	Combined Structue Function Index, RGC Estimates	-18,987 cells/y progressors, -8,808 cells/y non progressors	Joint Longitudinal Esitmates better than Structure or Function alone

Russell et al. (2012)	Regression	Bayesian Linear Regression	179 eyes	MS from 24-2 VF tests, RA from CLST HRT	8 follow-ups, 5.8 years	Significant negative slope ($p < 0.05$)	OLSLR	Rate of change in MS	RMSE 0.14dB smaller than OLSLR	BLR with MS and RA outperforms OLSLR for short time series, OLSLR more accurate for long time series with only VF
Sedai et al. (2020)	Regression	3D CNN + ML Forecasting	Train: 859 subjects, Test: 230 subjects	cpRNFL from OCT, age, IOP, 24-2 VF tests	3 visits, 3.65 years	Glaucoma (2 consecutive test ONL) and abnormal ONH	Linear Trend Based Estimation	RNFL Global and Sectoral Means	MAE: 1.10, 1.79, 1.87 for healthy, suspect and glaucoma	Model consistent across suspect and glaucoma subjects
Medeiros et al. (2014)	Regression	JLSM with RA and VF	492 eyes suspect	RA from CSLO, SAP 24-2 VF, IOP	5 CSLO tests, 2 years	3 consecutive abnormal VF tests with PSD ($p < 0.05$)	-	RA loss rate, Survival adapted R2, proportion of treatment effect (PTE)	R2 62% univariate model, 81% multivariate, PTE 65%	Progressive RA loss predictive of VF loss

Lee et al. (2021)	Regression	Machine to Machine (M2M) with JLSM	1072 eyes	Color Fundus, SDOCT RNFL thickness, 24-2 SAP tests	4.2 fundus tests, 9.6 VF tests, 5.9 years	2 consecutive abnormal VF (PSD with $p < 0.05$)	-	progres- sion: sig- nificant slopes from M2M pre- dictions	-1.02 um/y vs -0.67um/y between converter and non- converter	Longi- tudinal changes from DL can predict progression
Pham et al. (2023)	Regression	ResNET50 and LSTM	Train: 266 eyes, Test: 99 eyes	30-2 VF HFA SITA tests, RNFL map from cirrus OCT tests	Train: 5.7 visits, 5 years; Test: 2.3 visits, 3.3 years	-	-	Future VF points	MAE 3.31, RMSE 4.58	VF and OCT data improves predictive performance, model is useful with noisy data
Zhalechian et al. (2022)	Regression	Kalman Filter Estimator	362 sub- jects	demo- graph- ics, IOP, VF MD, VF PSD, global RN- FLT	10.6, 19.9, 11.7 follow-ups, 13.6, 12.1, 5.7 years	-	OLS Linear Regression	future MD, PSD and RNFL val- ues	Predictive accuracy: 73.5% vs 58% with LR	global RNFL min- imally im- proved MD prediction than with MD alone

Lee et al. (2022)	Regression	Random Forest	712 eyes with OAG	demographics, IOP, LCCI, peripapillary CT, global RNFLT, VF MD, PSD, AXL, CCT	5.3-11.5 years	-	Regression and Decision Trees	Rate of change in RNFL Thickness wrt Baseline	MAE: 0.075, 0.115, 0.128 for RF, LR, DT	baseline ONH characteristics predict risk of faster progression
Yousefi et al. (2013)	Classification	ML Classifiers: Bayesian Net, Lazy K Star, Meta Classifiers, AD Tree, CART	107 eyes - progressing, 72 - stable	52 + MD + PSD VF SAP Points, Global + Sectoral OCT RNFL Thickness	4.3 follow-ups, 2.2 years	PGON criteria + GPA	-	progressed vs non-progressed	0.88 AUC for Random Forest with RNFL and SAP; 0.88 AUC for Lazy K Star with only RNFL	RNFL measurements provide more discriminating power
Lee et al. (2020)	Classification	Random Forest and Extra Trees	Train: 110 eyes, Test: 45 eyes	IOP, CCT, 30-2 SAP VF tests, mGCIL thickness, cpRNFL thickness HDOCT	6.2 follow-ups, 3.39 years	event based GPA	Linear Regression Slopes	progressing vs non-progressing	0.881 AUC for Extra Trees, 0.811 AUC for Random Forest	ML Classifiers can predict progression effectively in young myopic patients

Nouri-Mahdavi et al. (2021)	Classification	Elastic Net Logistic Regression, MLC	104 eyes	cpRNFL, GCIPL thickness from Macular SD-OCT	5 tests, 3years	PLR deterioration on 24-2 SAP tests <-1dB/yr, p<0.01	PLR Method	progressing vs non-progressing	AUC 0.79 with ENR, 0.81 with ML	VF progression can be predicted from baseline and longitudinal structural data
Bowd et al. (2012)	Classification	Relevance Vector Machine (RVM)	264 eyes (10 fold CV)	117 CSLO points from HRT II and 52 SAP points from 24-1 SITA HFA II	5.35 years	SAP GPA or stereo-photo assessment	Glaucoma Probability Score	progressing vs non-progressing	AUC: 0.640, 0.762, 0.805 using CSLO, SAP, combined parameters	RVM with baseline parameters predicts future progression
Kamalipour et al. (2023)	Classification	Gradient Boosting (GB) Classifier	110 eyes	OCT scans, OCTA scans	3 follow-ups, 4.1 years	SAP GPA, - significant negative slope of VF MD, PPLR event	-	progressing vs non-progressing	AUC 0.89 with both OCT and OCTA features	ML with OCT and OCTA predicts clinical VF progression

2.7 Glaucoma Progression Detection with EHR and Clinical Data

Deep learning has also been successfully applied to detect glaucoma progression using structured clinical data and text notes from Electronic Health Records (EHR). These techniques offer a paradigm shift from traditional uses of deep learning methods using structure or functional progression characteristics and have been shown to predict progression accurately. Research by Wang and Stein (2023) and Baxter et al. (2019) explores several machine learning classifiers using EHR data to predict if the data is indicative of progressive characteristics and if the patient needs surgery. The models obtained a moderate AUC of 0.623-0.673 on the test sets, suggesting further research is required during inference, especially for different demographics. Another research Tao et al. (2023) by the same group studied survival-based AI algorithms to predict if a patient is showing characteristics of glaucomatous progression to surgery. They showed that using more complex algorithms such as DeepSurv (DL method) has a better predictive AUC of 0.802 due to its ability to capture information from high-dimensional data. The addition of clinical text notes with EHR data has also boosted the performance of deep learning models in classifying whether patients undergoing surgeries show signs of progression, obtaining an AUC of 0.873 (Jalamangala Shivananjaiah et al. (2023)). Exploring the utility of DL methods to predict progression from unstructured data, a Natural Language Processing (NLP) based DL algorithm was developed to predict progression from free-text clinical notes (Wang et al. (2022)). Although a combination of free text and EHR data obtained a higher AUC of 0.73 in the NLP model, only free-text data also had an appreciative AUC of 0.70. Making the DL model more complex has been shown to enhance its accuracy. For example, research by Hu and Wang (2022) demonstrated this by using BERT-based models on clinical notes obtained from ophthalmologists. This approach predicted which patients might need glaucoma surgery with a reliability

score, AUC of 0.734. Although the performance was not better than DL methods with just structured EHR data, this research showed the potential of using massive pre-trained models to predict progression using free text notes, which are abundantly available.

2.8 Conclusion

In this chapter, we have seen various models and algorithms using different modalities or combinations of modalities to detect, predict, and forecast glaucoma progression from longitudinal data. We observed various advantages of using complex techniques, trade-offs between structure and function, and challenges in the modeling of medical data. Identifying a holistic method for predicting glaucoma progression with a reliable reference standard is found to be quintessential. In addition, trade-offs between structural and functional assessment for progression suggest the need for a precise, reproducible, and comprehensive feature set that can accurately represent glaucomatous characteristics with the ability to detect and separate age-related variability. Obtaining longitudinal image data can be time-consuming and expensive, which adds another layer of constraints to the model development. However, with the advent of complex models such as deep learning, the availability of computational resources and data from large cohorts can be used to make powerful models that can predict glaucoma progression accurately and with minimal clinical expertise. In subsequent chapters, we introduce and formulate novel deep-learning strategies for detecting glaucoma progression within a longitudinal cohort characterized by data ambiguity, leveraging anatomical information of progression characteristics.

Methodology

3.1 Dataset Overview

The study, acquisition and documentation of the dataset in this chapter was carried in collaboration with Alessandro A. Jammal, MD, PhD and Felipe A. Medeiros, MD, PhD.

3.1.1 Duke Ophthalmic Registry

The data set used in this study is obtained from the Duke Ophthalmic Registry (DOR), currently the largest single Institution clinical database for ophthalmic records in the world. The database contains several millions of clinical and imaging data for patients with eye diseases. Taking over three decades of routine follow-up in a multi-ethnic and culturally diverse group of people in central-eastern North Carolina, the database has been used for multiple AI studies by researchers at the Duke Eye Center at Duke University. The DOR database is an extension of the Duke Glaucoma Registry (DGR) (Jammal et al. (2021)) by the Vision, Imaging, and Performance (VIP) laboratory at the Duke Eye Center whose main aim was to aggregate a large population and create an accessible pool of 'real-world' clinical information database of glaucoma. The DOR contains patient eye disease information collected at the main eye center and six satellite eye clinics of the Duke University Health Clinics (DUHS), boasting over 485,339 patient data undergoing routine ophthalmic care. Advanced imaging data stored in the DOR is one of the largest sources of longitudinal studies in glaucoma progression and has been the foundation of many researches involving AI and DL applications in evaluating glaucoma progression.

The DOR is an amalgamation of comprehensive health information of the patients undergoing ophthalmic care. It consists of demographic data (age, sex, location, etc.), medical history, clinical diagnosis and encounters, lab test results, and complete ophthalmic examination acquired over several visits of Medical Eye Care of each patient. The ophthalmic examination contains critical clinical and imaging data used in ophthalmic care, such as IOP, visual acuity (VA), fundus photographs, SDOCT scans, and SAP tests. Data hierarchies managed by the DOR were extracted using the Duke Enterprise Data Unified Content Explorer (DEDUCE). This web-based query tool efficiently searches patient Care information compiled using EHR. A protected Analytics Computing Environment (PACE), a virtual network space for data analysis, adds another layer of protection by de-identifying or masking patient data during research, in adherence with the standard of ethics in academic research. A de-identified population characteristics data from the DOR is provided in the following section.

3.1.2 Population Characteristics

The DOR is a growing retrospective database of all available electronic health records from patients' visits at the Duke Eye Center and its satellite clinics undergoing medical care. A wide array of clinical data from diverse populations was collected using relaxed inclusion criteria approved by the Duke Institutional Review Board (IRB). The DOR represents an unbiased sample of the population with demographic characteristics similar to the population of North Carolina U.S. Census Bureau. (2022). This can be seen by comparing the population from DOR and the US Census Bureau, which shows racial and ethnic similarity. For example, 20.7% of the population self-reported as Black or African American in DOR vs. 22.2% in US Census, 64.3% were White or Caucasian vs. 69.9% in US Census and 3.5% Asian vs. 3.6% in US Census, with a majority of the population being non-Hispanic or Latino

(Figure 3.1).

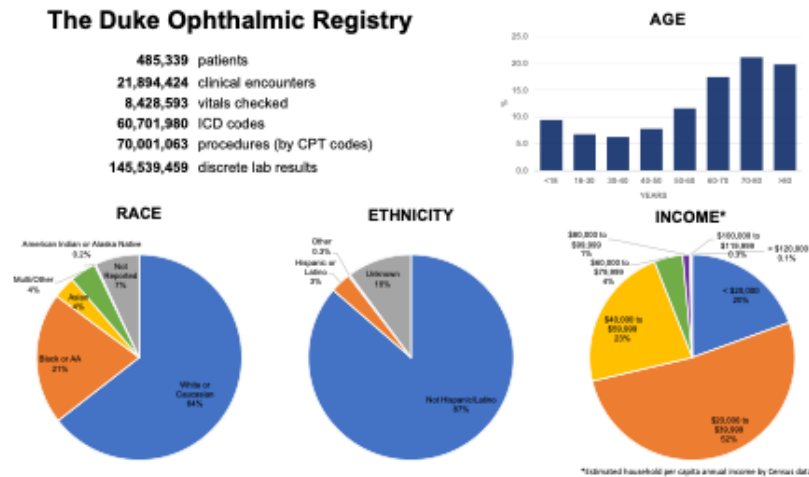


FIGURE 3.1: Demographic Characteristics of patients in the Duke Ophthalmic Registry.

Aimed to provide better care for improved eye health and vision quality of life, the DOR has a collection of rich samples of common and rare eye diseases. Analyzing the significant health aspects, 77,516 subjects in the database have or are suspected of glaucoma diagnosis, 24,431 subjects have age-related macular degeneration (AMD), and 20,692 subjects have diabetic retinopathy (DR) - the top three causes of irreversible blindness (Figure 3.2). The database also includes information on more than 111,170 cataract surgeries, one of the most common surgical procedures worldwide, and a wide array of rare eye diseases affecting select vulnerable populations and diseases with a risk of blindness and eye disease progression. This makes DOR one of the most unique and critical sources of ophthalmic data for clinicians, especially at Duke Eye Center, for developing innovative data-centric solutions for eye care. In this research, we will use data from the DOR database to study and establish DL algorithms for glaucoma progression with implications for improving the vision quality of life.

Major causes of irreversible blindness

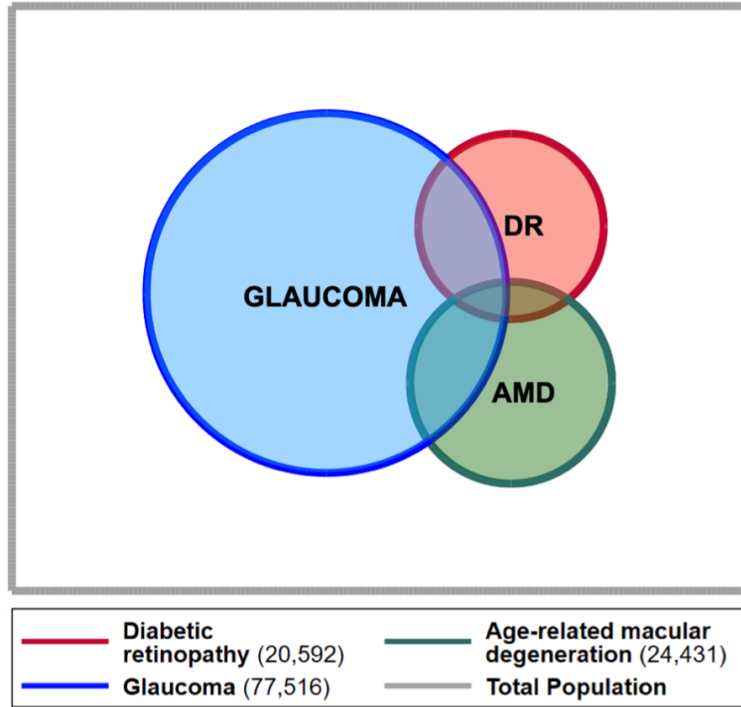


FIGURE 3.2: Comparison of top three causes of irreversible blindness in the DOR database.

3.2 Experiment Design and Setup

Building on previous research, we describe our study design as a longitudinal retrospective cohort study. Specifically, we develop innovative DL models to discern progression patterns in glaucomatous eyes. The data for this study is derived from the DOR database, organized as longitudinal sequential data for each eye across all the patients involved. Structural assessment is used to define the input features for the DL models. This is because advanced imaging techniques in structural assessment have been shown to effectively capture important anatomical features of the eye, such as RNFL and ONH, which are indicative of progressive changes. This approach is favored as it offers a more precise and reproducible dataset for DL, thereby minimizing the possibility of errors. Since the ultimate objective of this research is

to improve the visual quality of life, we use functional outcomes as the benchmark to assess the performance of the solutions derived from our study.

3.2.1 Input Features for the Model: Longitudinal SDOCT Scans

Longitudinal scans of the retina, specifically around the ONH, obtained from the Spectralis SDOCT (Heidelberg Engineering, Heidelberg, Germany) as part of standard clinical care are used as the primary input for the study. The Spectralis OCT is an advanced imaging system that combines CSLO from Heidelberg Retina Angiography with the dual beam SDOCT to obtain micrometer accurate representation of RNFL, GCIPL, Bruch's membrane (BM), and other layers that form the RGC in the ONH (Leite et al. (2011)). Spectralis OCT uses a real-time eye-tracking mechanism to adjust for eye movements and Ensure consistent retina scanning during the visit. It generates a set of different scans with a peripapillary circular scanning pattern of diameter 3.5mm around the ONH, a gold standard scan pattern for detecting structural glaucomatous damage in the RNFL (Chen (2009)). These scans include Amplitude-scans (A-scans) - one-dimensional, depth-resolved reflection profiles of the tissue across the ONH, B-scans - two-dimensional cross-sectional images of the tissue by combining multiple A-scans, 3D Volume scans - combining consecutive B-scans, infrared (IR) photograph of the optic disc, cpRNFL thickness pie chart and cpRNFL thickness profile (Figure 3.3) along with various secondary data (Zembarain et al. (2020)).

For relevance, 2D SDOCT B-scan images were used as the input features for the model due to their high precision and reproducibility to capture the complete RNFL profile characteristics in a micrometer scale (Sampani et al. (2020)). The study included B-scan images for each patient's eyes with scan rates of 768 and 1536 A-scan points, and all resized to 768 x 496 points using bilinear interpolation. The global RNFL mean thickness for each scan was also recorded from the OCT report to de-

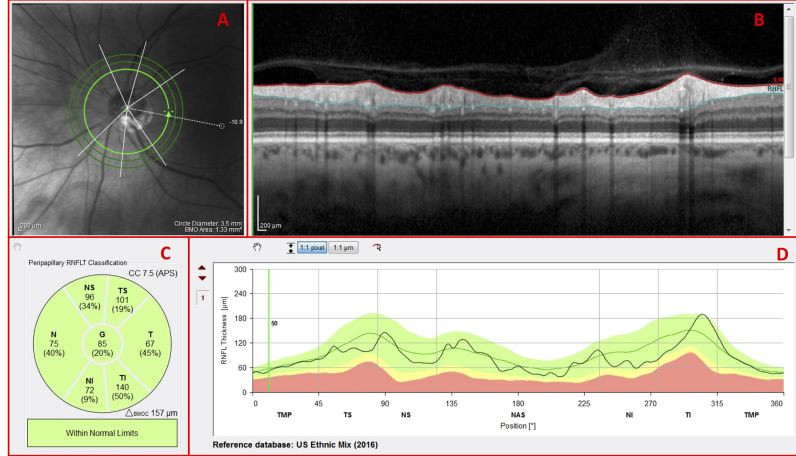


FIGURE 3.3: An SDOCT report of a normal eye showing (A) infrared projection of disc, (B) circular B-scan, (C) cpRNFL pie chart and (D) cpRNFL thickness profile obtained from Spectralis (Heidelberg Engineering, Heidelberg, Germany) (Zemborain et al. (2020)).

velop baseline models. Scans with segmentation or artifact errors were discarded. Scan quality scores less than 15 were also excluded according to the manufacturer’s recommendations. This process was repeated for all eyes across patient visits, obtaining a sequence of multiple OCT scans spaced over a follow-up period (Figure 3.4).

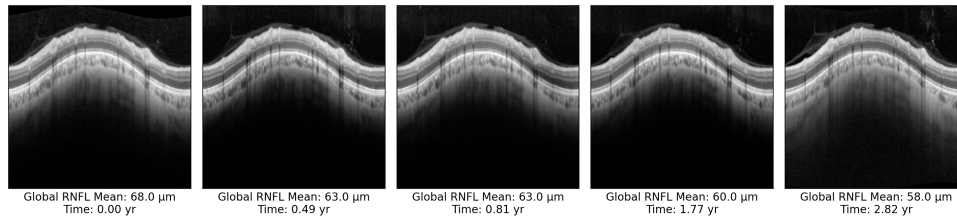


FIGURE 3.4: A longitudinal sequence of SDOCT B-scan images used as DL model input (resized to 224×224 pixels).

3.2.2 Reference Standard: Guided Progression Analysis

Glaucoma progression assessment can be a complex and nuanced process whose understanding is often challenging to non-experts. The intricate nature of the disease and its subtle manifestations make it essential to create an objective and simplified

method to communicate its progression effectively. A clear and analytical reference is not just beneficial for clinicians but also helpful in explaining patients and stakeholders who are unfamiliar with glaucoma. This underscores a need for an analytical approach to detect progression by tracking deterioration in vision quality of life. Therefore we use Visual Field Guided Progression Analysis (GPA) on SAP tests from the Humphrey Field Analyzer (Carl Zeiss Meditec, Inc., Dublin, CA) as a reference standard due to its ability to detect or predict glaucoma progression in a structured way and overcomes uncertainty.

GPA is a point-wise event-based analysis in which every point in the new VF test is compared with the values from two baseline tests. Points on the VF tests are flagged with (statistically) significant loss of sensitivity ($p < 0.05$) or "events" when the measured point-wise pattern deviation becomes greater than a predefined expected variability (derived from repeated tests from a population of stable glaucoma patients). The GPA algorithm then marks the points based on the number of times the "events" repeat at the same location in consecutive tests as:

- **Empty Triangles:** Locations with a significant change ($p < 0.05$) from baseline observed once.
- **Half Triangles:** VF loss change at that point is confirmed with a second test.
- **Solid Triangles:** Significant change at the same point is reconfirmed with a third VF test.

All the flagged points are locations where the GPA algorithm identifies a potential disease progression. If GPA observed changes at three or more points (at least two solid triangles) in two consecutive follow-up tests, the eye is labeled as "*possible progression*,". If changes in these points (at least three solid triangles) are repeated in three consecutive tests, the eye is marked as "*likely progression*" (Vianna and

Chauhan (2015)). This makes GPA a reliable qualitative measure that is relatively simple to implement and accounts for variability associated with VF location, threshold sensitivity, and patient age (Hood et al. (2022); Giraud et al. (2010)). Besides events, the GPA can also report statistical parameters (probability plots), which can help understand the significance of the changes (Figure 3.5).

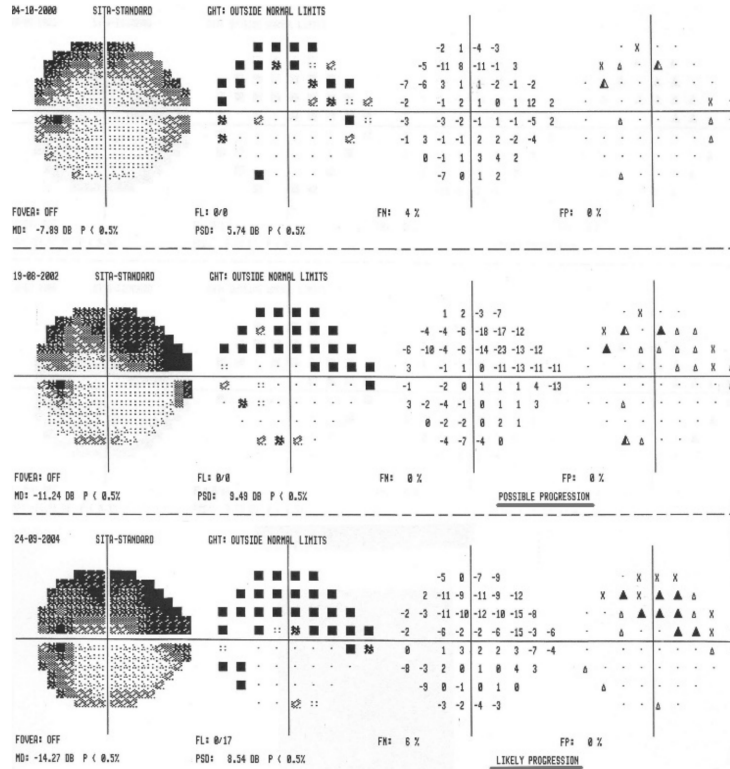


FIGURE 3.5: A GPA report representing different progression events: no-progression, possible progression and likely progression (top to bottom) (Diaz-Aleman et al. (2009)).

GPA’s method to directly contrast follow-up results with a stable baseline helps reduce test-retest variability and provides a better estimate of progression. Moreover, a standardized approach such as GPA ensures consistency, making it easier to compare results across different settings. For simplicity, we formulate our problem in the binary classification scheme with labels as ”progression and no-progression,” even though GPA produces three outcomes: ”no progression,” ”possible progression,” and

”likely progression.”

3.2.3 Baseline Comparison: Ordinary Least Squares Regression Method

Our baseline comparison method, unless otherwise specified, is the Ordinary Least Squares (OLS) Linear Regression model, which provides trend estimates of progression by quantifying its rate of change. OLS is a foundational statistical method used to analyze linear relationships between dependent variables with one or more independent variables. The output of OLS is the best-fitting linear equation line that describes the data after minimizing the sum of squares of the difference between observed and estimated values. In the context of Glaucoma Progression, OLS LR can be applied to fit global, sectoral, or point-wise values from diagnoses (e.g., sequence of global RNFL thickness values in μm from SDOCT taken during follow-ups) with time (yr) to obtain the slopes for the rate of change of values (deterioration in global RNFL thickness in $\mu m/yr$). The definitions of eyes detected as progressing with glaucoma vary across research, but obtaining a statistically significant negative slope ($p < 0.05$) is the most widely used reference.

3.2.4 Evaluation Metrics

Binary classification in disease progression prediction refers to the process of categorizing subjects into dichotomous outcomes: ”progressing” or the positive class and ”non-progressing” or the negative class, as evaluated by models. For classes C_1 and C_2 with class prior probabilities $P(C_1)$ and $P(C_2)$, the total data distribution and total probability for binary classification can be modeled as

$$P(\text{data}) = P(C_1) \cdot P(\text{data}|C_1) + P(C_2) \cdot P(\text{data}|C_2) \quad (3.1a)$$

$$P(C_1) + P(C_2) = 1 \quad (3.1b)$$

Where $P(\text{data}|C_1)$ represents the conditional distribution of data given class C .

Predictive models for classification try to assign the most probable "class" of data by categorizing it into one of the two classes. Maximum Likelihood Estimation (MLE) is used by complex models to estimate the parameters of the model. Assuming the true data distribution assigns data points to C_1 with probability y and to C_2 with probability $1 - y$ (3.1b) and the predictive model assigns data points to C_1 with probability p and assigns to C_2 with probability $1 - p$, we can derive the cross entropy of our classification problem as:

$$H(y, p) = - \sum_{i=1}^2 P(C_i) \log P(\text{data}|C_i) \quad (3.2a)$$

$$H(y, p) = -y \log(p) - (1 - y) \log(1 - p) \quad (3.2b)$$

Which gives the binary cross entropy from the total probability perspective. Here, $P(\text{data}|C_1)$ is viewed as observing the expected encoding length using the predicted distribution for events from the true distribution. Without going into much details, we can also derive the binary cross entropy (BCE) loss from MLE as:

$$\mathbf{J}(\theta) = - \sum_{i=1}^N [y_i \log(p_i) + (1 - y_i) \log(1 - p_i)] \quad (3.3)$$

minimizing which gets the best estimate for model parameters θ to predict class C_1 and C_2 .

Evaluating the model's predictive performance in medical data analyses is not only important for disease progression detection but also critical due to frequent encounters with class imbalance. It is imperative to get the "progressing" samples categorized correctly while ensuring extra care is taken to prevent false alarms (calling progressing samples "non-progressing") (Hicks et al. (2022)). The predictive performance of classification models can be estimated from the confusion matrix by comparing predictions to ground truth. A confusion matrix is given by (Figure 3.6):

$$\text{Confusion Matrix} = \begin{pmatrix} \text{True Positive (TP)} & \text{False Positive (FP)} \\ \text{False Negative (FN)} & \text{True Negative (TN)} \end{pmatrix} \quad (3.4)$$

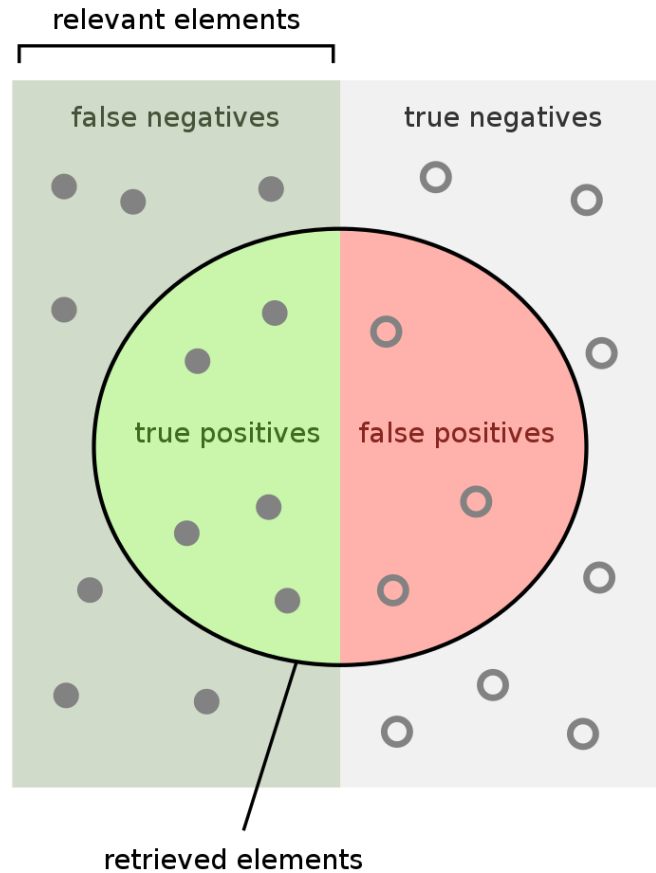


FIGURE 3.6: Classification Confusion Matrix based on items retrieved from all relevant examples (Walber (2014)).

Sensitivity, or the true positive rate, is one of the important metrics used to evaluate models for medical analysis. It calculates the rate of classifying positive (progressing) samples correctly:

$$\text{Sensitivity (or True Positive Rate)} = \frac{\text{TP}}{\text{TP} + \text{FN}} \quad (3.5)$$

Specificity, an equal if not greater significance than sensitivity, evaluates the model’s performance to classify the negative (non-progressing) samples correctly. It is also called the true negative rate and is given by:

$$\text{Specificity (or True Negative Rate)} = \frac{\text{TN}}{\text{TN} + \text{FP}} \quad (3.6)$$

Additionally, given the emphasis on minimizing false alarms (false positives) in medical settings, there are often benchmarks like ”sensitivity at 95% specificity” to provide a clinical view of model evaluation. Clinicians obtain this value by calculating the sensitivity (hit-ratio) by changing the probability or significance threshold to equalize specificity to 95%. This allows the model to balance between capturing true cases and avoiding overdiagnosis. Unless otherwise stated, our research will use these values extensively to report model performance.

Extending the above criterion, the Area Under the Curve of the Receiver Operator Characteristics (AUC-ROC) will be used to measure the classification model’s discerning capability across different probability thresholds, with higher scores denoting higher classification power and 0.5 equating random guessing. Finally, since the accuracy provides a holistic view of both progression and non-progression samples classified correctly, it will be used as the basic metric for initial evaluations of the model:

$$\text{Accuracy} = \frac{\text{TP} + \text{TN}}{\text{TP} + \text{TN} + \text{FP} + \text{FN} \text{ (Total Observations)}} \quad (3.7)$$

The ensemble of the metrics discussed in this section will provide enough evidence for a detailed and robust evaluation of the model’s clinical utility.

3.2.5 *Post-Hoc Statistical Analysis*

Post-hoc statistical analyses play a pivotal role in evaluating the clinical relevance of medical image classification systems. Once the predictive model has been developed and validated on a dataset, it is crucial to discern its real-world clinical applicability and acceptability. Linear Mixed Models (LMM), often used in this context, are suitable for analyzing clinical datasets with hierarchical or nested data structures, such as multiple measurements from the same patient or, specifically in ophthalmology, from each eye of the patient. LMM can model the predictions of classification systems with covariates like clinical or demographic features nesting random effects at the patient or eye level. The outputs of the LMM can be used to understand the behavior of the classifier against a covariate across different subgroups. Researchers can ascertain the clinical relevance of the classifier model if the LMM for model predictions obtains a similar performance or significance with true values as determined by the reference standard. This method often offers a nuanced understanding of the classifier's performance and can help identify areas of improvement from a clinical perspective.

Comparing population characteristics is also an important factor for ascertaining the medical applicability of the model. Chi-squared tests play a crucial role in determining if there are significant differences in populations, especially well-observed demographics like gender and race. This ensures the predictive model isn't inadvertently biased towards any particular demographic or subgroup, owing to generalizability and fairness. Additionally, McNemar's test can be used for a quick comparison of the performance of the developed model against traditional methods, like OLS Linear Regression, highlighting significant improvements from the latter (if it exists). The posthoc statistical analysis thus ensures that medical image classification systems, once developed, not only guarantee robustness beyond predictive

accuracy but also have clinical applicability in real-world medical applications.

3.3 The Time-Series Deep Learning Model

Glaucoma progression detection is a longitudinal study of disease progression. In our research, we focus on longitudinal structural assessments (SD-OCT B-scan images) taken over a follow-up period to determine if the OCT exams are indicative of subsequent progressive loss of visual fields by acceptable clinical metrics. For this, we develop time-series deep learning models that use the longitudinal OCT image sequence to learn both the spatial features within each image as well as the temporal evolution across image sequences. Unlike traditional image classification, we define our dataset (D) with N points as a time-series model where each datapoint contains τ B-scans $x^{(t)}$ taken over a time period T . We can express n^{th} datapoint in the time-series dataset as $(x^{(1)}, x^{(2)}, \dots, x^{(\tau)})_n \rightarrow y_n$, where y_n is the class label for that point. Outcome y is derived from the reference standard, which is typically obtained at endpoints after the final follow-up time \mathcal{T} , where $T \leq \mathcal{T}$. Therefore, the time-series model or "oracle" for the dataset can be written as:

$$f(x^{(1)}, x^{(2)}, \dots, x^{(\tau)}) \rightarrow y \tag{3.8}$$

Where $x^{(t)}$ represents the spatial features derived from SD-OCT B-scan image at time instance t , τ denotes the total number of instances in the series, and the output y is the classification output of the longitudinal data. The function $f(\cdot)$ is the oracle function which maps the temporal vector $X_n = (x^{(1)}, x^{(2)}, \dots, x^{(\tau)})_n$ to ground truths y_n . Given that we are dealing with binary classification, our labels have $K = 2$ classes, which can be represented as a K -dimensional vector using 1 – of – K encoding.

Our objective is to develop a time-series deep learning model, \mathcal{H} , that can encode

the spatiotemporal feature vector X_n . The goal is to optimize the parameters of \mathcal{H} so that the predicted labels \hat{y} closely match the true probability distributions of y . We use MLE to find the optimal parameter values θ of the DL model \mathcal{H} that maximizes the likelihood of observing data given model. The probability of observing the dataset \mathcal{D} is the likelihood (density) function given as:

$$\mathcal{L}(\theta|\mathcal{D}) = \prod_{i=1}^N P(y_i|X_i, \theta) \quad (3.9)$$

Rewriting $P(\cdot)$ with its probability distribution (binomial), replacing probabilities with appropriate estimates \hat{y} and taking the likelihood function's negative log-likelihood, we get a more tractable function:

$$\mathbf{J}(\theta) = -\log \mathcal{L}(\theta|\mathcal{D}) = -\sum_{i=1}^N [y_i \log(\hat{y}_i) + (1 - y_i) \log(1 - \hat{y}_i)] \quad (3.10)$$

Which is the exact BCE formula in Equation (3.3) derived in the previous section. Minimizing this loss (maximizing likelihood) with respect to model parameters θ obtains the most optimal parameters.

In the following subsections we discuss the specific parts of our time-series DL model which makes it unique.

3.3.1 Pre-trained CNN Networks: 3DCNN + ResNet50

The first layer of our deep learning architecture is a 3D Convolutional Neural Network (3D-CNN). We use 3D-CNN because of its intrinsic ability to capture not only the spatial features of each image but also the short-term temporal dynamics across the longitudinal image data. This dual encoding is crucial, especially in the first layer, since the input sequence contains high-dimensional images where the feature space is large (Manttari et al. (2020)). By concentrating on contiguous spatial patches in the

image sequence, the 3D-CNN extracts the most salient features for both spatial and temporal learning. These features are then passed on to a subsequent pre-trained ResNet50 model. This way, the 3D-CNN ensures that the ResNet50 model receives the most relevant and concise spatial-temporal encodings.

A pre-trained ResNet50 model follows the initial 3DCNN layer to encode the spatial features further. ResNet50, a 50-layer deep residual neural network (DNN), is known for its capability to extract complex spatial patterns and hierarchies from image data due to its ability to solve the vanishing gradient problem in deep networks (He et al. (2016)). ResNet50 has been widely used in the development of novel deep learning algorithms and transfer learning tasks in smaller datasets, producing state of the art results. Due to this, Residual Networks have also been widely used in the field of medical image analysis. Thus, we develop our spatial encoder by leveraging the weights and architecture of ResNet50 pre-trained on a large-scale ImageNet1K dataset. This way, our model can use prior knowledge and complex spatial feature representations to enhance the performance of the DL model on the glaucoma progression detection task. A representation of 34-layer ResNet model architecture is shown in Figure 3.7.

3.3.2 Sequence Learning: LSTM Networks

Long Short-Term Memory (LSTM) networks, an advanced type of recurrent neural network, are then used to capture the temporal evolution of the spatial encodings derived from the ResNet50 model. An LSTM model is made of memory cells controlled by gate mechanisms (Hochreiter and Schmidhuber (1997)) (Figure 3.8). Due to this, LSTMs are excellent in encoding the long-term dependencies in the time-series data, making them particularly suitable for handling the longitudinal OCT image sequence. By processing the sequential spatial features derived from the ResNet50, the LSTM layer learns to recognize intricate temporal patterns, capturing both intra-patient

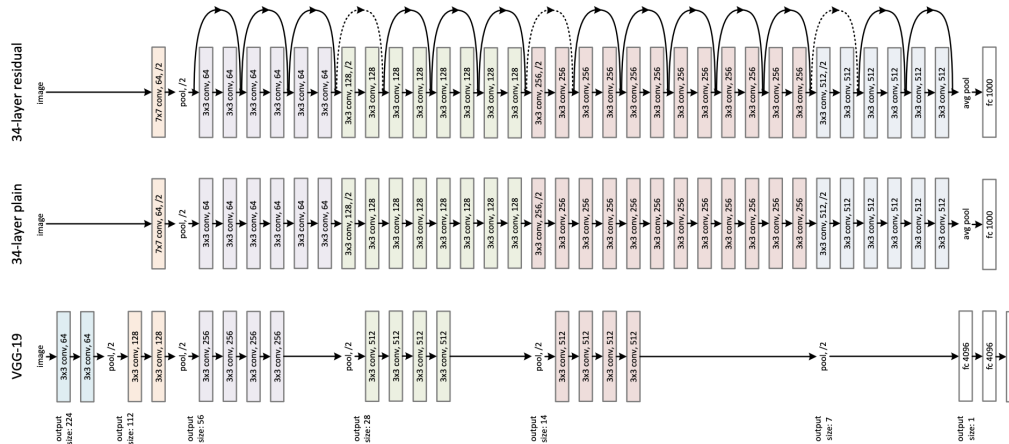


FIGURE 3.7: Representative example of 34-layer Deep Residual Network architecture (top) compared to a plain network (middle) and VGG-19 (bottom) (He et al. (2016)).

variabilities — such as the progression rate within the image sequence of an individual — and inter-patient variabilities — like differences in progression patterns across individuals (Mousavi and Afghah (2019)). This nuanced yet thorough understanding of temporal patterns allows for a more comprehensive representation of the glaucoma progression, allowing accurate representation of spatiotemporal features z .

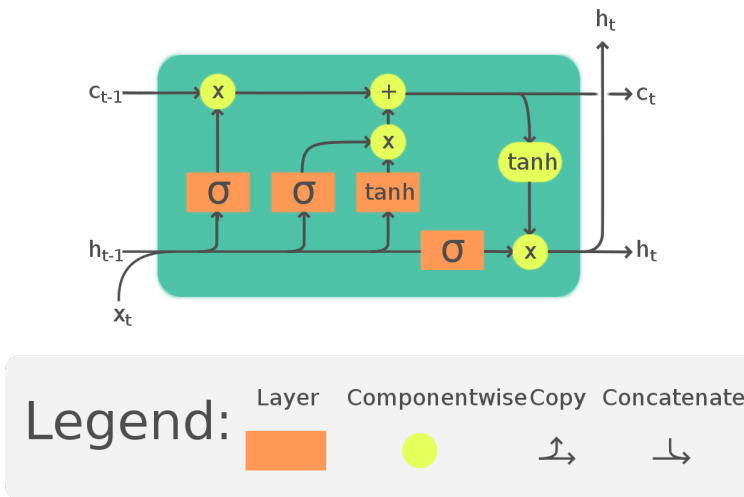


FIGURE 3.8: A schematic of the Long Short-Term Memory cell explaining components of the Recurrent Neural Networks (Chevalier (2018)).

3.3.3 Spatio-temporal Learning: Combining CNN and LSTM

Spatio-temporal learning effectively integrates both the CNN and LSTM networks to analyze both spatial and temporal features in longitudinal datasets together. In our model, the CNN module is made of a 3D-CNN layer followed by a pre-trained model. ResNet50 extracts the spatial and short-term temporal patterns from image data, ensuring important features are highlighted. These encodings are then fed into the LSTM network, which captures the long-term dependencies to recognize evolving patterns over time, combining both methods overall. This combined approach offers a unique perspective of the disease, leveraging both CNNs and LSTMs to achieve the most accurate representations of glaucoma progression.

3.3.4 Classification Head

A classification head is used at the end of the learning task to convert the complex feature representations, parsed by the CNN and LSTM layers, into a clinically relevant diagnostic outcome for glaucoma progression. The classification head typically contains fully connected layers to compress high-level encodings, activation functions to introduce non-linearities for complex patterns and relationships, and a final *softmax* function to get logits or probabilities to generate predictions for the binary classification task. Assuming the model contains parameters θ , the label distribution of classes k from the softmax becomes:

$$P_{\theta}(y = k|X_n) = \frac{e^{\mathcal{H}_{\theta}(X_n)}}{\sum_{k \in K} e^{\mathcal{H}_{\theta}(X_n)}} \quad (3.11)$$

where $\mathcal{H}_{\theta}(X_n)$ is the spatiotemporal encodings obtained from the model till the final layer and $P_{\theta}(y = k|X_n)$ signifies the probability of the model predicting data X_n to k^{th} class. Therefore, the model's output can be interpreted as the likelihood of the model to predict glaucoma progression for an input image sequence. An overview

of the combined CNN-LSTM network for spatiotemporal encoding is given in Figure 3.9

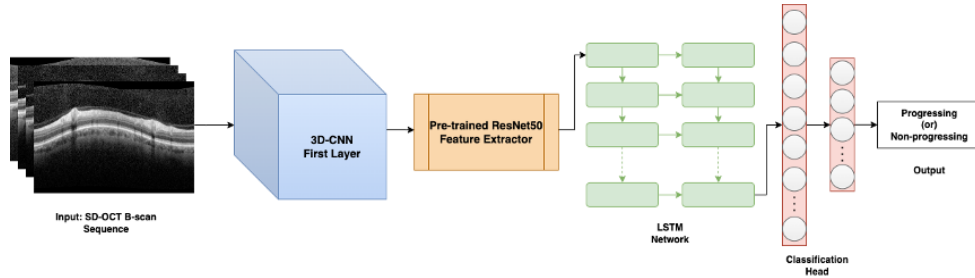


FIGURE 3.9: An overview of the combined CNN-LSTM Network with a Classification Head: CNN-LSTM encodes spatiotemporal features and Classification Head predicts progression from representations.

We observe that the longitudinal data for each eye obtained from the DOR database has variable follow-up lengths depending on the patient’s follow-up time. We employ various strategies to make the sequence size uniform and empirically select a sequence of 5 OCT images as the input for the model. Model-specific input sequence generation processes are shown in their respective chapters. In the following sections, we will explain in brief two of the most prominent problems in the detection of disease progression and subsequently formulate our research solution.

3.4 Modelling with Healthy Patient Data: Modified Positive Unlabeled Learning

The accuracy of the DL model for glaucoma progression detection and its clinical relevance highly depends on the reference standard. Since there is no consensus for a universally accepted reference gold standard, we use surrogate methods to evaluate predictions. A change detection model was developed by Belghith et al. (2015), which used OCT image pairs to identify regions in the OCT scans that were likely to predict progression. Other research by Leung et al. (2013) and Jammal et al. (2020) showed that the cpRNFL layer naturally undergoes age-related deterioration,

which can increase the susceptibility of identifying glaucoma progression. We extend these concepts to our dataset consisting of longitudinal SD-OCT image sequences and predict glaucomatous progression by analyzing the structural change characteristics observed in the data. This dataset contains longitudinal data with a diagnosis of open-angle glaucoma but is unlabeled for glaucoma progression. To reinforce the notion of progressing eyes from non-progressing eyes, we introduce a new subset of normal eyes from a small cohort of patients identified as healthy using the International Classification of Diseases (ICD) and Current Procedural Terminology (CPT) codes from the DOR database (the exact inclusion/exclusion criteria is defined in the following chapters). The problem effectively becomes Positive Unlabeled (PU) learning, which is one of the most common yet complex learning paradigms for discriminating positive and negative classes from a partially labeled positive dataset (Li and Liu (2005); Bekker and Davis (2020)). It’s important to note that in our scenario, the terminology for PU becomes counterintuitive as the ”positive” set contains ”healthy eyes,” which are typically ”negative” samples in traditional settings, but this does not change the inner working of PU learning (technically Negative-Unlabeled Learning). In this section, we formally introduce the modified PU learning and attempt to obtain error bounds for the learning task to show the feasibility of the method.

Unlike traditional PU methods, which rely on the calculation of a class prior to modeling classification systems, we let the DL model estimate class densities directly (Bekker and Davis (2020)). This is done by a modified PU learning task, which breaks down the learning process into two tasks:

- **PU Learning Phase:** A one-class classifier identifies the negative class (healthy eyes) from the unlabeled set (eyes that might or might not be progressing).
- **Noise Learning Phase:** The unlabeled samples are treated in two subsets: a pseudo-progressing group based on the original sequence showing systematic

time-related changes in glaucoma and a non-progressing group that is shuffled with time to remove any temporal dependencies. Noise Learning effectively becomes a binary classification to distinguish between the positive (pseudo-progressing) class and the negative (non-progressing) class.

3.4.1 Hypothesis and Mathematical Formulation

Let $\mathcal{S}_{healthy}$ be the set of healthy eyes (positive set in the PU learning context) and $\mathcal{S}_{unlabeled}$ (negative set in PU learning context), therefore PU dataset:

$$\mathcal{D}_{PU} = \mathcal{S}_{healthy} \cup \mathcal{S}_{unlabeled} \quad (3.12)$$

Positive Unlabeled (PU) Learning Task:

Objective: To differentiate between $\mathcal{S}_{healthy}$ and $\mathcal{S}_{unlabeled}$ using:

$$f_{PU} : \mathcal{D}_{PU} \rightarrow \{0, 1\} \quad (3.13)$$

where

$$f_{PU}(x) = 1 \implies x \in \mathcal{S}_{unlabeled}, \quad (3.14)$$

$$f_{PU}(x) = 0 \implies x \in \mathcal{S}_{healthy}. \quad (3.15)$$

We formulate our loss objective L_{PU} for PU learning as BCE over all samples of PU dataset (equation (3.3))

Noise Learning Task:

We synthetically create a pseudo-progressing criteria for glaucoma progression. Assuming $\mathcal{S}_{unlabeled} = \{X_1, X_2, \dots, X_{N'}\}$ are the N' unlabeled samples in the set. Shuffling with a random shuffling function Π with k permutation yields a set $\mathcal{S}_{shuffled} = \mathcal{S}_{\Pi(unlabeled)} = \{\tilde{X}_1, \tilde{X}_2, \dots, \tilde{X}_{N'}\}$ where each $\tilde{X}_i = \{X_{\Pi(i),1}, X_{\Pi(i),2}, \dots, X_{\Pi(i),k}\}$ contains k randomly shuffled input sequences. Here random shuffling is defined as $X_{\Pi(i)} = (x^{\pi(1)}, x^{\pi(2)}, \dots, x^{\pi(\tau)})_i$, where $\pi(i)$ is a random number in $1, 2, \dots, \tau$.

Based on the definitions discussed above:

- $\mathcal{S}_{\text{pseudo-progressing}}$ = Original sequence in $\mathcal{S}_{\text{unlabeled}}$ (pseudo-positives).
- $\mathcal{S}_{\text{non-progressing}}$ = Shuffled sequences from $\mathcal{S}_{\text{shuffled}}$ (pseudo-negatives).

Therefore, the shuffled dataset becomes:

$$\mathcal{D}_{\text{shuffled}} = \mathcal{S}_{\text{pseudo-progressing}} \cup \mathcal{S}_{\text{non-progressing}} \quad (3.16)$$

Objective: To differentiate between $\mathcal{S}_{\text{pseudo-progressing}}$ and $\mathcal{S}_{\text{non-progressing}}$ using:

$$f_{\text{noise}} : \mathcal{D}_{\text{shuffled}} \rightarrow \{0, 1\} \quad (3.17)$$

where,

$$f_{\text{noise}}(x) = 1 \implies x \in \mathcal{S}_{\text{pseudo-progressing}}, \quad (3.18)$$

$$f_{\text{noise}}(x) = 0 \implies x \in \mathcal{S}_{\text{non-progressing}}. \quad (3.19)$$

Similar to PU learning, we model the loss objective $L_{\text{noise-model}}$ for the noise learning as BCE (equation 3.3) over the shuffled dataset.

Joint Objective Function for Noise-PU Model

Combining both the losses, we model the objective for the joint learning task as the weighted sum of the two losses:

$$J(\theta, \mathcal{D}_{\text{PU}}, \mathcal{D}_{\text{shuffled}}) = L_{\text{PU}}(\theta, \mathcal{D}_{\text{PU}}) + \alpha \cdot L_{\text{noise-model}}(\theta, \mathcal{D}_{\text{shuffled}}) \quad (3.20)$$

Where θ represents the CNN-LSTM model parameters and α is the weighting factor for our learning scheme, which instructs the algorithm to focus on a particular learning task.

3.4.2 Objective Rationale

To show that joint training offers an advantage over standard Positive-Negative learning formulation, we need to identify the tradeoff between the performance of deep learning model on the unlabeled samples in the PU model and the negative samples in the noise model. In general, assuming that the shuffled sequences provide non-progressing information, it is expected that optimising for combined loss for the PU and Noise Model would be lower than the loss for PU model alone, especially if the pseudo-negative sequences can capture non-progressing conditions effectively. Since the $i \cdot i \cdot d$ conditions are lost when shuffling the time-series sequence in the Noise Model, it is challenging to quantify the improvements observed in joint training in terms of error bounds. Modeling error bounds requires information about the data characteristics and assumptions, which is out of scope. In the following chapters, we provide empirical evidence to show that the joint training model with PU and Noise learning offers a competitive advantage in learning inherent progressive characteristics in medical times-series data.

3.5 Modelling DL with External Labels: A Contrastive Learning Approach

U.S. Food and Drug Administration (FDA) recommends event-based analysis of SAP deterioration as endpoints for progression (Weinreb and Kaufman (2011)). Inspired by the EMGT study, GPA has been gaining traction as one of the reliable reference standards for event-based progression due to its clinical acceptance, objectivity, high sensitivity, and supportive research base (Arnalich-Montiel et al. (2009)). Many pieces of research have shown GPA progression has moderate to good agreement with glaucoma experts with potentially detecting early progression (Aref and Budenz (2017); Tanna et al. (2012)). We have already shown the relevance of GPA as

an endpoint for reference standards in Sections 2.4.1 and 3.2.2. Using the modeling procedures described in Section 3.4, we extend the definitions of the DL process to a labeled case where the labels are obtained from an external source. Specifically, we propose a DL approach that uses longitudinal sequences of SDOCT B-scan images from the DOR database to predict VF GPA indicative of glaucoma progression. The SDOCT images are derived from the detailed longitudinal structural assessments in the DOR, whereas VF GPA labels, which are binary (originally ternary - non-progressing, possible progressing, and likely progressing), come from VF SAP tests belonging to the same patients. Potential mismatches in the visit dates for SDOCT scans and SAP tests and the inherent discrepancy between early and late-stage progression detection between structure and function might introduce noise or other inconsistencies in labels. Furthermore, challenges in obtaining enough data points during VF SAP follow-ups lead to imbalances, making the modeling process complex. To overcome these difficulties, we use a three-step training method with a DL model that’s built on the SimCLR-based contrastive learning framework.

In the first step, the base model acts as a binary classifier, differentiating between progression and non-progression using the original SD-OCT image sequences and their corresponding VF GPA labels. Parallely, a second step focuses on discerning VF-derived glaucoma progression (GPA) with non-progressing by introducing controlled randomness (shuffling) in the sequence of images, aiming to mimic non-progressing eyes. Images are adversarially augmented to regularize the model for structural invariance. In addition, label-smoothing binary cross-entropy is used to address imbalances that arise from the shuffling criteria. In the last phase, the latent representations from both training stages are mapped into two distinct spaces using two projection heads. We then use the SimCLR framework to extract contrastive features from these spaces, enhancing the model’s precision in differentiating true VF-derived glaucoma progression from test variability due to non-progressing eyes.

This tripartite training process is designed to improve the model’s performance in detecting progression while solving important data ambiguities observed in medical datasets. The processes are elaborated in the following subsections.

3.5.1 Hypothesis and Mathematical Formulation

Extending the definitions in Section 3.4, we describe SDOCT-GPA dataset $\{X_i, y_i\} \sim \mathcal{D}$, where $X_i = (x^{(1)}, x^{(2)}, \dots, x^{(\tau)})_i$ is the i^{th} longitudinal SDOCT image sequence with followup T , and $y_i \in \{0, 1\}$ is the VF GPA label representing glaucoma progression at an endpoint \mathcal{T} where $\mathcal{T} \geq T$. Here 0 represents non-progressing while 1 represents progressing.

Using the above data as input, we want to develop a time-series DL model h with parameters θ that can predict glaucoma progression using \mathcal{D} . The h model is a CNN-LSTM network discussed earlier, which consists of three parts:

- CNN: $\mathbb{R}^{T \times H \times W} \rightarrow \mathbb{R}^{T \times F}$ Is a 3DCNN + pretrained ResNet50 deep CNN that extracts feature vector of dimension F from T images of size $H \times W$.
- LSTM: $\mathbb{R}^{T \times F} \rightarrow \mathbb{R}^Z$ is the LSTM network that processes the longitudinal sequence of feature vectors and outputs a fixed-size feature vector of dimension Z .
- Classification Head: $\mathbb{R}^Z \rightarrow [0, 1]$, is the classifier made of fully connected layers and the sigmoid activation. It returns the probability of progression based on the CNN-LSTM output.

Typically, unless otherwise stated, the DL output \hat{y}_i ,

$$\hat{y}_i = \begin{cases} 1 & \text{if } h(X_i) \geq 0.5 \\ 0 & \text{otherwise} \end{cases} \quad (3.21)$$

Since \mathcal{D} is imbalanced and noisy, the learning algorithm is derived by a Regularized Contrastive Learning Model which consists of three learning steps:

Binary Classification with Original Data

Objective: To differentiate between progression and non-progression using original labels. To do this, we train the model h on \mathcal{D} using the original labels, referred as \mathcal{D}_{orig} . We use L_{BCE} as the loss objective which is the standard BCE loss (equation 3.3) defined earlier.

Augmented Learning with Pseudo-Progression

This step is inspired by the modified PU learning model described in Section 3.4. In this step, we introduce strong adversarial augmentations to the input features X_i to ensure that our model captures the most discriminative and robust representations of X_i . This makes the DL model resilient to adversarial perturbations and label noise, which enhances the generalizability by focusing on consistent and invariant features of X_i .

We generate a new shuffled dataset from \mathcal{D} where $X_{shuffle;i}$ represents shuffling of X_i with permutation 1. We define probability p as a parameter, where a sample from the original dataset is shuffled with p if $y_i = 0$ (non-progressing), and with $(1-p)$ if $y_i = 1$ (progressing). The labels for these samples are set to $Y_{shuffle;i} = 0$ to represent characteristics of "true" non-progression. If \mathcal{A} represent strong adversarial augmentations applied to image sequences, the new data pairs $(X_{shuffle}^*, y_{shuffle}) \sim \mathcal{D}_{augmented,shuffle}$ becomes:

$$\{X_{shuffle;i}^*, y_{shuffle;i}\} = \begin{cases} \{\text{shuffle}(\mathcal{A}(X_i)), 0\} & \text{if } y_i = 0 \text{ with probability } p, \\ \{\text{shuffle}(\mathcal{A}(X_i)), 0\} & \text{if } y_i = 1 \text{ with probability } 1 - p, \\ \{\mathcal{A}(X_i), y_i\} & \text{otherwise,} \end{cases} \tag{3.22}$$

We see that the label imbalance increases with p . The loss objective for the augmented dataset, $L_{smooth-BCE}$ is formulated as label smoothed BCE loss which uses BCE loss on y_{smooth} by converting labels y using formulae:

$$y_{smooth} = (1 - \epsilon) \cdot y + \frac{\epsilon}{2} \quad (3.23)$$

Where ϵ is a smoothing constant.

The shuffling scheme, therefore, generates a criterion for the model to distinguish between progression and non-progression samples by shuffling a subset of sequences to generate eyes with "true" non-progressing characteristics.

Contrastive Learning with SimCLR

We use contrastive learning in this project due to its effectiveness in handling label noise and imbalanced datasets (Li et al. (2022b); Xue et al. (2022)). This approach is essential because of its ability to extract subtle variations in the data. In our approach, this method dissects and contrasts features from the shuffled sequences (hard negatives) and the original dataset (potential glaucoma progression) to enhance the model's ability to differentiate between them. The adversarial augmentations in the second step allow for contrastive learning not only to regularize but also to teach invariances in images that are critical for structural progression determination. To this effect, we employ contrastive learning by implementing SimCLR, an unsupervised method for learning variations (Chen et al. (2020)) because of its ability to inherently learn representations from datasets where explicit labeling might be noisy or inconsistent, like our dataset.

Let ϕ and ψ be the parameters of the two projection heads in the DL model. Using the model definitions explained above, we derive the latent features of the CNN-LSTM base model with parameters θ as:

$$Z_{orig} = h(X_{orig}; \theta) \quad (3.24)$$

$$Z_{aug} = h(X_{augmented}; \theta) \quad (3.25)$$

Where $X_{augmented} = X_{shuffle}^*$. We obtain the projections of the original and augmented (with shuffling) images using the projection heads as:

$$Z_{orig-proj} = h_\phi(Z_{orig}; \phi) \quad (3.26)$$

$$Z_{aug-proj} = h_\psi(Z_{aug}; \psi) \quad (3.27)$$

SimCLR is used to maximize agreement between positive pairs (similar sequences) while pushing negative pairs (dissimilar sequences) apart in both the projected spaces. The objective function for SimCLR is:

$$L_{SimCLR} = \frac{1}{2N} \sum_{i=1}^N [L_{con}(Z_{orig-proj}, Z_{aug-proj}) + L_{con}(Z_{aug-proj}, Z_{orig-proj})] \quad (3.28)$$

Where L_{con} is the contrastive loss between representation pairs from the respective projection heads. The formula for L_{con} with projections z is:

$$L_{con}(i, j) = -\log \left(\frac{\exp(sim(z_i, z_j)/\tau)}{\sum_{k=1}^{2N} \mathbb{1}_{[k \neq i]} \exp(sim(z_i, z_k)/\tau)} \right) \quad (3.29)$$

where $sim(\cdot)$ is the cosine similarity function defined as $sim(u, v) = \frac{u \cdot v}{\|u\|_2 \cdot \|v\|_2}$, τ is the temperature parameter which scales the similarity and $\mathbb{1}_{[\cdot]}$ is an indicator function which is 1 when the argument in $[\cdot]$ is true, 0 otherwise.

Joint Objective Function

The final objective function, considering all three training steps, becomes:

$$\begin{aligned}
J_{joint}(\theta, \phi, \psi, \mathcal{D}_{orig}, \mathcal{D}_{augmented,shuffle}) &= L_{BCE}(\theta, \mathcal{D}_{orig}) \\
&+ \alpha \cdot L_{smooth-BCE}(\theta, \mathcal{D}_{augmented,shuffle}) \\
&+ \beta \cdot L_{SimCLR}(\theta, \phi, \psi, \mathcal{D}_{orig}, \mathcal{D}_{augmented,shuffle})
\end{aligned} \tag{3.30}$$

where α and β are weighting factors for smooth-BCE and SimCLR loss objectives respectively

3.5.2 Objective Rationale

To show that the joint training offers an advantage over standard training on GPA labels, we need assumptions about the distributions of data and noise, the complexity of the DL models, and more. In general, adding adversarial augmentations with shuffling (emulating "true" non-progression) and leveraging contrastive learning aims to make the model more robust and generalizable, thus reducing generalization error. However, quantifying these improvements in terms of error bounds is complicated and depends on the complex characteristics of the data, model, and augmentations, which is out of scope. We provide empirical evidence to show that the joint model is better than the base model trained on original data.

Weakly Supervised Time Series Learning to Detect Glaucoma Progression from Optical Coherence Tomography B-scans

The research discussed in this chapter was collaboratively carried out with Alessandro A. Jammal, MD, PhD and Felipe A. Medeiros, MD, PhD.

An abstract was presented in *Investigative Ophthalmology & Visual Science*, ARVO, 2023. Refer to Mandal et al. (2023) for details.

A preliminary version of this work is in review at the *American Journal of Ophthalmology*, AJO, 2024 as a Full Length Article.

4.1 Introduction

This chapter proposes a novel DL algorithm to detect glaucoma progression using OCT images, in the absence of a reference standard. Recent years have witnessed a surge in research centered around the development of DL and AI algorithms aimed at improving glaucoma assessment (Thompson et al. (2020)). While most of these algorithms have been developed for cross-sectional assessment, only some have addressed the critical need for tracking longitudinal change - a fundamental element in monitoring the progression of glaucoma.

A common thread among traditional DL methods that utilize supervised learning is the dependence on accurate and precisely labeled datasets. These are crucial for training the models based on universally accepted reference standards, ensuring trustworthy classifications (Thompson et al. (2020)). In the context of glaucoma progression, however, no such reference standard exists. While the detection of dis-

ease progression can be aided by clinical software based on parameters from OCT and SAP over time (Heijl et al. (2003)), the determination of progression is ultimately dependent on the clinician’s subjective evaluation. Such evaluations include the complex task of discerning true glaucomatous changes from normal aging effects (Bussel et al. (2014); Vianna et al. (2015)). Even when performed by expert graders, this assessment suffers from the low agreement and reproducibility (Öhnel et al. (2016)). For training AI algorithms, this reliance on human evaluation as the reference standard can be problematic, reducing the accuracy of the algorithm if an imperfect classification is used as the ”gold standard.”

Alternative approaches have been suggested for dealing with the need for a perfect reference standard when assessing changes over time. For instance, one method used to assess progression on OCT randomly rearranges sequences of images from glaucomatous eyes, effectively eliminating any systematic changes over time (Belghith et al. (2015)). The rearranged sequences are then classified as stable or ”non-progressing” cases. The algorithm is trained to recognize these stable sequences, and any sequence not classified as stable is presumed to show progression. The ”hit ratio”, or the percentage of images not identified as stable, serves as an indirect measure of the algorithm’s sensitivity in detecting progression.

However, this approach overlooks a key factor: the presence of age-related changes in OCT images (Sung et al. (2009)). An algorithm trained solely on scrambled images could be confounded by these changes, which it might mistakenly identify as ”progression.” Prior research indicates that age-related changes in OCT B-scans are pretty common and can impact multiple layers (Margolis and Spaide (2009); Ramrattan et al. (1994); Shigueoka et al. (2021)), which may lead to a high false-positive ratio for an algorithm trained exclusively on scrambled images.

In the current study, we propose an innovative approach for training a DL algorithm for detecting glaucoma progression on OCT scans by combining training on

scrambled images with a parallel training process for recognizing age-related changes. We demonstrate that such an approach performs superiorly to standard approaches based on summary parameters for detecting changes over time while maintaining high specificity.

4.2 Methods

Data for this study was obtained from a database registry designed to investigate longitudinal structural and functional changes in glaucoma. The database involves retrospective data retrieved from Electronic Health Records of subjects seen at the Bascom Palmer Eye Institute, University of Miami, Florida, and Duke University, Durham, North Carolina. The Institutional Review Board from both institutions approved the study, and the methods conformed with the tenets of the Declaration of Helsinki and the regulations of the Health Insurance Portability and Accountability Act for research involving human subjects.

The study included subjects with a diagnosis of open-angle glaucoma as well as healthy individuals followed over time. Glaucoma subjects had evidence of glaucomatous optic neuropathy and reproducible visual field defects on SAP, defined as Glaucoma Hemifield Test outside normal limits or pattern standard deviation with $P < 5\%$ (Keltner et al. (2005)). Normal controls were obtained from a subset of eyes with IOP below 22 mmHg and no history of elevated IOP, normal ophthalmologic examination, normal appearance of the optic disc on stereo photographs, and at least two reliable normal VFs in both eyes. Subjects with a history of other ocular or systemic diseases that could affect the optic nerve were excluded.

All eyes were required to have at least 5 Spectralis SDOCT (Heidelberg Engineering GmbH, Dossenheim, Germany) images over time. Scans were acquired using a circular scanning pattern with a 3.5mm diameter around the ONH. The sequences of B-scan images for each eye were used as input features to the deep learning model,

with each SD-OCT B-scan being a grayscale image of 768×496 points resized to 224×224 pixels. Each series of five consecutive SDOCT B-scans from each eye was treated as a separate observation in the model. For eyes with more than five reliable SDOCT tests, all possible sequences of five consecutive tests from each eye were included in the dataset (e.g., n_1 to n_5 ; n_2 to n_6 , etc.).

4.2.1 Weakly Supervised Time Series Learning

We developed a weakly supervised time-series learning model, called Noise Positive-Unlabeled (Noise-PU) deep learning, to classify whether sequences of OCT B-scans showed progression. Positive-Unlabeled (PU) learning is a machine learning scenario where the training data consists of a set of labeled instances (positive) and a set of unlabeled instances (Bekker and Davis (2020)). 'Noise' refers to irrelevant or meaningless data in the dataset that can negatively impact the performance of a model. Therefore, a "Noise-PU" model refers to a deep learning model that is specifically designed to handle datasets with high levels of noise or mislabeled instances. The Noise-PU model was built in two steps, which used a parallel learning scheme: (a) PU Learning and (b) Noise Learning models. Both models' bases were CNN and LSTM networks, which were combined to form a CNN-LSTM model, which was then used as a spatiotemporal encoder for time series learning.

The first learning scheme (PU-learning) was used to discriminate healthy eyes from glaucoma eyes using a sequence of OCT B-scans from a highly imbalanced class dataset (i.e., many more glaucoma than healthy eyes). To do this, all healthy eyes from the dataset were identified and labeled as "normal," as any change over time would be considered related to normal aging only and not from glaucoma. All other observations obtained from glaucoma eyes were kept unlabeled for progression as they might or might not be actually progressing. A one-class classifier was used to discriminate healthy eyes from unlabeled eyes (Bekker and Davis (2020); Wolf et al.

(2022); Yang et al. (2012)).

A second learning scheme was used to distinguish between possible systematic time-related changes in glaucoma from test-retest variability (i.e., noise). For that, noise was defined as a sequence of images where any possible temporal changes were removed by randomly scrambling the order of the images. These sequences were treated as negative labels (i.e., pseudo-labeled for non-progressing), while the original sequence of SD-OCT B-scans for the same eye was marked as a positive label (pseudo-labeled for progression). Of course, not all original sequences of images from glaucoma eyes would, in fact, be truly progressing, as some might be stable or exhibit age-related changes. However, this training step ensures that the model learns to identify test-retest variability in the process of building the final model. The learned parameters from this model were used to tune the PU classifier directly without the need for estimating class priors (Wang et al. (2021)).

Finally, features from the PU and Noise learning models that were learned simultaneously were combined at the classification stage and jointly trained using two classification heads (one for PU learning and the other for noise learning) against the original PU labels to determine eyes with progression while accounting for normal age-related loss. The architecture for the weakly supervised time-series model is shown in Figure 3.9.

The model used a Residual Deep Neural Network, ResNet50, pre-trained on the ImageNet1K dataset as the CNN encoder to learn spatial features from SD-OCT b-scans (He et al. (2016)). The use of pre-trained ResNet50 and transfer learning has been widely used in the development of new deep learning algorithms to save computational power while still being able to produce state-of-the-art results on smaller datasets. A 3D-CNN replaced the top layer of the ResNet50 to encode the short-term temporal dependencies. 3D-CNN is a variant of CNN used for processing 3D images, usually MRI or CT scans, but recently, it has been applied to a series

of 2D images to encode time dependencies while preserving spatial features (Singh et al. (2020); Parmar et al. (2020)). LSTM network uses the sequence of spatial encoding obtained from the 3DCNN-ResNet50 network further to encode the long-term temporal dependencies in the data. A classification head made of FC layers was used to decode the spatiotemporal encodings into logits from which a softmax function computes the probability distribution of labels. The overall CNN-LSTM architecture is shown in Figure 4.1.

4.2.2 Training and Validation

Inputs to the DL model consisted of observations simultaneously from both the PU dataset and the artificially generated Noise dataset with 2-fold scrambling (i.e., for every observation in the training set pseudo-labeled for progression, two different randomly shuffled observations were created and pseudo-labeled for non-progression). Each observation in the dataset was made of a series of 5 consecutive SD-OCT B-scan images. A batch size of 16 was used for both datasets with a data split 70% training set, 15% validation set, and 15% testing set for the PU learning. Importantly, data split was performed at the subject level to avoid data leakage from having eyes of the same subject in more than one partition.

Image augmentations were introduced during the training phase to increase the variability in the dataset. Both one-shot and binary classification from PU learning and Noise learning, along with the predictions from the combined model used cross-entropy loss¹ as the objective function. All the losses obtained from the DL model were added up², and the net loss was optimized. Stochastic gradient descent (SGD) with an initial learning rate of $8.9e-4$, momentum 0.9 was used along with a scheduler of step size five and gamma 0.5 for 30 epochs. The evaluation was done after every

¹ Binary Cross-Entropy Loss (Equation 3.3)

² Losses were equally weighted i.e $\alpha = 1$ in equation 3.20

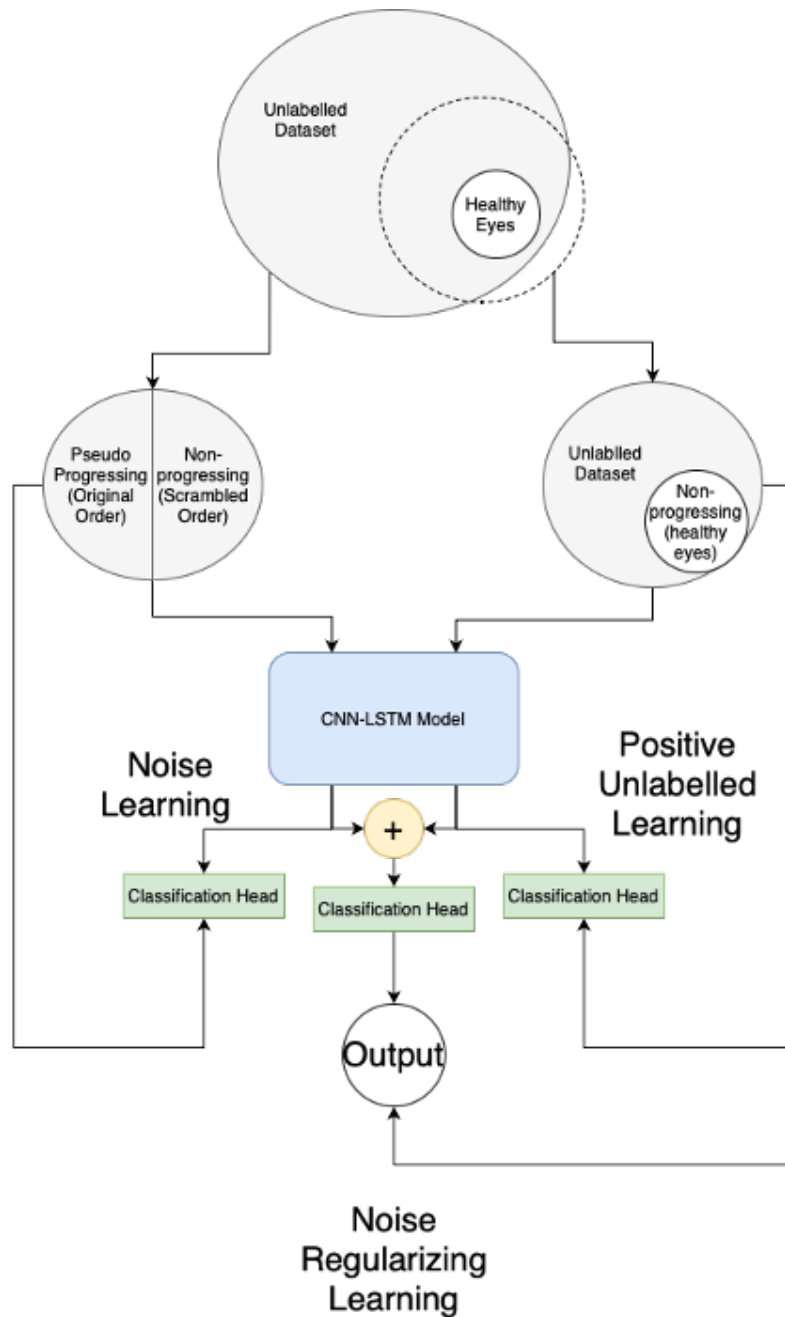


FIGURE 4.1: An overview of the Noise-PU learning scheme, which simultaneously incorporates both positive unlabeled learning and noise learning.

epoch, and the model with the lowest validation loss was saved. Optimizing for the best cumulative sum of the sensitivity and specificity on the validation set was used to obtain the optimal weakly supervised time series model and used for further

analysis on the test set. All the training and testing were done in Pytorch, Python 3.8.

4.2.3 Model Evaluation and Statistical Analysis

The performance of the DL model was compared to that of OLS regression of global retinal nerve fiber layer (RNFL) thickness, one of the clinical standards currently used for glaucoma progression detection for clinical validation (Abe et al. (2016)). A sequence was declared as progressing with OLS if it got a statistically significant negative slope ($\mu\text{m}/\text{year}$) with $p < 0.05$. Since there was no 'true label' or 'gold standard' test for glaucoma progression to provide a ground truth for comparison of OLS vs. the DL method, relative measures were used. Therefore, instead of sensitivity, the hit ratio served as a proxy for comparisons between the DL and OLS predictions. The DL method was said to be better at detecting glaucoma progression if its hit rate was higher than that of the OLS method when the specificities were equalized in the test set. The DL method's and OLS methods' specificities were matched by adjusting the DL method's probability threshold for predictions.

To assess the technical performance, the DL models AUC and hit-ratio (sensitivity) at matched specificities were compared to various machine learning (ML) and DL techniques used for identifying glaucoma progression. These techniques included classic ML methods like multi-layer perceptron (MLP) classifiers (Bizios et al. (2010)), feature engineering methods such as fast Fourier transform or wavelet Fourier transforms with support vector machines (FFT-SVM and WFT-SVM; Kim et al. (2013)), and unsupervised methods like Logistic Regression with principal component analysis (PCA; Christopher et al. (2018)). All these methods used RNFL thickness measures from OCT scans as inputs. DL methods for detecting progression included techniques like convolutional long short-term memory (ConvLSTM) networks (Dixit et al. (2021)) and transformers with image stitching inputs using

the SWIN based classifier (Liu et al. (2021)). These methods used a sequence of 2D OCT B-scan images as inputs.

Additionally, two ablation studies were also done to assess individual components of our learning approach: the PU learning method (Bekker and Davis (2020)) and the Noise learning method (Belghith et al. (2015)). The training was done on the same dataset for fair evaluations against a common baseline. Performance evaluations were carried out on the held-out test set comprising original image sequences from eyes not included in the training or validation datasets.

McNemar’s test was used to compare the hit rates of the methods. A mixed effect model nested at patient and eye level was used to check for correlation between the DL model predictions and age to ensure that the DL method predicts true glaucoma progression rather than age-related changes. Demographics and clinical characteristics of eyes determined as progressing and not progressing by the DL model were compared using linear mixed models to account for inherent correlations between eyes of the same subject and sequences of the same eye.

4.3 Results

This study included 21,797 SDOCT B-scans from 3,253 eyes of 1,859 subjects with 8,785 sequences of 5 consecutive SD-OCT tests. Table 4.1 shows demographic and clinical characteristics of glaucoma and healthy eyes included in the study. The dataset was split at a patient level with a split ratio of 70:15:15 for training, validation, and testing. The model was fit to the dataset by training using the SGD algorithm. Model training was stopped when training loss and accuracy reached a stable and satisfactory state, also called convergence. The training process to convergence is given in Figure 4.2.

From the 1225 sequences of OCT scans of the 446 glaucoma eyes in the test set, the fully trained Noise-PU DL model identified 462 sequences (38%) as non-

Table 4.1: Baseline Demographics and Clinical Characteristics for glaucoma and healthy eyes for all subjects included in the study.

	Glaucoma	Normal	Total
No. Subjects	1802	57	1859
No. eyes	3142	111	3253
No. sequences	8165	620	8785
Female Sex (%)¹	54%	66%	55%
Race, Black or AA (%)^{1,3}	24%	60%	25%
Age at baseline (years)¹	65.8 ± 10.4	59.7 ± 11.0	65.6 ± 10.5
Baseline RNFL thickness (μm)^{2,3}	79.4 ± 15.5	96.2 ± 10.1	80.6 ± 15.7
Mean Follow-Up time (years)²	3.6 ± 1.5	2.2 ± 1.0	3.5 ± 1.5
Global RNFL thickness slope (μm/year)^{2,3}	-0.73 ± 1.36	-0.51 ± 1.53	-0.72 ± 1.56

¹ Reported on a patient level.

² Reported on a sequence level.

³ AA = African American; RNFL = retinal nerve fiber layer.

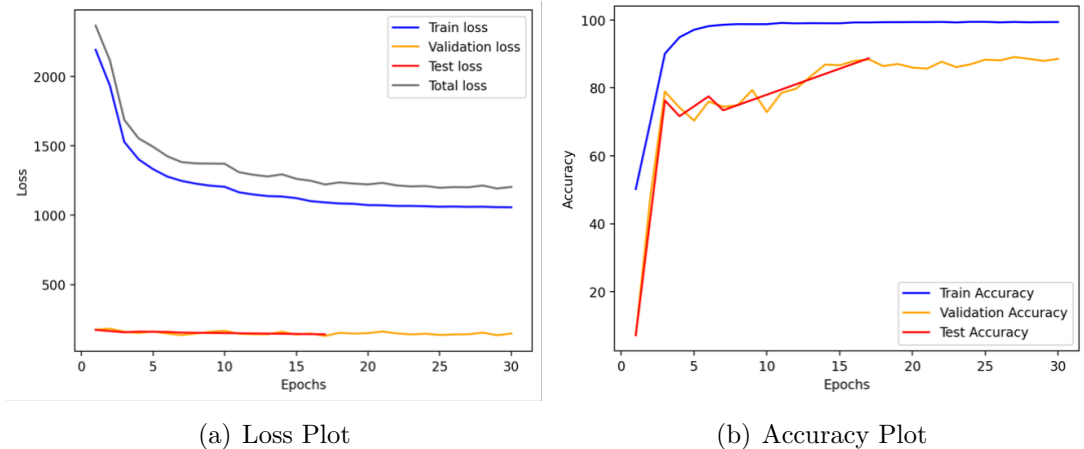


FIGURE 4.2: The Net Loss vs Epochs (left) and Accuracy vs Epochs (right) plots for predictions obtained from the deep learning model trained on the Noise-PU dataset.

progressing and 763 (62%) as progressing. Of note, since the predictions were made at the sequence level and each eye had multiple sequences, the same eye could have

different sequences predicted as non-progressing and progressing. The hit-ratios of the DL and OLS methods were 0.623 (95% CI, 0.595—0.649) and 0.069 (95% CI, 0.056—0.084) respectively ($P < 0.001$) when the specificities were equalized to 0.947 (95% CI, 0.883—0.977). A comparison of performance metrics for the DL model against various conventional, ML and DL methods evaluated on the testing set is summarized in Table 4.2.

Eyes deemed as progressing by the DL algorithm presented significantly faster rates of global RNFL loss compared with those not progressing ($-0.82 \pm 1.50 \mu\text{m}/\text{year}$ vs. $-0.63 \pm 1.54 \mu\text{m}/\text{year}$, respectively; $P = 0.008$). A comparison of the demographic and baseline clinical characteristics of eyes classified as progressing versus non-progressing by the DL model is given in Table 4.3. Glaucoma eyes that were classified as progressing had a significantly longer follow-up time ($P < 0.001$) but presented similar disease severity as determined by the baseline age ($P = 0.395$) and baseline RNFL thickness ($P = 0.704$).

Table 4.2: Comparison of Performance Metrics obtained from predictions by various Machine Learning and Deep Learning methods with the Noise-PU model.

	Input	AUROC¹ (95% CI)	Specificity¹ (95% CI)	Hit-ratio² (95% CI)
OLS				
Regression Method	Global RNFL Mean -		0.947 (0.883–0.977)	0.069 (0.056–0.084)
MLP Classifier	RNFL Thickness	0.509 (0.441 – 0.581)	1.000 (1.000–1.000)	0.000 (0.000–0.000)
FFT-SVM Method	RNFL Thickness	0.779 (0.734 – 0.821)	0.947 (0.899–0.989)	0.441 (0.415–0.467)
WFT-SVM Method	RNFL Thickness	0.749 (0.704 – 0.792)	0.947 (0.896–0.989)	0.418 (0.391–0.446)
PCA-Logistic Method	RNFL Thickness	0.821 (0.779 – 0.859)	0.947 (0.901–0.989)	0.439 (0.415–0.467)
ConvLSTM Network	2D OCT B-scan	0.719 (0.670 – 0.766)	0.947 (0.899 – 0.989)	0.154 (0.136 – 0.174)
SWIN Base Transformer	2D OCT B-scan	0.792 (0.733 – 0.850)	0.915 (0.859 – 0.971)	0.187 (0.164 – 0.208)
Noise Learning Model	2D OCT B-scan	0.583 (0.529 – 0.644)	1.000 (1.000 – 1.000)	0.000 (0.000 – 0.000)
PU Learning Model	2D OCT B-scan	0.711 (0.662 – 0.760)	0.947 (0.899 – 0.989)	0.159 (0.139 – 0.180)
Noise-PU Learning Model	2D OCT B-scan	0.858 (0.832 – 0.885)	0.947 (0.883 – 0.977)	0.623 (0.595 – 0.649)

¹ 95% Confidence Interval obtained from DeLong Method.

² Reported at matched Specificities at 95%.

Two representative examples of the sequence of tests predicted as progression and non-progression, along with the activation heatmaps by the DL model, the RNFL thickness profile change from baseline, sector averages, and global RNFL thickness trend-line, are given in Figures 4.3 and Figure 4.4. Figure 4.3, an eye characterized as progressing by the DL model, shows a significant change in the global average RNFL thickness over time, with prominent loss in the inferior temporal and superior temporal sectors. Although little change would have been seen under manual inspection of the B-scans, the heatmaps emphasize the temporal superior, and temporal inferior regions as the most relevant areas for determining this eye as progressing by our model, in agreement with the expected pattern of glaucomatous damage. In contrast, when an eye was predicted as non-progressing, the heatmaps often highlighted non-retinal structures, like parts of the sclera and vitreous or the nasal sector (Figure 4.4).

Table 4.3: Baseline Demographics and Clinical Characteristics for Glaucoma Eyes in the test set Predicted as Progressing versus Non-Progressing by the Deep Learning model.

	Progression	Non-progression	p-value
No. Subjects	210	145	-
No. eyes	336	195	-
No. sequences	763	462	-
Female Sex (%)¹	51%	51%	1.000 ³
Race, Black or AA (%)¹	24%	29%	0.452 ³
Age at baseline (years)²	68.2 ± 9.9	65.0 ± 10.3	0.395 ⁴
Baseline RNFL Thickness (μm)²	77.4 ± 14.1	84.3 ± 13.9	0.704 ⁴
Mean Follow-Up Time (years)²	3.8 ± 1.6	3.0 ± 1.6	0.001⁴
Mean RNFL Slope ($\mu\text{m}/\text{year}$)²	-0.82 ± 1.50	-0.63 ± 1.54	0.008⁴
Median RNFL Slope ($\mu\text{m}/\text{year}$)²	-0.74 (-1.52 - -0.098)	-0.57 (-1.30 - 0.107)	-

¹ Reported on a patient level.

² Reported on a sequence level.

³ Chi² test.

⁴ LMM nested at the patient and eye levels.

4.4 Discussion

In this study, we developed and validated a novel time-series DL algorithm to detect glaucoma progression in the absence of ground truth labels. The DL method consisted of a CNN-LSTM encoder to learn the spatiotemporal features of a series of SDOCT B-scans taken over a follow-up period. The algorithm was based on weak supervision on a severely imbalanced, partially labeled dataset (PU dataset) aimed to learn the true characteristics of structural progression for glaucoma while accounting for normal age-related loss. This was made possible by dividing the learning process into two steps: (a) PU learning and (b) Noise learning, where PU learning identifies age-related changes, and noise learning discriminates between progressing and non-

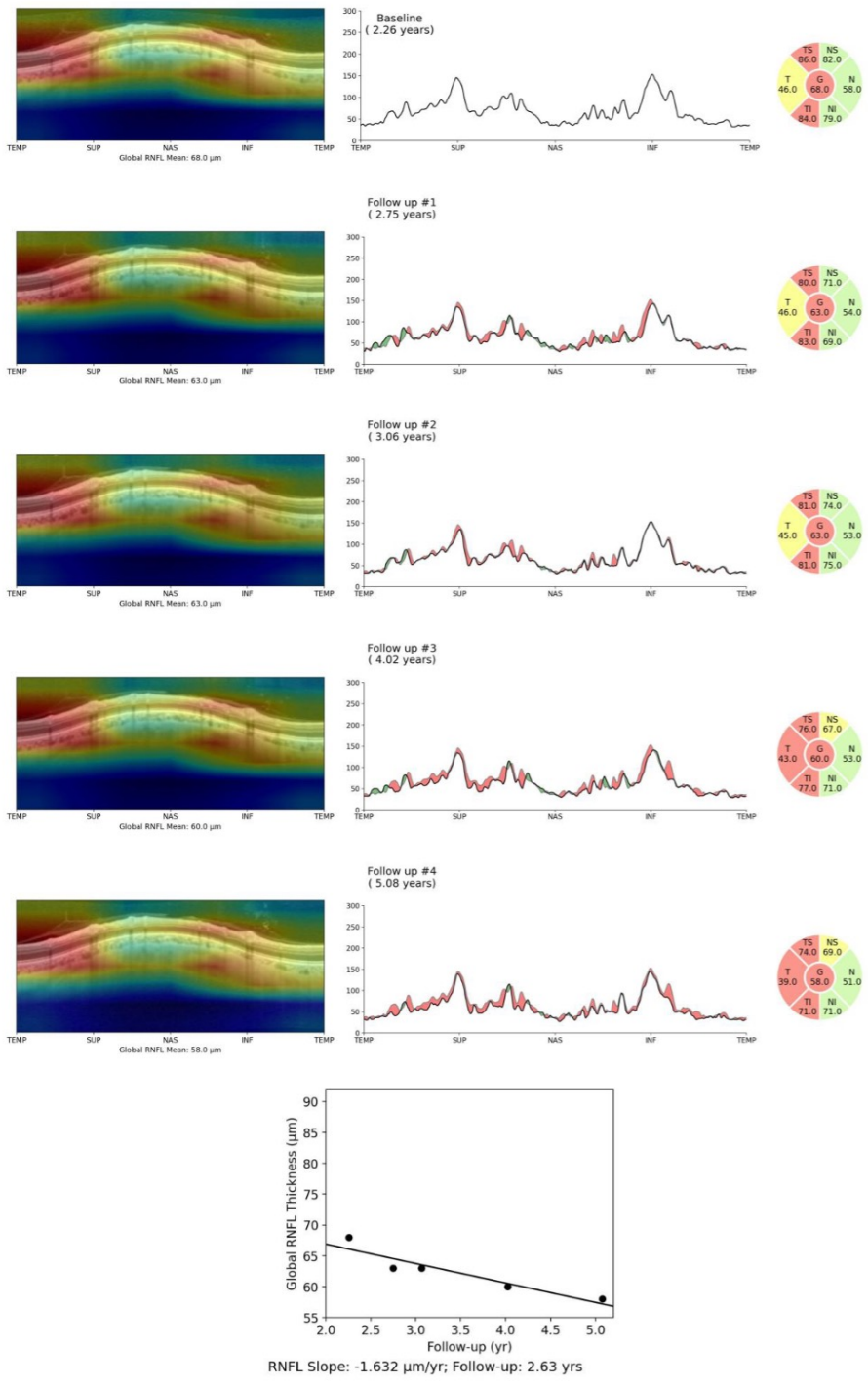


FIGURE 4.3: Representative sequence of a glaucoma eye predicted as progressing by the Noise-PU Model: DL Heatmap (left), RNFL thickness profile (center), RNFL thickness sectors (right), global RNFL trend-line (bottom).

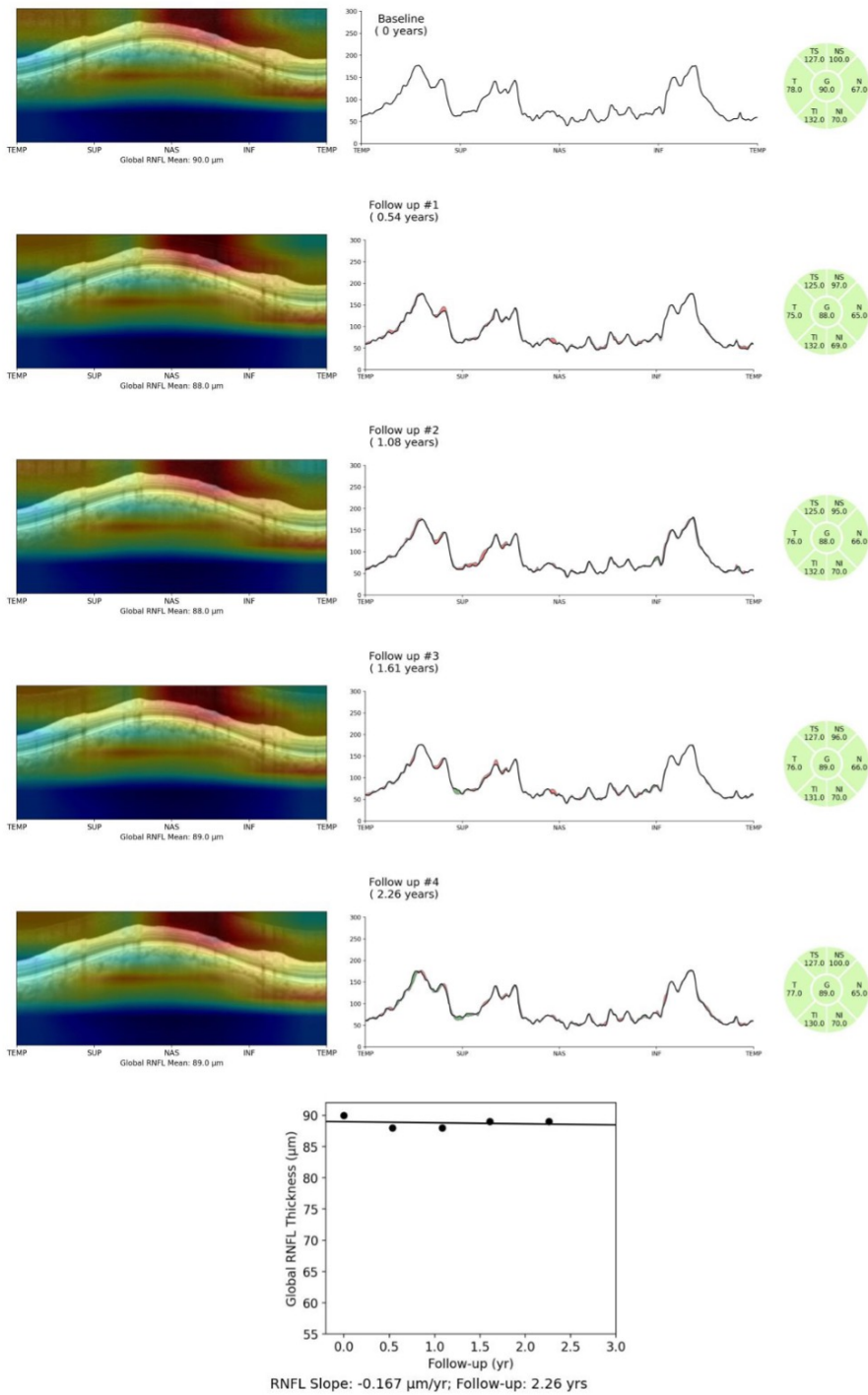


FIGURE 4.4: Representative sequence of a glaucoma eye predicted as non-progressing by the Noise-PU Model: DL Heatmap (left), RNFL thickness profile (center), RNFL thickness sectors (right), global RNFL trend-line (bottom).

progressing RNFL loss. Our methods showed statistically significant improvement over the conventional OLS linear regression for progression detection by obtaining a hit ratio of 62.3% when compared to a hit ratio of 6.9% by the OLS method when the specificities were equalized to 95% ($P < 0.001$). The DL method was also found to outperform other classical ML and DL methods, including advanced methods such as transformers. Ablations studies showed that the combined Noise-PU model performed better than the individual components of the model when tested on the same dataset. In contrast to other works in this area, our algorithm did not rely on any reference standard to detect glaucoma progression.

Although SD-OCT of the retina and optic nerve head has become a widespread diagnostic tool for detecting structural damage, its application for identifying true glaucoma progression remains challenging. Inconsistent structure-function relationship, test-retest variability, age-related loss, and absence of clear reference standards are some of the reasons which have challenged clinicians and researchers in developing new approaches for glaucoma progression analysis (Thompson et al. (2020); Jammal et al. (2020); Abe et al. (2016); Giangiacoimo et al. (2006); Harwerth et al. (1999); Heijl et al. (1989); Medeiros et al. (2012c)). So far, several traditional ML and DL methods have been proposed to diagnose glaucoma progression using human gradings or trend-based analysis as the reference standard (Christopher et al. (2018); Yousefi et al. (2013); Murata et al. (2014)); although they achieve high performance, these methods have considerable drawbacks. For example, human gradings are prone to subjectivity and bias, along with reproducibility issues. On the other hand, it is difficult to differentiate pathological progression from age-related losses, although some statistical approaches have been proposed to improve its specificity (Leung et al. (2013); Wu et al. (2017)). In the absence of a perfect reference standard, some studies have used unsupervised learning to identify patterns for glaucoma progression (Christopher et al. (2018); Sample et al. (2005)). Still, these techniques have

produced either subpar results or present difficulties in real-world implementation (Thompson et al. (2020)), limiting their incorporation into clinical practice. Our approach overcomes these challenges by eliminating the need for a ground truth or a reference standard for progression.

While most PU learning research has focused on utilizing simple features or simple classifiers to model noisy imbalanced data, the DL method we presented estimates the class priors internally by regularizing the PU learning with a surrogate noise learning in the classification stage. This gives the classifier sufficient information to reweight both for class imbalances and partial labeling, thereby preventing overfitting. Our model also bypasses the need for estimating the class priors and reweighting the label frequency to account for sampling bias ahead of time or through a separate density estimator (Huang et al. (2006); Sugiyama et al. (2007)), which are often unavailable and inaccurate for highly imbalanced data, such as datasets in medicine (Su et al. (2021)). Since the DL model uses state-of-the-art expressive neural networks, the algorithm can be easily replicated for complex datasets with unknown class priors while preserving model performance. Therefore, our algorithm has the potential to be translated to other disease progression tasks if similar data on a control group of stable subjects is available. In our case, our model was supplemented by learning features related to age-related change in the SDOCT B-scans from normal eyes in the PU dataset to detect glaucoma progression, but the same architecture could be used for datasets for other progressive eye diseases that affect the retina, such as age-related macular degeneration.

Studying the activation heatmaps from the DL model’s predictions can both provide insight into the most important features used by the model and may help clinicians identify crucial regions in the images that may be missed by the human eye. For instance, in Figure 4.3, the DL model focused on the temporal, temporal superior, and temporal inferior regions of the B-scan images. This essentially means

that the DL model identified that such regions behaved differently than what the model learned was expected from normal aging or noise, ultimately identifying that sequence as progressing. In sequences of images classified as non-progressing (Figure 4.4), the DL method frequently highlighted areas outside the retina, such as parts of the sclera or vitreous, or areas with less probability of progression, such as the nasal sector.

The DL method in this study used information from the whole B-scan image to make determinations about glaucoma progression. While hit ratios indicated a superior ability to detect glaucomatous changes compared to simple OLS linear regression, a limitation of the DL method is that it cannot produce quantitative estimates of the rate of glaucoma progression (Abe et al. (2016)). On the other hand, although rates can be estimated from the OLS model, it is a simplistic approach that relies on the global peripapillary RNFL thickness, making it susceptible to information loss and possibly affected by segmentation errors. Although trend analysis can also be applied to sectors, it is often unclear how to consider the many different slopes from all possible sectors for the assessment of change. It is interesting to note that the performance of OLS regression in this study was inferior to those of some previous investigations. The likely reason for that was because the evaluation was done on sequences of only 5 tests over time, which may have limited the precision of OLS estimates. However, in clinical practice clinicians are often faced with the challenge of making decisions based on a small number of tests available over time.

This study had limitations . Despite the superior hit-ratio at matched specificities of the deep learning algorithm compared to OLS, at this time, there is no other way to confirm cases of progression. Although subjective assessment could be used, this would negate the very motivation of using the proposed approach to train the models. Although the heatmaps contribute to indicate the clinical relevance of the findings, these maps were obtained through a method called score-based class

activation maps (CAM) technique. Findings from CAM methods are solely built to highlight CNN activations and caution should be exercised when extrapolating its results for clinical interpretation. Of note, we have also limited the present analysis to sequences of 5 images over time. However, the model could be expanded to consider longer sequences in the future. Finally, while our work shows promising results for the proposed approach, external validation should still be performed in datasets from different populations.

In conclusion, we demonstrated that a DL model can identify glaucomatous progression using a weakly supervised learning framework that learned features related to normal aging, and was able to differentiate change from test-retest noise. The proposed approach could potentially be expanded to other imaging modalities or diseases where a perfect reference standard for progression is lacking.

Regularized - Contrastive Learning to Predict Functional Glaucoma Progression Using Longitudinal OCT Scans.

The research discussed in this chapter was collaboratively carried out with Alessandro A. Jammal, MD, PhD and Felipe A. Medeiros, MD, PhD.

An abstract of the work is in review at the Investigative Ophthalmology & Visual Science, ARVO, 2023.

5.1 Introduction

This chapter builds on the previous chapter to propose a novel DL algorithm to predict SAP progression from longitudinal OCT scans. The rate of glaucoma progression can be difficult to predict due to confounding risk factors, uncertainty in prognosis, and limitations in tests, which has allowed detecting and predicting glaucoma progression as an emerging field in glaucoma research (Susanna Jr (2009); Omodaka et al. (2022); Termote and Zeyen (2010)). The above reasons along with the evolution and reliance on computer-aided algorithms for clinical diagnosis have motivated researchers to focus on the development of new algorithms to capture disease characteristics (Giangiacomo et al. (2006)). Recently, DL methods have been the forefront for computer-aided diagnosis and detection of glaucoma progression (Thompson et al. (2020); Guergueb and Akhloufi (2023)).

There is no gold standard test nor unified approach to evaluate glaucoma progression. Subjective clinical judgments for glaucoma progression require expertise and are prone to biases, uncertainty, and judgment errors (Thompson et al. (2020);

Mariottoni et al. (2023)). Thus, clinicians prefer assessment using objective criteria and quantitative methods to assess glaucoma progression. Amongst all forms, SAP testing and Optic Disc photography are the most common and emerging measures for diagnosis, screening, and assessment of the rate of change of glaucoma (Alencar and Medeiros (2011); Yaqoob et al. (2005)). SAP test measures visual field loss and changes over time by mapping patients' responses to contrast stimuli (Lucy and Wollstein (2016)). Due to subjectivity and cognitive fatigue accrued during testing, SAP tests are subject to limitations such as test-retest variability and reproducibility (Yohannan et al. (2017)). On the other hand, SDOCT, an important test for glaucoma diagnosis, is a non-invasive test that measures structural loss by quantifying the ONH and RNFL Thickness (Gracitelli et al. (2015b); Strouthidis et al. (2010)). In contrast to SAP tests, SD-OCT is objective and precise, producing high-resolution RNFL information with excellent reproducibility (Abe et al. (2016)). However, monitoring glaucoma through SDOCT is sometimes slow, requires a high degree of expertise, and becomes unreliable in advanced stages (Thenappan et al. (2021)).

Previous studies have shown an association between RGC loss and visual field damage (Garway-Heath et al. (2002)). Research has shown that decreased RGC count usually precedes the vision loss observed through SAP tests (Harwerth et al. (1999)). Clinicians and researchers have applied different statistical approaches such as joint survival, longitudinal and event-based, and mixed-effect models to predict glaucoma progression using structure and function relationship (Medeiros et al. (2011, 2009a); Nouri-Mahdavi et al. (2021)). However, no consensus has been found on the modeling criteria that can accurately capture glaucoma progression (Abe et al. (2016)). Owing to the nuances and subtleties in glaucoma progression, the DL approach becomes a potential way to identify complex patterns in raw structural data.

Artificial intelligence (AI) algorithms, especially DL methods, are becoming an emerging field for glaucoma progression prediction and detection. Recent studies have shown that DL methods can overcome some statistical methods' limitations in understanding the glaucoma progression criteria (Mariotoni et al. (2023); Hou et al. (2023); Meira-Freitas et al. (2013)). These studies have emphasized using RNFL information from longitudinal SD-OCT scans to predict visual field worsening. But ubiquitously, these studies still need to address data imbalance, covariate shift, and noise. These also need universal gold standard criteria for evaluation. Recently, a gated transformer network (GTN) obtained state-of-the-art performance to predict visual field worsening with longitudinal OCT RNFL Thickness data. This study used an ensemble of objective and subjective criteria to obtain visual field worsening (Hou et al. (2023)). This study showed the critical need for an accurate gold standard criterion to measure the DL method's performance. A proper gold standard represents an accurate structure-function relationship and reduces false positives in the DL model's predictions for glaucoma progression. In another study, a CNN-LSTM DL model trained on longitudinal SD-OCT images was able to distinguish between glaucoma progressing and non-progressing using only the knowledge of a healthy cohort (Mandal et al. (2023)). This study used weak supervision to teach age-related structural deterioration and showed that the DL model generalizes well on progressing samples.

In this study, we developed a DL method that improves the previous models to detect glaucoma progression. We use a combination of 1) standard binary classification to predict SAP progression using original OCT sequences; 2) training on a subset of adversarially augmented, selective shuffled sequences to improve model robustness; and 3) applying self-supervised contrastive learning between original and shuffled datasets to discern "true" representations of change over time. The selective shuffling process is an extension of the research in the previous chapter, which uses

random shuffling to generate "hard negatives" for progression (Mandal et al. (2023)). SimLR contrastive learning was added to learn contrastive artifacts between original and adversarially augmented images, learning underlying data distribution from potentially noisy data (Chen et al. (2020); Xue et al. (2022)). Overall, the combined approach, in conjunction with the label-smoothed classifier and contrastive learning, was aimed to reduce classification noise, improve performance stability, and enhance the predictive accuracy of the base classifier. We use SAP GPA, an event-based method, to determine clinically relevant visual field loss outcomes as the reference criteria. It reports consistently high specificity amongst all other SAP progression techniques (Nguyen et al. (2019); Rabiolo et al. (2019)). We compare and evaluate the DL model's performance in identifying glaucomatous progression, specifically specificities and hit ratios, against clinically validated and recent state-of-the-art algorithms for glaucoma progression (Nouri-Mahdavi et al. (2021); Medeiros et al. (2009a); Hou et al. (2023); Medeiros and Jammal (2023)).

5.2 Methodology

The data set used in this study is derived from a retrospective cohort study of patients from a database registry containing tests with longitudinal structural and functional changes in eyes. The database contains EHRs of subjects seen at the Bascom Palmer Eye Institute, University of Miami, Florida, and Duke University, Durham, North Carolina. This study was approved by the institutional review board from both institutes, along with a waiver of informed consent for being a retrospective study. Data collection methods adhered to the Declaration of Helsinki's tenets and the Health Insurance Portability and Accountability Act regulations for Human Research.

To qualify for the study, subjects needed to have a diagnosis of open-angle glaucoma based on the international classification of disease (ICD) codes, a minimum of 5 reliable VF SAP tests (Humphrey Field Analyzer II, Carl Zeiss Meditec, Inc.),

and 5 reliable SDOCT (Spectralis, Heidelberg Engineering GmbH, Dossenheim, Germany) scans at an age over 18 years. Glaucoma was defined as having the Glaucoma Hemifield Test outside normal limits or Pattern Standard Deviation with $P < 5\%$. Individuals who did not conform to the criteria mentioned above or had a history of other ocular or systemic diseases that could affect the optic nerve or visual field were excluded. Subjects were also excluded if the tests were performed after treatment with photocoagulation as per CPT codes.

The dataset consisted of longitudinal scans of the retina around the optic nerve head (ONH) obtained from the Spectralis SD-OCT (Heidelberg Engineering, Heidelberg, Germany) over routine clinical care. The acquisition protocol has been described in detail previously (Leite et al. (2011)). In summary, each SDOCT scan in the longitudinal series consisted of a cross-sectional image of the retina (B-scans; 768 x 496 points) with the peripapillary circular scanning pattern of 3.5 diameters around the ONH. This scan pattern has been established as the gold standard for the evaluation of structural glaucomatous damage by identifying the thinning of the RNFL thickness at a micrometer scale. The global average of the RNFL thickness for each scan was recorded and used as a comparison for the model (see Model Evaluation section below). Scans were excluded if they had segmentation or artifact errors or the quality score was lower than 15, according to the manufacturer’s recommendation. Each observation for an eye consisted of five equally spaced sequences of successive good-quality SDOCT Bscan images.

5.2.1 Definition of Glaucoma Progression

We used the Guided progression analysis (GPA; Humphrey Field Analyzer II (HFA II), Carl Zeiss Meditec, Inc., Dublin, USA) as the definition for glaucoma progression criteria. GPA is a proprietary algorithm of HFA that uses pointwise event-based analysis on repeatable visual field loss observed in longitudinal 24-2 SAP tests (Gi-

raud et al. (2010)). The algorithm flags a point on the SAP pattern deviation plot as progression if it exceeds the expected test-retest variability in the follow-up exams in comparison to two baseline exams. If three or more points over three consecutive tests present such deterioration, the algorithm flags the test as “likely progressing” (Wu et al. (2017)). This method produces a relatively simple qualitative measure of glaucoma progression and improves on the other methods by accounting for point-wise test-retest variability, sensitivity, and age (Nguyen et al. (2019)). The results of the algorithm were summarized under a binary classification (progressing vs. non-progressing) and applied to each series of SDOCT B-scan images as the label for the event of glaucoma progression. The date of the first event (out of the three consecutive events of progression) was considered as the date of progression. After a glaucoma progression event, the baseline was reset at the date of the event, and successive SAP tests were again considered to create a new event window. Such event windows were repeated until at most three glaucoma progression events were marked by GPA or no glaucoma progression was observed.

5.2.2 DL Method

A novel DL method was developed to predict whether a longitudinal sequence of SDOCT B-scan images presented glaucoma progression or remained stable. A recent study showed that a hybrid CNN-LSTM model can learn spatiotemporal relationships exhibited by the time series image sequences (Figure 3.9) (Mandal et al. (2023)). We employed a similar architecture for our research. A pretrained ResNet50 residual deep neural network was used as the CNN encoder due to its ability to produce state of the art results even on smaller datasets (He et al. (2016)). 3D-CNN, a 3D variant of CNN, was used as the top layer for its ability to encode short-term time dependencies and relevant spatial features (Parmar et al. (2020)). Due to its ability to learn sequential data, a bidirectional LSTM network was used as a time-series encoder,

which encodes long-term temporal dependencies in the spatial encoding sequence obtained from the encoder. LSTM networks also have memory blocks believed to retain inter and intra-test variability in the data, thereby improving sequence predictions (Mousavi and Afghah (2019)).

Regularized – Contrastive (RegCon) Learning

The DL model used a classification head of several fully connected (FC) layers to generate logits for the classification task. Softmax function was used to compute the probability distribution of labels from the logits to train with categorical cross-entropy (CCE) loss (Equation 5.1) ¹. The data acquisition to generate features and outcomes for the model is expected to subsume label noise. As studies have shown that DL methods trained with CCE loss are sensitive to label noise (Feng et al. (2021)), finding a training protocol robust to noisy data is of utmost importance. Following the research outcomes of the previous chapter, which showed that identifying test variability due to normal aging in longitudinal SDOCT images could improve DL model performance (Mandal et al. (2023)), we create a parallel learning step to generate a subset of randomly shuffled sequence data to introduce "hard negatives." This step, called selective shuffling, generates negative (non-progressing) samples by shuffling image sequences with probability p if they are progressing set and $(1 - p)$ if they are non-progressing set in the training data. All the images in each image sequence are adversarially augmented (Wang and Qi (2022)) to introduce sufficient regularization and structural invariance. Using the novel DL algorithm discussed earlier, we create this learning step as a label-smoothed binary classifier due to increased imbalance in the modified dataset (Equation 5.2).

A third learning step with self-supervised contrastive learning was introduced to

¹ The loss objective CCE is used interchangeably with BCE from Section 3.5 since the CCE is done over two categories.

mitigate the effects of label noise. Unlike other methods that improve robustness, contrastive learning produces generalizable and transferable results. Specifically, we use the SimCLR contrastive learning framework over the CNN-LSTM encoder on the original and modified dataset to identify reliable time-series representations of image sequences. Without going into details, SimCLR is an unsupervised learning method used to generate good representations of the data by comparing and contrasting with different perspectives of the original sequences through strong data augmentations (Wang and Qi (2022)). The loss function for SimCLR is given in Equation 3. The use of selective shuffling with adversarial (strong) data augmentation helps the model discern "true" representation of structural loss over time.

Overall, the original and augmented sequences were passed through the CNN-LSTM encoder to obtain their respective time-series feature encodings. A Classification Head generated logits or probability measures for both the datasets simultaneously, which was used for Binary classification (Equation 5.1) and Label-Smoothed Binary Classification (Equation 5.2). With the time-series encodings as input, two different projection heads made of FC layers were used to learn contrastive representations of the original and augmented features from the DL model. A contrastive loss given by Equation 5.3 was used to maximize the agreement between representations by aligning the data distributions (negative and hard negatives) of the original and augmented sequences. This small addition improves the model's performance on real-world data exhibiting label noise and variability. Equation 5.4 defines the overall objective function for the DL model. α and β represent the contributions of the Label-Smoothed Classifier and SimCLR loss in the joint training approach. The RegCon Learning model architecture is shown in Figure 5.1.

$$L_{CCE} = -\frac{1}{N} \sum_{i=1}^N Y_{t,i} \log(Y_{p,i}) \quad (5.1)$$

$$L_{smooth-CCE} = -\frac{1}{N} \sum_{i=1}^N \bar{Y}_{t,i} \log(Y_{p,i}); \bar{Y}_{ti} = (1 - \mu)Y_{ti} + \frac{\mu}{K} \quad (5.2)$$

$$L_{simCLR} = \frac{1}{2N} \sum_{k=1}^N [L_{\text{pos}(2k-1,2k)} + L_{\text{pos}(2k,2k-1)}] \quad (5.3)$$

where, $L_{\text{pos}(i,j)} = -\log\left(\frac{\exp(\text{sim}(Z_i, Z_j)/\tau)}{\sum_{k=1}^{2N} \mathbb{1}_{[k \neq i]}\exp(\text{sim}(Z_i, Z_j)/\tau)}\right)$ and $\text{sim}(u_i, u_j) = \frac{u_i \cdot u_j}{\|u_i\|_2 \cdot \|u_j\|_2}$;

$$L_{\text{Joint}} = L_{\text{CCE}} + \alpha \cdot L_{\text{smooth-CCE}} + \beta \cdot L_{\text{simCLR}} \quad (5.4)$$

5.2.3 Training and Validation

The DL model’s inputs consist of a pair of original observation sequences for glaucoma progression prediction, a selectively shuffled, adversarially augmented view of the same observation of label-smoothed classification, and a subsequent contrastive learning loop. Each observation comprised a series of 5 successive SD-OCT B-scan images resized to 224×224 pixels. The model was trained with a data split of 70% training set, 10% validation set, and 20% testing set with a batch size 48.

The model was trained to optimize the objective function given in Equation 5.4. The values of α and β were set to 1 each after empirical analysis. A likely reason for this hyperparameter setting might be that a lower value prioritizes CCE, which might overfit, and a higher value prioritizes label smoothing or contrastive learning, which over regularizes. The objective function was optimized with an l_2 regularized stochastic gradient descent (SGD) algorithm with a learning rate of 0.002, a momentum of 0.9, and a weight decay of 0.1 for 120 epochs. Cosine Annealing with Warm Restarts was used to search the learning rate space for optimal learning rate. Models at training epochs were saved if the validation loss of the model at that epoch was lower than in previous epochs. The cumulative sum of original validation

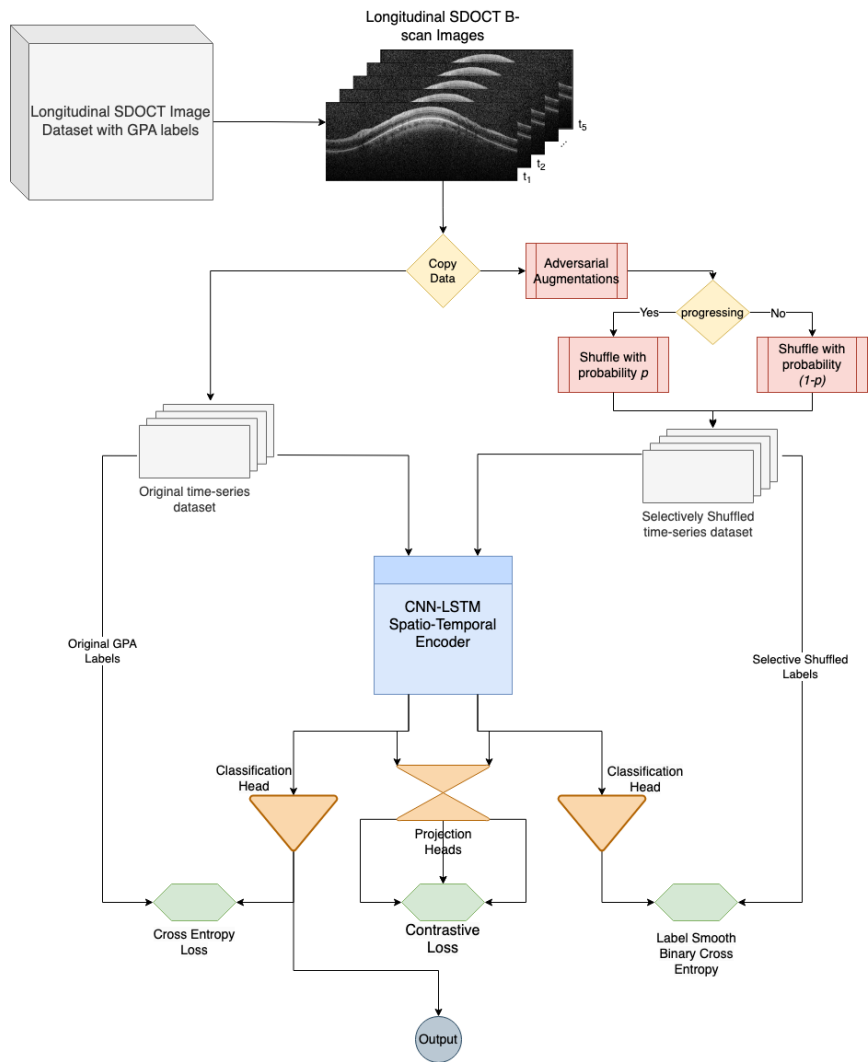


FIGURE 5.1: An overview of the RegCon CNN-LSTM Network: made of three DL loops, main VF GPA classifier (left), selective shuffled label smoothed classifier (right) and self-supervised contrastive learning (center).

specificity and sensitivity was compared for every such model to obtain the best DL model setting. All training and testing were done on the latest Pytorch snapshot in Python 3.8. Logit predictions produced by the classification head of the DL model represented the final outcome of glaucoma progression.

5.2.4 Model Evaluation and Statistical Analysis

We determined that the DL model achieved convergence when the validation loss stabilized and accuracy reached a satisfactory plateau. The receiver operator characteristic (ROC) curve, with the AUC, and the precision-recall (PR) curve, with the average precision (AP), was used to assess the discriminative power of the overall DL model. Accuracy, sensitivity (hit ratio; specificity matched at 95%), precision, f1-score, and Matthew’s correlation coefficient (MCC) were some metrics used to assess model performance. To appraise the model’s performance regarding true prediction ability and relevance, these performance metrics were compared with the GTN-based DL algorithm (Hou et al. (2023)) and a conventional non-DL approach, OLS Linear Regression. OLS is the currently widely accepted clinical standard that determines eyes as glaucoma progressing if the rates of change of the peripapillary RNFL thickness shows a significant ($P < 0.05$) negative slope during analysis (Wu et al. (2017)).

All these models underwent training and evaluation on the same dataset to ensure fair comparison metrics. Two ablation studies, by removing (a) Contrastive Learning, and (b) both the Label-Smoothed Classifier and contrastive Learning, were performed. The ablation studies necessitated evidence that joint training was essential for the study. The DL model was considered superior if it outperformed other methods in most metrics. As a final indicator of model performance, hit ratios and specificities for the DL method were compared to others. McNemar’s test between our DL model’s predictions and other methods provided significance in the prediction ability. Additionally, the demographics and clinical characteristics of the eyes were compared for clinical validation. Cohen’s kappa between the model’s prediction and GPA progression criteria for the test set showed the level of agreement between the two. Finally, a real-life test example of the predicted progressing eye was presented

to analyze the DL model’s interpretation of input sequences to classify from complex data.

5.3 Results

Table 5.1: Baseline Demographics and Clinical Characteristics for Progressing and Non-progressing Subjects based on the GPA criteria.

	Non-progression by GPA	Progression by GPA	Total
No. Subjects	415	42	424
No. eyes	593	45	614
No. sequences	593	56	649
Female Sex (%)¹	51.1%	41.1%	50.2%
Race, Black or AA (%)^{1,3}	27.5%	19.6%	26.8%
Age at baseline (<i>years</i>)¹	65.1 ± 10.1	70.3 ± 9.3	65.5 ± 10.2
Baseline RNFL thickness (μm)^{2,3}	77.5 ± 16.0	67.0 ± 14.0	76.6 ± 16.1
Mean OCT Follow-Up time (<i>years</i>)²	5.6 ± 1.3	3.2 ± 1.2	5.4 ± 1.5
Mean RNFL thickness slope ($\mu\text{m}/\text{year}$)^{2,3}	-0.64 ± 1.04	-0.70 ± 1.47	-0.65 ± 1.08
Mean SAP Follow-Up time (<i>years</i>)^{2, 3}	7.2 ± 2.8	4.6 ± 3.3	7.0 ± 2.9
SAP MD at Baseline (<i>dB</i>)^{2, 3}	-3.4 ± 4.5	-10.8 ± 7.0	-4.0 ± 5.2
Mean SAP MD slope (<i>dB/year</i>)^{2,3}	-0.09 ± 0.30	-0.52 ± 0.34	-0.13 ± 0.33

¹ Reported on a patient level.

² Reported on a sequence level.

³ AA = African American; RNFL = retinal nerve fiber layer; SAP = standard automated perimetry.

The demographics and clinical characteristics of the dataset used in this study are given in Table 5.1. The study included 3178 SD-OCT B-scans and 4091 SAP tests from 614 eyes of 424 subjects. 9% or 56 of the original sequences (45 eyes) were classified as progressors based on the GPA. The average age at baseline was

65.5 ± 10.2 years, with a mean follow-up of 5.4 ± 1.5 years for the SD-OCT test and 7.0 ± 2.9 years for the SAP tests. The dataset comprised 50.2% females, and 26.8% individuals self-identified as Black or African Americans (AA). Of the 649 SAP series, 56 (8.6%) were identified as glaucoma progressing, and 593 (91.4%) were non-progressing. The baseline SAP mean deviation was -4.0 ± 5.2 dB. The average rate of SAP MD loss was -0.52 ± 0.34 dB/year for the glaucoma progressing group and -0.09 ± 0.30 dB/year for the stable group ($P < 0.001$).

Table 5.2: Dataset distribution used by the DL model at eyes and observation levels for training, validation, and testing set (Sub = Subjects, Seq = Sequences).

	Non-progression by GPA			Progression by GPA			Total		
	No. Sub	No. Eyes	No. Seq	No. Sub	No. Eyes	No. Seq	No. Sub	No. Eyes	No. Seq
Training	252	355	355	25	27	34	258	367	389
Validation	65	89	89	7	7	8	66	93	97
Testing	98	149	149	10	11	14	100	154	163
Total	415	593	593	42	45	56	424	614	649

The data was split at a patient level for training, validation, and testing, shown in Table 5.2. The demographics and clinical characteristics of progressing and non-progressing eyes in the test set are shown in Table 5.3. The training was done to fit the DL model to the dataset using the SGD algorithm till the loss and accuracy reached a stable and satisfactory state. Figure 5.2 shows the loss and accuracy plots for training and testing the DL model. Evaluation of the testing set showed that the model identified 14 sequences (11 eyes; 8.6%) as glaucoma progressing and 149 sequences (145 eyes; 91.4%) as non-progressing. It is to be noted that each eye could have multiple GPA progressing or non-progressing events. Table 5.4 compares performance metrics between different models used in other studies. Figure 5.3 shows

the predictive performance of glaucoma progression (ROC curve and PR curve plots) for all the methods. Both Table 5.3 and Figure 5.3 suggest that our DL model outperforms all other approaches. Our DL obtained an AUC score of 0.894 (95% CI; 0.825 - 0.963). In comparison, AUC for other methods was 0.861 (95% CI; 0.785 - 0.937) for CNN-LSTM + Selective Shuffling (ablation study 1), 0.861 (95% CI; 0.783 - 0.940) for GPA trained GTN (Hou et al. (2023)), 0.842 (95% CI; 0.757 - 0.926) for CNN-LSTM model (ablation study 2). The average precision of our model (0.448) was higher than all other methods as well (0.273 - 0.407). A comparison of hit ratios at equalized specificities showed that our DL method produces better predictions when compared to other methods. Our DL Model correctly identified OCT test sequences as glaucoma progressing with a hit ratio of 0.500 (95% CI; 0.492 - 0.508) versus 0.286 (95% CI; 0.278 - 0.293; $P < 0.001$) for CNN-LSTM + Selective Shuffling, 0.143 (95% CI; 0.137 - 0.149; $P < 0.001$) for GPA trained GTN, 0.071 (95% CI; 0.067 - 0.076; $P < 0.001$) for CNN-LSTM, 0.071 (95% CI; 0.067 - 0.076; $P < 0.001$) for OLS Regression method, current widely used to evaluate glaucomatous structural progression in routine care (all specificities matched at 95%).

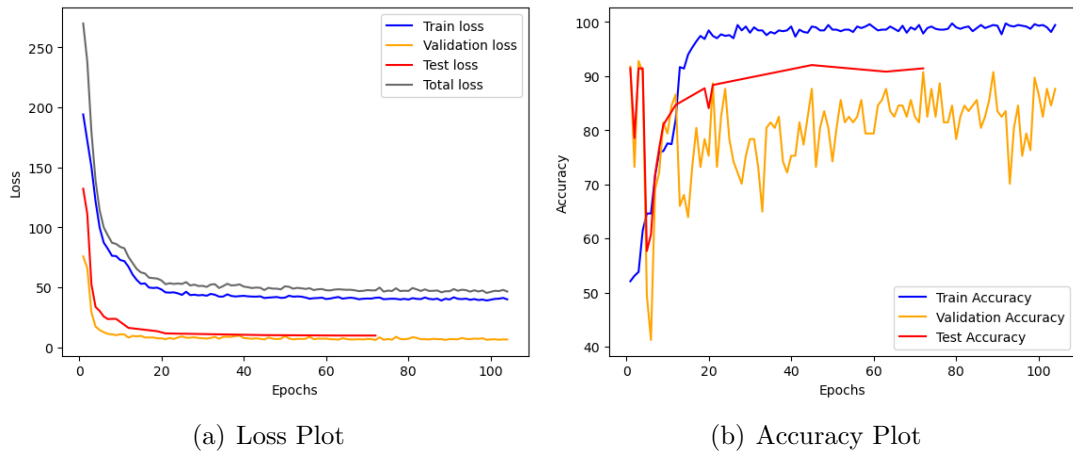


FIGURE 5.2: The (a) Net Loss vs Epochs and (b) Accuracy vs Epochs plots during Reg-CON Model training for glaucoma progression detection.

Table 5.3: Baseline Demographics and Clinical Characteristics of the Test Set based on GPA reference standard.

	Non-progression by GPA	Progression by GPA	p-value
No. Subjects	98	10	-
No. eyes	149	11	-
No. sequences	149	14	-
Female Sex (%)¹	42.9%	30.0%	0.653 ³
Race, Black or AA (%)¹	28.6%	10.0%	0.374 ³
Age at baseline (years)²	63.1 ± 11.7	73.4 ± 6.2	0.167 ⁴
Baseline RNFL thickness (μm)²	77.8 ± 14.7	65.7 ± 12.5	0.180 ⁴
Mean OCT Follow-Up time (years)²	5.4 ± 1.3	3.0 ± 1.1	0.000⁴
Mean RNFL slope (μm/year)²	-0.35 ± 1.40	-0.58 ± 1.28	0.998 ⁴
Mean SAP Follow-Up time (years)²	7.3 ± 2.9	4.5 ± 3.0	0.009⁴
Mean SAP MD slope (dB/year)²	-0.07 ± 0.33	-0.51 ± 0.42	0.007⁴

¹ Reported on a patient level.

² Reported on a sequence level.

³ Chi² test.

⁴ LMM nested at the patient and eye levels.

⁵ Boldface indicated statistical significance ($P < 0.05$).

Table 5.5 compares the demographic and clinical characteristics of the classifications obtained from our DL model. Eyes that were predicted as glaucoma progressing had a faster rate of RNFL Thickness loss ($-0.59 \pm 1.30\mu m/year$ vs. $-0.27 \pm 1.25\mu m/year$; $P = 0.695$) although significance was not obtained. Comparing the SAP MD slopes, the DL model obtained a significantly faster rate of SAP MD loss over time ($-0.39 \pm 0.30dB/year$ vs $-0.09 \pm 0.35dB/year$; $P = 0.013$) when comparing progressing and non-progressing sequences. These clinical characteristics resembled the clinical and demographic characteristics obtained from the GPA progression criteria with moderate agreement (cohen’s kappa, $\kappa = 0.453$). Fig-

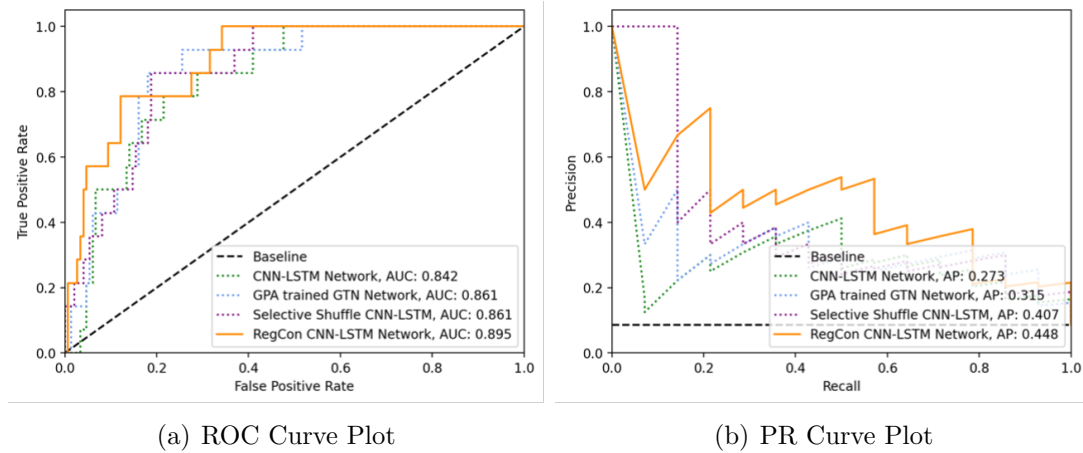


FIGURE 5.3: (a) Receiver Operating Characteristic (ROC) Plot and (b) Precision Recall Plot for different DL methods with the RegCon Model evaluated on the test set for glaucoma progression.

Figure 5.4 shows a representative example of the SDOCT B-scan sequence predicted as progressing by our DL model. The class activation heatmaps (CAM) from the DL method show that the model focuses on the Nasal Superior and Nasal Inferior regions as most progressing, which is reflected by the RNFL Thickness profile.

Table 5.4: Comparison of Performance Metrics across conventional and different DL model configurations trained and evaluated on our dataset.

Model	Input	AUROC (95% CI)	Accuracy (95% CI)	Sensitivity (95% CI)	Specificity (95% CI)	Precision (95% CI)	F1 Score (95% CI)	MCC Score (95% CI)
GPA trained								
GTN Classifier	RNFL Thickness Estimates	0.861 (0.783 - 0.940)	0.890 (0.888 - 0.891)	0.143 (0.137 - 0.149)	0.960 (0.959 - 0.961)	0.250 (0.241 - 0.260)	0.182 (0.177 - 0.187)	0.133 (0.133 - 0.134)
CNN-LSTM Classifier	SDOCT B-scans Images	0.842 (0.757 - 0.926)	0.883 (0.882 - 0.885)	0.071 (0.067 - 0.076)	0.960 (0.959 - 0.961)	0.143 (0.135 - 0.151)	0.095 (0.091 - 0.099)	0.043 (0.043 - 0.043)
Selective Shuffle CNN-LSTM	SDOCT B-scans Images	0.861 (0.785 - 0.937)	0.896 (0.894 - 0.897)	0.286 (0.278 - 0.293)	0.953 (0.952 - 0.954)	0.364 (0.355 - 0.373)	0.320 (0.314 - 0.326)	0.267 (0.266 - 0.267)
RegCon CNN-LSTM	SDOCT B-scans Images	0.895 (0.825 - 0.963)	0.920 (0.919 - 0.922)	0.500 (0.492 - 0.508)	0.960 (0.959 - 0.961)	0.538 (0.530 - 0.547)	0.519 (0.512 - 0.525)	0.475 (0.475 - 0.476)

¹ All metrics reported at a specificity equalized to 95%.

² 95% Confidence Interval for AUROC obtained from DeLong Method.

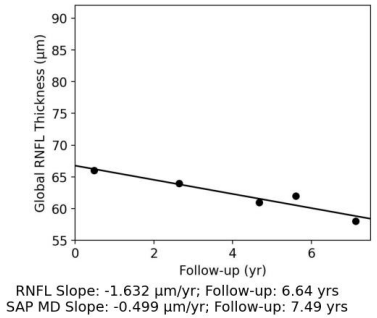
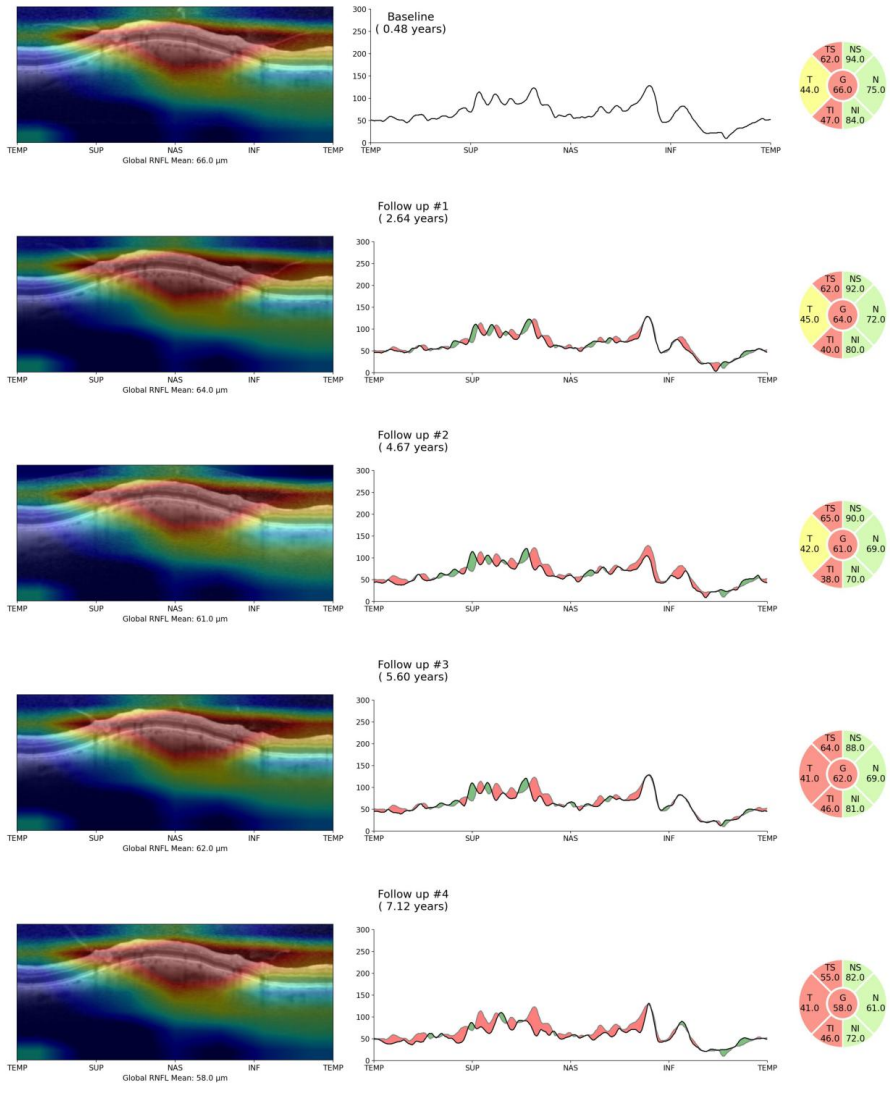


FIGURE 5.4: Representative example sequence of an eye predicted as glaucoma progressing by the RegCon CNN-LSTM Model: DL Heatmap (left), RNFL thickness profile (center), RNFL thickness sectors (right), global RNFL trend-line (bottom).

Table 5.5: Comparison of Baseline Demographics and Clinical Characteristics for eyes predicted as Progressing versus Non-Progressing by RegCon CNN-LSTM model.

	Non-progression by DL Model	Progression by DL Model	p-value
No. Subjects	97	12	-
No. eyes	146	12	-
No. sequences	149	14	-
Female Sex (%) ¹	41.2%	25.0%	0.440 ³
Race, Black or AA (%) ¹	28.9%	16.7%	0.582 ³
Age at baseline (years) ²	63.3 ± 11.8	71.4 ± 7.5	0.757 ⁴
Baseline RNFL thickness (μm) ²	78.1 ± 14.4	62.3 ± 11.7	0.161 ⁴
Mean OCT Follow-Up time (years) ²	5.3 ± 1.4	4.1 ± 1.8	0.877 ⁴
Mean RNFL slope (μm/year) ²	-0.27 ± 1.25	-0.59 ± 1.30	0.695 ⁴
Mean SAP Follow-Up time (years) ²	7.2 ± 2.9	5.5 ± 4.5	0.449 ⁴
Mean SAP MD slope (dB/year) ²	-0.09 ± 0.35	-0.39 ± 0.30	0.013 ⁴

¹ Reported on a patient level.

² Reported on a sequence level.

³ Chi² test.

⁴ LMM nested at the patient and eye levels.

⁵ Boldface indicated statistical significance ($P < 0.05$).

5.4 Discussion

In this study, we developed and validated a novel DL algorithm that detects the presence of glaucoma progression from data and labels obtained from different sources. The DL model used longitudinal structural SD-OCT B-scan images as inputs and functional VF GPA as the reference standard for model training. The DL model used a CNN-LSTM spatiotemporal encoder to identify progression artifacts from longitudinal scans. In addition to standard classification, the algorithm consisted of joint learning with a label smoothing classification step and a self-supervised contrastive

learning step to learn the underlying data distribution from noisy labeled - highly imbalanced data. The label-smoothed selective shuffling process increases the specificity by teaching the DL model to discern non-progressing samples using a subset of "hard negatives." The representations of the original and augmented data were further used to regularize the CNN-LSTM encoder with SimCLR-based contrastive learning to identify any time-series or structural image invariances and other sources of noise and discern "true" representations of change over time. The DL model we developed addressed several data challenges, such as small dataset size, label noise, and class imbalance issues observed in glaucoma progression detection.

Our model improves on the previous methods by producing a good approximation of functional outcomes from longitudinal structural scans without reliance on clinical expertise or post-acquisition software algorithms. Unlike other methods, including the state-of-the-art GTN model, which uses clinical data preprocessing, tabular biomarkers, or clinicians' supervision while data acquisition (Hou et al. (2023)), our approach uses a longitudinal sequence of SDOCT B-scan images, which are readily available at acquisition, without further processing or application of segmentation algorithms. This algorithm is one of the recent advances of its kind to detect functional glaucoma progression using direct longitudinal structural OCT image data requiring minimal expertise.

Since this study used events of progression as flagged by the GPA clinical algorithm as the reference standard for glaucoma progression, the longitudinal structural features learned by the DL model from the OCT images can be assumed to be a close approximation of the structure-function relationship that would lead to clinically relevant functional damage in glaucoma. The temporal features observed in longitudinal SDOCT B-scans by our model can reveal patterns of functional loss. Thus, our models overcome the difficulties observed in traditional approaches, which could not formulate true glaucoma progression criteria. Furthermore, ablation stud-

ies prove incorporating contrastive learning ensures the DL model learns functional deficits from structural changes accurately. This is particularly important because earlier methods could not identify at which stage test variability exceeds the limits for advancing glaucoma progression. Since glaucoma progression manifests as RNFL Thinning over time, our DL method can learn the variability and distinguish between "true" representations glaucomatous damage over time from other factors.

It is worth mentioning that the lower performance of the other methods on our dataset stems from the fact that other techniques are still needed to resolve data distribution and label noises. Our algorithm tries to mitigate this noise using an additional classification step with selective shuffled, adversarially augmented data. The selectively shuffled, adversarially augmented data generates a better decision boundary between progressing and non-progressing sequences by introducing hard negatives in the dataset. This classification step uses a label smoothing classifier, which teaches the model to accurately distinguish non-progressing eyes, thereby increasing specificity (Mandal et al. (2023)). As longitudinal analysis of SD-OCT B-scans by design might be prone to test-retest variability and hinder the model's performance, a SimCLR-based contrastive learning step was added to identify and regularize time-series and structural image invariance (Xue et al. (2022)). It pushes the model to recognize only relevant features across different time points and reduce the influence of noise while learning artifacts in the SDOCT B-scans, improving prediction stability and adding generalization to the model. The joint learning makes our model more robust to variations during image acquisition conditions, increasing the DL model's performance, as seen in the ablation studies (Table 5.4).

Clinicians and researchers like to understand specific SD-OCT characteristics that contribute to glaucoma progression at various stages of the patient's life and their impact on the disease outcomes. Saliency heatmaps obtained by our DL model's activation layers using the CAM method highlight regions of interest for glaucoma

(Figure 5.4). These regions of interest show evidence that the DL model looks at specific RNFL layers for discrimination. In the representative example, the DL method focuses more on Nasal Superior, Nasal Inferior, and parts of Temporal Inferior regions to determine progression. This was also reflected in the adjoining RNFL thickness profile and RNFL sector maps. We also saw that some Temporal regions showing signs of progression in the RNFL thickness profile were not highlighted by the DL model. A likely reason for this might be these regions showed uniform RNFL thickness loss, which might not have significant slopes and, therefore, not picked by our DL method. Since our study did not focus on pinpointing the exact conditions or features that influence glaucoma’s progression, additional investigation of the DL model’s interpretability of glaucoma features should be done with caution. However, our DL method improves over traditional interpretation techniques by adding a time-series component of glaucoma, facilitating the identification of glaucoma progression features. While it is not investigated in this study, a statistical analysis of the representation space holds significant potential to explore disease progression mechanisms, identify severity stages, and provide insights into localized deterioration for more targeted and effective treatment strategies.

The DL model we developed achieved high performance for predicting progression (AUC 0.894 (95% CI; 0.825 - 0.963), hit ratio 0.500 (95% CI; 0.492 – 0.508), specificity equalized at 95%; 0.960 (95% CI; 0.959 – 0.961)). Compared to other methods, our model outperformed in almost all metrics with statistical significance ($P < 0.001$). A likely explanation is that the GPA-trained GTN and trend-based analysis are trained with the RNFL Thickness profile, which is prone to outlier sensitivity, uncertainty, and test variability (Thompson et al. (2020); Hou et al. (2023); Hu et al. (2020)). GTN method might have to overfit to the high imbalance in the training data and label noise. Trend-based analysis, on the other hand, assumes changes are linear to derive glaucoma progression, which might not reflect actual

progression (Wu et al. (2017)). Since we use SD-OCT B-scan images directly, the DL model can capture complex features, interdependent RNFL profile characteristics, and progressive attributes in local receptive fields to increase the model’s ability to capture high-dimensional time series image representations accurately. Another notable advantage of using our time series DL model is that it can characterize glaucoma attribute manifestations at different stages of the disease in different individuals. By leveraging the spatiotemporal and contextual information in longitudinal B-scans, our model can identify subtle changes and differential patterns across local sectors and time windows that other methods might miss.

Analysis of the clinical and demographic characteristics of the predictions from the DL method showed mixed results. Even though the rates of RNFL thickness loss in eyes predicted as progressing had faster rates of loss in average, it did not show statistical significance difference from non-progressing eyes as classified by the algorithm ($-0.59 \pm 1.30 \mu\text{m}/\text{year}$ vs. $-0.27 \pm 1.25 \mu\text{m}/\text{year}$; $P = 0.695$) but showed significantly faster rates of SAP MD loss ($-0.39 \pm 0.30 \text{dB}/\text{year}$ vs $-0.09 \pm 0.35 \text{dB}/\text{year}$ respectively, $P = 0.013$). A reason for this might be in the data modeling process. We used a longitudinal sequence of SDOCT B-scans from Spectralis as input features for the DL method. On the other hand, GPA labels were obtained as an end-point of event-based analysis of VF SAP data. This might cause inconsistencies in the data generation stage as visits in the OCT data might not coincide with visits in the VF SAP data.

It is important to emphasize that our model requires little clinical expertise to make predictions, as it only uses SDOCT B-scan images as inputs. This removes the dependency on manual data annotations or expertise in glaucoma diagnosis while providing inference. Relying on human gradings may make the model susceptible to biases. Using human-generated global or sectoral averages of the RNFL Thickness profile may not accurately capture pointwise variability and fail to learn the complex-

ity of glaucoma progression. By learning glaucoma progression attributes directly from the SDOCT B-scan images and visual field SAP GPA criteria, our model learns subtle and intricate details that human graders can miss.

Despite its superior performance, this study had some limitations. One limitation of the model is its complexity, which requires significant computational resources and training times. We understand that there might be more straightforward techniques to solve label noise and data imbalance, but these methods only work for specific cases, are susceptible to data variations, and require study assumptions (Natarajan et al. (2013)). As of now, only semi-supervised techniques provide us with the capabilities necessary for modeling such data variations. Unfortunately, in the current setting, we do not offer any analysis or study of model performance in different population settings. As with any DL model, since the performance varies across datasets, an exhaustive set of tests is required to validate for real-world use, mainly when evaluated with diverse demographic characteristics, which is affected more by the scarcity of benchmarking datasets. The comparisons provided in this study are done on our proprietary datasets constructed from different data sources and not tested for noise severity. Other models have assumed cleaner data for training and thus predictably underperformed on our dataset. Therefore, researchers should take caution when comparing statistics.

Although the regularized contrastive learning framework proposed in this study achieved comparative performance, if it not outperform other methods, it has inherent risks. The selective shuffling process might change the inherent characteristics of the data which is used to determine progression. While this process is shown to enhance specificity by introducing hard negatives, the training process still lacks information on true glaucoma-progressing samples and thus might generate a decision boundary that does not reflect the actual VF deterioration observed in glaucoma progression. Another limitation to note is using the visual field GPA as the gold

standard itself. It is already understood amongst clinicians and researchers that glaucoma progression does not have a universal gold standard. However, the GPA algorithm demonstrates a clinically relevant functional progression, which has been associated with worse quality-of-life outcomes. A clinician’s validation of the model performance and correlation with other clinical parameters might overcome this and strengthen the rationale behind such grading criteria. Further research on grading standards’ applicability and relevance to structural progression can help optimize the model’s efficacy and generalizability, addressing some of the above-mentioned limitations and ensuring its applicability in various clinical settings.

In conclusion, we developed a DL framework that combines classification with selective shuffling and contrastive learning over a CNN-LSTM network to detect glaucoma progression in noisy, imbalanced datasets. Our model demonstrates superior performance and surpasses current conventional and state of the art techniques by utilizing longitudinal SD-OCT B-scans and visual field GPA outcomes. Since the DL model is impervious to label noise, our model can be generalized and translated to other clinical practices that utilize real-world EHR data sources. By directly using SD-OCT B-scan images as inputs, our model was able to capture complex information and provide a more comprehensive evaluation of glaucoma progression. Further clinical validation for model performance and relevance with medical experts offers the potential for automated, accurate glaucoma progression detection, aiding clinicians to monitor glaucoma patients effectively.

Conclusion and Future Work

In this thesis, we developed various DL algorithms for detecting glaucoma progression using structural changes in the eye. Owing to the clinical need for precise glaucoma progression detection and the inherent challenges in medical image analysis, we explored the current landscape of conventional and DL methods for glaucoma progression in Chapter 2. The investigation was marked by understanding how structural, functional, or structure-function relationships improve glaucoma progression detection when integrated with complex algorithms. We observed three primary challenges in developing algorithms for progression detection: the lack of comprehensive longitudinal datasets, the absence of reliable reference standards, and complexities in structure-function relationship in glaucoma. The advent of powerful computer-aided algorithms, the accessibility to computational resources, and the availability of large datasets have helped develop innovative data-driven solutions for predicting glaucoma progression.

In Chapter 3, we introduced the extensive Duke Ophthalmic Registry Dataset, which contains structural and functional assessments of the eye over routine clinical care of patients over two decades. Using the dataset and insights from Chapter 2, we established the input features for our DL algorithms as Longitudinal SDOCT scans. The subtleties and nuances in the structural sequences of SDOCT scans motivated us to design a time-series DL model utilizing CNN-LSTM networks to extract intricate spatiotemporal encodings. We also elaborated on the GPA reference standard and OLS linear regression-based trend analysis for glaucoma progression, which is currently widely used in clinical settings. We showed its relevance for

comparison and post-hoc analysis in our studies.

Addressing specifically the challenges of the absence of reliable reference standards and the intricacies in the structure-function relationship, in Chapter 4, we developed a novel DL algorithm. This DL model used a CNN-LSTM encoder-based approach to discern progressing eyes by training on longitudinal SDOCT scans without reliance on any reference standard. We showed that the DL model can generalize well on a time-series dataset by creating pseudo-progression criteria using age-related structural deterioration and knowledge of stable (healthy) eye characteristics. We provide a simple proof of concept for the DL algorithm in section 3.4 and show empirically with experiments in chapter 4 that the DL algorithm with modified Noise-PU learning scheme is, in fact, able to learn the intricate structural RNFL progression characteristics in glaucoma and differentiates well from natural age-related variability.

In Chapter 5, we refined our model to a more realistic scenario to detect vision impairments observed as functional deterioration in glaucoma using structural assessments. We repurposed the DL model that uses a longitudinal sequence of SDOCT images to predict progression, as characterized by VF GPA endpoints. Building on the concepts of Chapter 4, we introduced a novel algorithm, dubbed RegCon network, that jointly addresses two critical problems in medical image analysis: data imbalance and label noise. We implemented selective shuffling to produce hard negatives. We paired these features with contrastive learning to discern patterns of age-related variability and structural invariances in longitudinal images, which indicate glaucoma progression. We demonstrated empirically that the joint learning approach outperforms other conventional methods, even exceeding the performance of the current state of the art GTN method. Our experiments showed that the DL algorithm is impervious to label noise and adeptly manages class imbalances by learning intricate details directly from the spatiotemporal representations of the DL model. Overall,

the refined model showed superior performance in detecting functional deterioration in glaucoma from longitudinal structural assessments of the eye.

Despite the groundbreaking work, our research has limitations. The Noise-PU learning algorithm in Chapter 4 relied heavily on data modeling, especially the clinical characteristics of healthy subjects and the variability observed in age-related progression. The lack of positive samples (progressing eyes) possibly biased the results towards non-progressing sequences. This, coupled with the lack of benchmarking datasets, makes direct comparisons between the DL and conventional methods challenging. Our Noise-PU learning study primarily focused on detecting progression based on structural changes in the eyes. However, structural progression might not always reflect actual glaucoma progression. To ensure a comprehensive understanding, validating these findings against functional progression criteria is essential, an aspect we explored with the RegCon learning algorithm in Chapter 5. Although exhibiting competitive performance, the RegCon learning approach also had inherent risks. Specifically, the selective shuffling framework, a critical step in generating hard negatives, could change the intrinsic data distribution and manipulate the decision boundary. Even though this method showed improved sensitivity and a higher specificity, label noise (lack of knowledge of truly positive samples) might cause the DL model to generate suboptimal predictions. In both cases, validation against an external population is needed to draw accurate clinical insights into the performance of the DL models.

As the thesis concludes, several promising avenues of research emerge. Since we have shown that the DL algorithms can learn intrinsic disease characteristics from potentially noisy datasets, we can incorporate data from other sources with fewer assumptions. This allows researchers to implement a common DL algorithm across multiple datasets with minimal expertise and provide a comprehensive understanding of glaucoma progression across varied demographics, a notion wildly sought by

the medical community. Integrating data from different imaging modalities, such as fundus photographs, gonioscopy, etc., can uncover deeper insights into the structure, function, and clinical relationship in glaucoma progression. Even though the performance of the CNN-LSTM network was satisfactory, the clinical need for a real-time glaucoma progression detection tool requires further optimization of our models and possibly the exploration of alternative architectures. DL networks such as the transformers have been shown to produce state of the art results for combined image and time-series analysis; incorporating them in our research might be beneficial and outperform the current setup. For clinicians and the medical community, trust and collaboration are paramount. Therefore, further research is needed to design DL methods that yield transparent and interpretable results seamlessly integrating with EHR data. This improved framework can facilitate a thorough analysis of progression for those without expert knowledge and can empower clinicians to offer individualized routine care.

In sum, our thesis has laid a solid foundation for glaucoma progression research and tackled some crucial problems observed in medical research involving real-world datasets. The developments in our study have the potential to provide purposeful and impactful solutions to various clinical problems. Validation and further research can address the limitations of our methods and refine the model's applicability across diverse clinical contexts.

Bibliography

- Abe, R. Y., Gracitelli, C. P., and Medeiros, F. A. (2015), “The use of spectral-domain optical coherence tomography to detect glaucoma progression,” *The Open Ophthalmology Journal*, 9, 78.
- Abe, R. Y., Diniz-Filho, A., Zangwill, L. M., Gracitelli, C. P., Marvasti, A. H., Weinreb, R. N., Baig, S., and Medeiros, F. A. (2016), “The relative odds of progressing by structural and functional tests in glaucoma,” *Investigative ophthalmology & visual science*, 57, OCT421–OCT428.
- Abu, S. L., Marín-Franch, I., and Racette, L. (2020), “A framework for assessing glaucoma progression using structural and functional indices jointly,” *PloS one*, 15, e0235255.
- AGIS (1994), “The advanced glaucoma intervention study (AGIS): 1. Study design and methods and baseline characteristics of study patients,” *Controlled Clinical Trials*, 15, 299–325.
- Alaparthi, V., Mandal, S., and Cummings, M. (2021), “A comparison of machine learning and human performance in the real-time acoustic detection of drones,” in *IEEE Aerospace*.
- Alencar, L. M. and Medeiros, F. A. (2011), “The role of standard automated perimetry and newer functional methods for glaucoma diagnosis and follow-up,” *Indian journal of ophthalmology*, 59, S53.
- Anderson, D. R. (2003), “Collaborative normal tension glaucoma study,” *Curr Opin Ophthalmol*, 14, 86–90.
- Anderson, R. L., Cadena, M. d. I. A. R., and Schuman, J. S. (2018), “Glaucoma diagnosis: from the artisanal to the defined,” *Ophthalmology Glaucoma*, 1, 3–14.
- Antón, A., Pazos, M., Martín, B., Navero, J. M., Ayala, M. E., Castany, M., Martínez, P., and Bardavío, J. (2013), “Glaucoma Progression Detection: Agreement, Sensitivity, and Specificity of Expert Visual Field Evaluation, Event Analysis, and Trend Analysis,” *European Journal of Ophthalmology*, 23, 187–195, PMID: 23065852.
- Aref, A. A. and Budenz, D. L. (2017), “Detecting visual field progression,” *Ophthalmology*, 124, S51–S56.
- Arnalich-Montiel, F., Casas-Llera, P., Muñoz-Negrete, F. J., and Rebolleda, G. (2009), “Performance of glaucoma progression analysis software in a glaucoma population,” *Graefes’s Archive for Clinical and Experimental Ophthalmology*, 247, 391–397.

- Artes, P. H. and Chauhan, B. C. (2005), “Longitudinal changes in the visual field and optic disc in glaucoma,” *Progress in retinal and eye research*, 24, 333–354.
- Artes, P. H., O’Leary, N., Nicolela, M. T., Chauhan, B. C., and Crabb, D. P. (2014), “Visual Field Progression in Glaucoma: What Is the Specificity of the Guided Progression Analysis?” *Ophthalmology*, 121, 2023–2027.
- Asaoka, R. and Murata, H. (2023), “Prediction of visual field progression in glaucoma: existing methods and artificial intelligence,” *Japanese Journal of Ophthalmology*, pp. 1–14.
- Asaoka, R., Xu, L., Murata, H., Kiwaki, T., Matsuura, M., Fujino, Y., Tanito, M., Mori, K., Ikeda, Y., Kanamoto, T., et al. (2021), “A joint multitask learning model for cross-sectional and longitudinal predictions of visual field using OCT,” *Ophthalmology Science*, 1, 100055.
- Balasubramanian, M., Kriegman, D. J., Bowd, C., Holst, M., Weinreb, R. N., Sample, P. A., and Zangwill, L. M. (2012), “Localized glaucomatous change detection within the proper orthogonal decomposition framework,” *Investigative ophthalmology & visual science*, 53, 3615–3628.
- Baxter, S. L., Marks, C., Kuo, T.-T., Ohno-Machado, L., and Weinreb, R. N. (2019), “Machine learning-based predictive modeling of surgical intervention in glaucoma using systemic data from electronic health records,” *American journal of ophthalmology*, 208, 30–40.
- Bekker, J. and Davis, J. (2020), “Learning from positive and unlabeled data: A survey,” *Machine Learning*, 109, 719–760.
- Belghith, A., Balasubramanian, M., Bowd, C., Weinreb, R. N., and Zangwill, L. M. (2013), “Glaucoma progression detection using variational expectation maximization algorithm,” in *2013 IEEE 10th International Symposium on Biomedical Imaging*, pp. 876–879, IEEE.
- Belghith, A., Bowd, C., Medeiros, F. A., Balasubramanian, M., Weinreb, R. N., and Zangwill, L. M. (2014a), “Glaucoma progression detection using nonlocal Markov random field prior,” *Journal of Medical Imaging*, 1, 034504–034504.
- Belghith, A., Bowd, C., Weinreb, R. N., and Zangwill, L. M. (2014b), “A joint estimation detection of glaucoma progression in 3D spectral domain optical coherence tomography optic nerve head images,” in *Medical Imaging 2014: Computer-Aided Diagnosis*, vol. 9035, pp. 180–186, SPIE.
- Belghith, A., Bowd, C., Medeiros, F. A., Balasubramanian, M., Weinreb, R. N., and Zangwill, L. M. (2015), “Learning from healthy and stable eyes: a new approach for detection of glaucomatous progression,” *Artificial intelligence in medicine*, 64, 105–115.

- Berchuck, S. I., Mwanza, J.-C., and Warren, J. L. (2019a), “Diagnosing glaucoma progression with visual field data using a spatiotemporal boundary detection method,” *Journal of the American Statistical Association*.
- Berchuck, S. I., Mukherjee, S., and Medeiros, F. A. (2019b), “Estimating rates of progression and predicting future visual fields in glaucoma using a deep variational autoencoder,” *Scientific Reports*, 9, 18113.
- Betz-Stablein, B. D., Morgan, W. H., House, P. H., and Hazelton, M. L. (2013), “Spatial modeling of visual field data for assessing glaucoma progression,” *Investigative ophthalmology & visual science*, 54, 1544–1553.
- Bilonick, R., Sung, K., Wollstein, G., Ishikawa, H., Townsend, K., Kagemann, L., Noecker, R., and Schuman, J. (2008), “Evaluating Glaucoma Progression Using a Latent Class Model for MD, PSD, AGIS, and VFI With RNFL as Covariate,” *Investigative Ophthalmology & Visual Science*, 49, 3610–3610.
- Bizios, D., Heijl, A., Hougaard, J. L., and Bengtsson, B. (2010), “Machine learning classifiers for glaucoma diagnosis based on classification of retinal nerve fibre layer thickness parameters measured by Stratus OCT,” *Acta ophthalmologica*, 88, 44–52.
- Bowd, C., Lee, I., Goldbaum, M. H., Balasubramanian, M., Medeiros, F. A., Zangwill, L. M., Girkin, C. A., Liebmann, J. M., and Weinreb, R. N. (2012), “Predicting glaucomatous progression in glaucoma suspect eyes using relevance vector machine classifiers for combined structural and functional measurements,” *Investigative ophthalmology & visual science*, 53, 2382–2389.
- Bowd, C., Belghith, A., Christopher, M., Goldbaum, M. H., Fazio, M. A., Girkin, C. A., Liebmann, J. M., de Moraes, C. G., Weinreb, R. N., and Zangwill, L. M. (2021), “Individualized glaucoma change detection using deep learning auto encoder-based regions of interest,” *Translational vision science & technology*, 10, 19–19.
- Bryan, S. R., Eilers, P. H., Rosmalen, J. v., Rizopoulos, D., Vermeer, K. A., Lemij, H. G., and Lesaffre, E. M. (2017), “Bayesian hierarchical modeling of longitudinal glaucomatous visual fields using a two-stage approach,” *Statistics in Medicine*, 36, 1735–1753.
- Bussel, I. I., Wollstein, G., and Schuman, J. S. (2014), “OCT for glaucoma diagnosis, screening and detection of glaucoma progression,” *British Journal of Ophthalmology*, 98, ii15–ii19.
- Casas-Llera, P., Rebolleda, G., Muñoz-Negrete, F. J., Arnalich-Montiel, F., Pérez-López, M., and Fernández-Buenaga, R. (2009), “Visual field index rate and event-based glaucoma progression analysis: comparison in a glaucoma population,” *British Journal of Ophthalmology*, 93, 1576–1579.

- Chen, T., Kornblith, S., Norouzi, M., and Hinton, G. (2020), “A simple framework for contrastive learning of visual representations,” in *International conference on machine learning*, pp. 1597–1607, PMLR.
- Chen, T. C. (2009), “Spectral domain optical coherence tomography in glaucoma: qualitative and quantitative analysis of the optic nerve head and retinal nerve fiber layer (an AOS thesis),” *Transactions of the American Ophthalmological Society*, 107, 254.
- Chevalier, G. (2018), “Long short-term memory,” https://en.wikipedia.org/wiki/Long_short-term_memory, Last accessed on 2023-09-30.
- Cho, J. W., Sung, K. R., Yun, S.-C., Na, J. H., Lee, Y., and Kook, M. S. (2012), “Progression detection in different stages of glaucoma: mean deviation versus visual field index,” *Japanese journal of ophthalmology*, 56, 128–133.
- Christopher, M., Belghith, A., Weinreb, R. N., Bowd, C., Goldbaum, M. H., Saunders, L. J., Medeiros, F. A., and Zangwill, L. M. (2018), “Retinal nerve fiber layer features identified by unsupervised machine learning on optical coherence tomography scans predict glaucoma progression,” *Investigative ophthalmology & visual science*, 59, 2748–2756.
- Crabb, D. P., Smith, N. D., Glen, F. C., Burton, R., and Garway-Heath, D. F. (2013), “How does glaucoma look?: patient perception of visual field loss,” *Ophthalmology*, 120, 1120–1126.
- Czudowska, M. A., Ramdas, W. D., Wolfs, R. C., Hofman, A., De Jong, P. T., Vingerling, J. R., and Jansonius, N. M. (2010), “Incidence of glaucomatous visual field loss: a ten-year follow-up from the Rotterdam Study,” *Ophthalmology*, 117, 1705–1712.
- Dada, T., Sharma, R., Angmo, D., Sinha, G., Bhartiya, S., Mishra, S. K., Panda, A., and Sihota, R. (2014), “Scanning laser polarimetry in glaucoma,” *Indian journal of ophthalmology*, 62, 1045–1055.
- De Moraes, C. G., Ghobrial, S. R., Ritch, R., and Liebmann, J. M. (2012), “Comparison of PROGRESSOR and Glaucoma Progression Analysis 2 to detect visual field progression in treated glaucoma patients,” *The Asia-Pacific Journal of Ophthalmology*, 1, 135–139.
- Diaz-Aleman, V., Anton, A., de la Rosa, M. G., Johnson, Z., McLeod, S., and Azuara-Blanco, A. (2009), “Detection of visual-field deterioration by Glaucoma Progression Analysis and Threshold Noiseless Trend programs,” *British journal of ophthalmology*, 93, 322–328.

- Dielemans, I., Vingerling, J. R., Wolfs, R. C., Hofman, A., Grobbee, D. E., and de Jong, P. T. (1994), “The prevalence of primary open-angle glaucoma in a population-based study in the Netherlands: the Rotterdam Study,” *Ophthalmology*, 101, 1851–1855.
- Dixit, A., Yohannan, J., and Boland, M. V. (2021), “Assessing glaucoma progression using machine learning trained on longitudinal visual field and clinical data,” *Ophthalmology*, 128, 1016–1026.
- Dong, Z. M., Wollstein, G., and Schuman, J. S. (2016), “Clinical utility of optical coherence tomography in glaucoma,” *Investigative ophthalmology & visual science*, 57, OCT556–OCT567.
- Drance, S., Anderson, D. R., Schulzer, M., Group, C. N.-T. G. S., et al. (2001), “Risk factors for progression of visual field abnormalities in normal-tension glaucoma,” *American journal of ophthalmology*, 131, 699–708.
- Ekström, C. (2012), “Risk factors for incident open-angle glaucoma: a population-based 20-year follow-up study,” *Acta ophthalmologica*, 90, 316–321.
- Feng, L., Shu, S., Lin, Z., Lv, F., Li, L., and An, B. (2021), “Can cross entropy loss be robust to label noise?” in *Proceedings of the Twenty-Ninth International Conference on International Joint Conferences on Artificial Intelligence*, pp. 2206–2212.
- Fitzke, F. W., Hitchings, R. A., Poinoosawmy, D., McNaught, A. I., and Crabb, D. P. (1996), “Analysis of visual field progression in glaucoma.” *British Journal of Ophthalmology*, 80, 40–48.
- Founti, P., Bunce, C., Khawaja, A. P., Doré, C. J., Mohamed-Noriega, J., Garway-Heath, D. F., Group, U. K. G. T. S., et al. (2020), “Risk factors for visual field deterioration in the United Kingdom Glaucoma Treatment Study,” *Ophthalmology*, 127, 1642–1651.
- Frankfort, B. J., Khan, A. K., Dennis, Y. T., Chung, I., Pang, J.-J., Yang, Z., Gross, R. L., and Wu, S. M. (2013), “Elevated intraocular pressure causes inner retinal dysfunction before cell loss in a mouse model of experimental glaucoma,” *Investigative ophthalmology & visual science*, 54, 762–770.
- Fronimopoulos, J. and Lascaratos, J. (1991), *The terms glaucoma and cataract in the ancient Greek and Byzantine writers*, Springer.
- Garcia, G.-G. P., Nitta, K., Lavieri, M. S., Andrews, C., Liu, X., Lobaza, E., Van Oyen, M. P., Sugiyama, K., and Stein, J. D. (2019), “Using Kalman filtering to forecast disease trajectory for patients with normal tension glaucoma,” *American journal of ophthalmology*, 199, 111–119.

- Gardiner, S. K., Johnson, C. A., and Demirel, S. (2012), “The effect of test variability on the structure–function relationship in early glaucoma,” *Graefe’s Archive for Clinical and Experimental Ophthalmology*, 250, 1851–1861.
- Garway-Heath, D., Wollstein, G., and Hitchings, R. (1997), “Aging changes of the optic nerve head in relation to open angle glaucoma,” *British Journal of Ophthalmology*, 81, 840–845.
- Garway-Heath, D. F., Holder, G. E., Fitzke, F. W., and Hitchings, R. A. (2002), “Relationship between electrophysiological, psychophysical, and anatomical measurements in glaucoma,” *Investigative ophthalmology & visual science*, 43, 2213–2220.
- Garway-Heath, D. F., Lascaratos, G., Bunce, C., Crabb, D. P., Russell, R. A., Shah, A., Zeyen, T., Wormald, R., Garway-Heath, D. F., Crabb, D. P., Bunce, C., Anand, N., Azuara-Blanco, A., Bourne, R., Broadway, D., Cunliffe, I., Diamond, J., Fraser, S. G., Martin, K., McNaught, A., Negi, A., Spry, P., Amalfitano, F., and White, E. (2013), “The United Kingdom Glaucoma Treatment Study: a multicenter, randomized, placebo-controlled clinical trial: design and methodology,” *Ophthalmology*, 120, 68–76.
- Geevarghese, A., Wollstein, G., Ishikawa, H., and Schuman, J. S. (2021), “Optical coherence tomography and glaucoma,” *Annual review of vision science*, 7, 693–726.
- Gharahkhani, P., Jorgenson, E., Hysi, P., Khawaja, A. P., Pendergrass, S., Han, X., Ong, J. S., Hewitt, A. W., Segrè, A. V., Rouhana, J. M., et al. (2021), “Genome-wide meta-analysis identifies 127 open-angle glaucoma loci with consistent effect across ancestries,” *Nature communications*, 12, 1–16.
- Giangiaco, A., Garway-Heath, D., and Caprioli, J. (2006), “Diagnosing glaucoma progression: current practice and promising technologies,” *Current opinion in ophthalmology*, 17, 153–162.
- Giraud, J.-M., May, F., Manet, G., Fenolland, J.-R., Meynard, J.-B., Sadat, A.-M., Mouinga, A., Seck, S., and Renard, J.-P. (2010), “Analysis of progression with GPA (guided progression analysis) and mean deviation (MD) indexes of automated perimetry in ocular hypertension and glaucoma,” *Investigative Ophthalmology & Visual Science*, 51, 3997–3997.
- Glaucoma Laser Trial Research Group (1995), “The Glaucoma Laser Trial (GLT) and Glaucoma Laser Trial Follow-up Study: 7. Results,” *American Journal of Ophthalmology*, 120, 718–731.
- Goldbaum, M. H., Lee, I., Jang, G., Balasubramanian, M., Sample, P. A., Weinreb, R. N., Liebmann, J. M., Girkin, C. A., Anderson, D. R., Zangwill, L. M., et al.

- (2012), “Progression of patterns (POP): a machine classifier algorithm to identify glaucoma progression in visual fields,” *Investigative ophthalmology & visual science*, 53, 6557–6567.
- Gordon, M. O., Beiser, J. A., Brandt, J. D., Heuer, D. K., Higginbotham, E. J., Johnson, C. A., Keltner, J. L., Miller, J. P., Parrish, Richard K., I., Wilson, M. R., Kass, M. A., and for the Ocular Hypertension Treatment Study Group (2002), “The Ocular Hypertension Treatment Study: Baseline Factors That Predict the Onset of Primary Open-Angle Glaucoma,” *Archives of Ophthalmology*, 120, 714–720.
- Gracitelli, C. P., Abe, R. Y., Tatham, A. J., Rosen, P. N., Zangwill, L. M., Boer, E. R., Weinreb, R. N., and Medeiros, F. A. (2015a), “Association between progressive retinal nerve fiber layer loss and longitudinal change in quality of life in glaucoma,” *JAMA ophthalmology*, 133, 384–390.
- Gracitelli, C. P., Abe, R. Y., and Medeiros, F. A. (2015b), “Spectral-domain optical coherence tomography for glaucoma diagnosis,” *The Open Ophthalmology Journal*, 9, 68.
- Guergueb, T. and Akhloufi, M. A. (2023), “A Review of Deep Learning Techniques for Glaucoma Detection,” *SN Computer Science*, 4, 274.
- Harwerth, R. S., Carter-Dawson, L., Shen, F., Smith, E. L., and Crawford, M. (1999), “Ganglion cell losses underlying visual field defects from experimental glaucoma,” *Investigative ophthalmology & visual science*, 40, 2242–2250.
- Hassan, O. N., Sahin, S., Mohammadzadeh, V., Yang, X., Amini, N., Mylavarapu, A., Martinyan, J., Hong, T., Mahmoudinezhad, G., Rueckert, D., et al. (2020), “Conditional GAN for prediction of glaucoma progression with macular optical coherence tomography,” in *Advances in Visual Computing: 15th International Symposium, ISVC 2020, San Diego, CA, USA, October 5–7, 2020, Proceedings, Part II 15*, pp. 761–772, Springer.
- He, K., Zhang, X., Ren, S., and Sun, J. (2016), “Deep residual learning for image recognition,” in *Proceedings of the IEEE conference on computer vision and pattern recognition*, pp. 770–778.
- Heijl, A., Lindgren, A., and Lindgren, G. (1989), “Test-retest variability in glaucomatous visual fields,” *American journal of ophthalmology*, 108, 130–135.
- Heijl, A., Leske, M. C., Bengtsson, B., Bengtsson, B., Hussein, M., and group, E. (2003), “Measuring visual field progression in the Early Manifest Glaucoma Trial,” *Acta ophthalmologica Scandinavica*, 81, 286–293.

- Hemelings, R., Wong, D. W., Van Eijgen, J., Chua, J., Breda, J. B., Stalmans, I., and Schmetterer, L. (2023), “Predicting glaucomatous visual field progression from baseline fundus photos using deep learning,” *Investigative Ophthalmology & Visual Science*, 64, 380–380.
- Hicks, S. A., Strümke, I., Thambawita, V., Hammou, M., Riegler, M. A., Halvorsen, P., and Parasa, S. (2022), “On evaluation metrics for medical applications of artificial intelligence,” *Scientific reports*, 12, 5979.
- Hirooka, K., Izumibata, S., Ukegawa, K., Nitta, E., and Tsujikawa, A. (2016), “Estimating the rate of retinal ganglion cell loss to detect glaucoma progression: an observational cohort study,” *Medicine*, 95.
- Hochreiter, S. and Schmidhuber, J. (1997), “Long short-term memory,” *Neural computation*, 9, 1735–1780.
- Hood, D. C., Raza, A. S., de Moraes, C. G. V., Liebmann, J. M., and Ritch, R. (2013), “Glaucomatous damage of the macula,” *Progress in retinal and eye research*, 32, 1–21.
- Hood, D. C., La Bruna, S., Tsamis, E., Leshno, A., Melchior, B., Grossman, J., Liebmann, J. M., and De Moraes, C. G. (2022), “The 24-2 visual field guided progression analysis can miss the progression of glaucomatous damage of the macula seen using OCT,” *Ophthalmology Glaucoma*, 5, 614–627.
- Hosni Mahmoud, H. A. and Alabdulkreem, E. (2023), “Bidirectional Neural Network Model for Glaucoma Progression Prediction,” *Journal of Personalized Medicine*, 13, 390.
- Hou, K., Bradley, C., Herbert, P., Johnson, C., Wall, M., Ramulu, P. Y., Unberath, M., and Yohannan, J. (2023), “Predicting Visual Field Worsening with Longitudinal OCT Data Using a Gated Transformer Network,” *Ophthalmology*, 130, 854–862.
- Hu, R., Marin-Franch, I., and Racette, L. (2014), “Prediction accuracy of a novel dynamic structure–function model for glaucoma progression,” *Investigative ophthalmology & visual science*, 55, 8086–8094.
- Hu, R., Racette, L., Chen, K. S., and Johnson, C. A. (2020), “Functional assessment of glaucoma: uncovering progression,” *Survey of ophthalmology*, 65, 639–661.
- Hu, W. and Wang, S. Y. (2022), “Predicting glaucoma progression requiring surgery using clinical free-text notes and transfer learning with transformers,” *Translational Vision Science & Technology*, 11, 37–37.

- Huang, J., Gretton, A., Borgwardt, K., Schölkopf, B., and Smola, A. (2006), “Correcting sample selection bias by unlabeled data,” *Advances in neural information processing systems*, 19.
- Huang, X., Mahotra, S., Elze, T., Wang, M., Boland, M. V., Pasquale, L., Majoor, J. E. A., Lemij, H., Nouri-Mahdavi, K., Johnson, C. A., et al. (2021), “Detection of Glaucoma Progression from Retinal Nerve Fiber Layer Thickness Measurements Using Machine Learning,” *Investigative Ophthalmology & Visual Science*, 62, 1005–1005.
- Jalamangala Shivananjaiiah, S. K., Kumari, S., Majid, I., and Wang, S. Y. (2023), “Predicting near-term glaucoma progression: An artificial intelligence approach using clinical free-text notes and data from electronic health records,” *Frontiers in Medicine*, 10, 371.
- Jammal, A. A., Berchuck, S. I., Thompson, A. C., Costa, V. P., and Medeiros, F. A. (2020), “The effect of age on increasing susceptibility to retinal nerve fiber layer loss in glaucoma,” *Investigative ophthalmology & visual science*, 61, 8–8.
- Jammal, A. A., Thompson, A. C., Mariottoni, E. B., Urata, C. N., Estrela, T., Berchuck, S. I., Tseng, H. C., Asrani, S., and Medeiros, F. A. (2021), “Rates of glaucomatous structural and functional change from a large clinical population: the Duke Glaucoma Registry Study,” *American Journal of Ophthalmology*, 222, 238–247.
- Jones, I., Van Oyen, M. P., Lavieri, M., Andrews, C., and Stein, J. D. (2019), “Identifying Patients at Risk for Experiencing Rapid Progression of Open Angle Glaucoma Using Supervised Machine Learning,” *Investigative Ophthalmology & Visual Science*, 60, 2472–2472.
- Kamalipour, A., Moghimi, S., Khosravi, P., Mohammadzadeh, V., Nishida, T., Micheletti, E., Wu, J.-H., Mahmoudinezhad, G., Li, E. H., Christopher, M., et al. (2023), “Combining Optical Coherence Tomography and Optical Coherence Tomography Angiography Longitudinal Data for the Detection of Visual Field Progression in Glaucoma,” *American Journal of Ophthalmology*, 246, 141–154.
- Katz, J. (1999), “Scoring systems for measuring progression of visual field loss in clinical trials of Glaucoma treatment¹¹The author has no commercial or proprietary interest in the manufacturer of the Humphrey Field Analyzer. The author has not received payment as a consultant, reviewer, or evaluator of this product.” *Ophthalmology*, 106, 391–395.
- Katz, J., Congdon, N., and Friedman, D. S. (1999), “Methodological Variations in Estimating Apparent Progressive Visual Field Loss in Clinical Trials of Glaucoma Treatment,” *Archives of Ophthalmology*, 117, 1137–1142.

- Kaushik, S., Muljutkar, S., Pandav, S. S., Verma, N., and Gupta, A. (2015), “Comparison of event-based analysis of glaucoma progression assessed subjectively on visual fields and retinal nerve fibre layer attenuation measured by optical coherence tomography,” *International ophthalmology*, 35, 95–106.
- Keltner, J. L., Johnson, C. A., Levine, R. A., Fan, J., Cello, K. E., Kass, M. A., Gordon, M. O., Group, O. H. T. S., et al. (2005), “Normal visual field test results following glaucomatous visual field end points in the Ocular Hypertension Treatment Study,” *Archives of ophthalmology*, 123, 1201–1206.
- Kim, K. E., Kim, M. J., Park, K. H., Jeoung, J. W., Kim, S. H., Kim, C. Y., Kang, S. W., of the Korean, E. S. C., and Society, O. (2016), “Prevalence, awareness, and risk factors of primary open-angle glaucoma: Korea National Health and Nutrition Examination Survey 2008–2011,” *Ophthalmology*, 123, 532–541.
- Kim, P. Y., Iftexharuddin, K. M., Davey, P. G., Tóth, M., Garas, A., Holló, G., and Essock, E. A. (2013), “Novel fractal feature-based multiclass glaucoma detection and progression prediction,” *iee journal of biomedical and health informatics*, 17, 269–276.
- Koronyo-Hamaoui, M., Koronyo, Y., Ljubimov, A. V., Miller, C. A., Ko, M. K., Black, K. L., Schwartz, M., and Farkas, D. L. (2011), “Identification of amyloid plaques in retinas from Alzheimer’s patients and noninvasive in vivo optical imaging of retinal plaques in a mouse model,” *Neuroimage*, 54, S204–S217.
- Kotowski, J., Wollstein, G., Folio, L. S., Ishikawa, H., and Schuman, J. S. (2011), “Clinical use of OCT in assessing glaucoma progression,” *Ophthalmic Surgery, Lasers and Imaging Retina*, 42, S6–S14.
- Lazaridis, G. (2022), “Deep learning-based improvement for the outcomes of glaucoma clinical trials,” Ph.D. thesis, UCL (University College London).
- Le, A., Mukesh, B. N., McCarty, C. A., and Taylor, H. R. (2003), “Risk factors associated with the incidence of open-angle glaucoma: the visual impairment project,” *Investigative ophthalmology & visual science*, 44, 3783–3789.
- Lee, E. J., Kim, T.-W., Weinreb, R. N., Park, K. H., Kim, S. H., and Kim, D. M. (2011), “Trend-based analysis of retinal nerve fiber layer thickness measured by optical coherence tomography in eyes with localized nerve fiber layer defects,” *Investigative ophthalmology & visual science*, 52, 1138–1144.
- Lee, E. J., Kim, T.-W., Kim, J.-A., Lee, S. H., and Kim, H. (2022), “Predictive Modeling of Long-Term Glaucoma Progression Based on Initial Ophthalmic Data and Optic Nerve Head Characteristics,” *Translational Vision Science & Technology*, 11, 24–24.

- Lee, J., Kim, Y. K., Jeoung, J. W., Ha, A., Kim, Y. W., and Park, K. H. (2020), “Machine learning classifiers-based prediction of normal-tension glaucoma progression in young myopic patients,” *Japanese Journal of Ophthalmology*, 64, 68–76.
- Lee, T., Jammal, A. A., Mariottoni, E. B., and Medeiros, F. A. (2021), “Predicting glaucoma development with longitudinal deep learning predictions from fundus photographs,” *American journal of ophthalmology*, 225, 86–94.
- Lee, W. J., Kim, Y. K., Park, K. H., and Jeoung, J. W. (2017), “Trend-based analysis of ganglion cell–inner plexiform layer thickness changes on optical coherence tomography in glaucoma progression,” *Ophthalmology*, 124, 1383–1391.
- Leffler, C. T., Schwartz, S. G., Hadi, T. M., Salman, A., and Vasuki, V. (2015a), “The early history of glaucoma: the glaucous eye (800 BC to 1050 AD),” *Clinical Ophthalmology*, pp. 207–215.
- Leffler, C. T., Schwartz, S. G., Giliberti, F. M., Young, M. T., and Bermudez, D. (2015b), “What was glaucoma called before the 20th century?” *Ophthalmology and eye diseases*, 7, OED–S32004.
- Leite, M. T., Rao, H. L., Zangwill, L. M., Weinreb, R. N., and Medeiros, F. A. (2011), “Comparison of the diagnostic accuracies of the Spectralis, Cirrus, and RTVue optical coherence tomography devices in glaucoma,” *Ophthalmology*, 118, 1334–1339.
- Leske, M. C., Heijl, A., Hyman, L., Bengtsson, B., Group, E. M. G. T., et al. (1999), “Early Manifest Glaucoma Trial: design and baseline data,” *Ophthalmology*, 106, 2144–2153.
- Leske, M. C., Heijl, A., Hyman, L., Bengtsson, B., Dong, L., Yang, Z., group, E., et al. (2007), “Predictors of long-term progression in the early manifest glaucoma trial,” *Ophthalmology*, 114, 1965–1972.
- Leung, C. K., Ye, C., Weinreb, R. N., Yu, M., Lai, G., and Lam, D. S. (2013), “Impact of age-related change of retinal nerve fiber layer and macular thicknesses on evaluation of glaucoma progression,” *Ophthalmology*, 120, 2485–2492.
- Leung, C. K.-s., Cheung, C. Y. L., Weinreb, R. N., Qiu, K., Liu, S., Li, H., Xu, G., Fan, N., Pang, C. P., Tse, K. K., et al. (2010), “Evaluation of retinal nerve fiber layer progression in glaucoma: a study on optical coherence tomography guided progression analysis,” *Investigative ophthalmology & visual science*, 51, 217–222.
- Li, F., Su, Y., Lin, F., Li, Z., Song, Y., Nie, S., Xu, J., Chen, L., Chen, S., Li, H., et al. (2022a), “A deep-learning system predicts glaucoma incidence and progression using retinal photographs,” *The Journal of Clinical Investigation*, 132.

- Li, S., Xia, X., Ge, S., and Liu, T. (2022b), “Selective-supervised contrastive learning with noisy labels,” in *Proceedings of the IEEE/CVF Conference on Computer Vision and Pattern Recognition*, pp. 316–325.
- Li, X.-L. and Liu, B. (2005), “Learning from positive and unlabeled examples with different data distributions,” in *Machine Learning: ECML 2005: 16th European Conference on Machine Learning, Porto, Portugal, October 3-7, 2005. Proceedings 16*, pp. 218–229, Springer.
- Lin, C., Mak, H., Yu, M., and Leung, C. K.-S. (2017), “Trend-based progression analysis for examination of the topography of rates of retinal nerve fiber layer thinning in glaucoma,” *JAMA ophthalmology*, 135, 189–195.
- Lisboa, R., Weinreb, R. N., and Medeiros, F. A. (2013), “Combining structure and function to evaluate glaucomatous progression: implications for the design of clinical trials,” *Current opinion in pharmacology*, 13, 115–122.
- Liu, Z., Lin, Y., Cao, Y., Hu, H., Wei, Y., Zhang, Z., Lin, S., and Guo, B. (2021), “Swin transformer: Hierarchical vision transformer using shifted windows,” in *Proceedings of the IEEE/CVF international conference on computer vision*, pp. 10012–10022.
- London, A., Benhar, I., and Schwartz, M. (2013), “The retina as a window to the brain—from eye research to CNS disorders,” *Nature Reviews Neurology*, 9, 44–53.
- Lucy, K. A. and Wollstein, G. (2016), “Structural and functional evaluations for the early detection of glaucoma,” *Expert review of ophthalmology*, 11, 367–376.
- Mackenzie, W. (1855), *A Practical Treatise on the Diseases of the Eye*, Blanchard and Lea.
- Mandal, S., Chen, L., Alaparthi, V., and Cummings, M. L. (2020), “Acoustic detection of drones through real-time audio attribute prediction,” in *AIAA Scitech 2020 Forum*, p. 0491.
- Mandal, S., Jammal, A. A., and Medeiros, F. A. (2023), “Noise-PU Learning: Weakly Supervised Time Series Learning to Detect Glaucoma Progression from Optical Coherence Tomography B-scans,” *Investigative Ophthalmology & Visual Science*, 64, 977–977.
- Manttari, J., Broomé, S., Folkesson, J., and Kjellstrom, H. (2020), “Interpreting video features: A comparison of 3D convolutional networks and convolutional LSTM networks,” in *Proceedings of the Asian Conference on Computer Vision*.
- Margolis, R. and Spaide, R. F. (2009), “A pilot study of enhanced depth imaging optical coherence tomography of the choroid in normal eyes,” *American journal of ophthalmology*, 147, 811–815.

- Mariotti, A. and Pascolini, D. (2012), “Global estimates of visual impairment,” *Br J Ophthalmol*, 96, 614–8.
- Mariottoni, E. B., Datta, S., Shigueoka, L. S., Jammal, A. A., Tavares, I. M., Henao, R., Carin, L., and Medeiros, F. A. (2023), “Deep Learning–Assisted Detection of Glaucoma Progression in Spectral-Domain OCT,” *Ophthalmology Glaucoma*, 6, 228–238.
- Maslin, J. S., Mansouri, K., and Dorairaj, S. K. (2015), “Suppl 1: M2: HRT for the Diagnosis and Detection of Glaucoma Progression,” *The open ophthalmology journal*, 9, 58.
- Matlach, J., Wagner, M., Malzahn, U., Schmidtman, I., Steigerwald, F., Musacchio, T., Volkman, J., Grehn, F., Göbel, W., and Klebe, S. (2018), “Retinal changes in Parkinson’s disease and glaucoma,” *Parkinsonism & Related Disorders*, 56, 41–46.
- Mayama, C., Araie, M., Suzuki, Y., Ishida, K., Yamamoto, T., Kitazawa, Y., Shirakashi, M., Abe, H., Tsukamoto, H., Mishima, H. K., et al. (2004), “Statistical evaluation of the diagnostic accuracy of methods used to determine the progression of visual field defects in glaucoma,” *Ophthalmology*, 111, 2117–2125.
- Mayro, E. L., Wang, M., Elze, T., and Pasquale, L. R. (2020), “The impact of artificial intelligence in the diagnosis and management of glaucoma,” *Eye*, 34, 1–11.
- Medeiros, F. A. and Jammal, A. A. (2023), “Validation of Rates of Mean Deviation Change as Clinically Relevant End Points for Glaucoma Progression,” *Ophthalmology*, 130, 469–477.
- Medeiros, F. A., Zangwill, L. M., Alencar, L. M., Bowd, C., Sample, P. A., Sussanna, R., and Weinreb, R. N. (2009a), “Detection of glaucoma progression with stratus OCT retinal nerve fiber layer, optic nerve head, and macular thickness measurements,” *Investigative ophthalmology & visual science*, 50, 5741–5748.
- Medeiros, F. A., Alencar, L. M., Zangwill, L. M., Bowd, C., Sample, P. A., and Weinreb, R. N. (2009b), “Prediction of functional loss in glaucoma from progressive optic disc damage,” *Archives of ophthalmology*, 127, 1250.
- Medeiros, F. A., Leite, M. T., Zangwill, L. M., and Weinreb, R. N. (2011), “Combining structural and functional measurements to improve detection of glaucoma progression using Bayesian hierarchical models,” *Investigative ophthalmology & visual science*, 52, 5794–5803.
- Medeiros, F. A., Zangwill, L. M., Girkin, C. A., Liebmann, J. M., and Weinreb, R. N. (2012a), “Combining structural and functional measurements to improve estimates of rates of glaucomatous progression,” *American journal of ophthalmology*, 153, 1197–1205.

- Medeiros, F. A., Zangwill, L. M., and Weinreb, R. N. (2012b), “Improved prediction of rates of visual field loss in glaucoma using empirical Bayes estimates of slopes of change,” *Journal of glaucoma*, 21, 147.
- Medeiros, F. A., Weinreb, R. N., Moore, G., Liebmann, J. M., Girkin, C. A., and Zangwill, L. M. (2012c), “Integrating event-and trend-based analyses to improve detection of glaucomatous visual field progression,” *Ophthalmology*, 119, 458–467.
- Medeiros, F. A., Zangwill, L. M., Bowd, C., Mansouri, K., and Weinreb, R. N. (2012d), “The structure and function relationship in glaucoma: implications for detection of progression and measurement of rates of change,” *Investigative ophthalmology & visual science*, 53, 6939–6946.
- Medeiros, F. A., Lisboa, R., Zangwill, L. M., Liebmann, J. M., Girkin, C. A., Bowd, C., and Weinreb, R. N. (2014), “Evaluation of progressive neuroretinal rim loss as a surrogate end point for development of visual field loss in glaucoma,” *Ophthalmology*, 121, 100–109.
- Medeiros, F. A., Jammal, A. A., and Mariottoni, E. B. (2021), “Detection of progressive glaucomatous optic nerve damage on fundus photographs with deep learning,” *Ophthalmology*, 128, 383–392.
- Meira-Freitas, D., Lisboa, R., Tatham, A., Zangwill, L. M., Weinreb, R. N., Girkin, C. A., Liebmann, J. M., and Medeiros, F. A. (2013), “Predicting progression in glaucoma suspects with longitudinal estimates of retinal ganglion cell counts,” *Investigative Ophthalmology & Visual Science*, 54, 4174–4183.
- Miglior, S., Zeyen, T., Pfeiffer, N., Cunha-Vaz, J., Torri, V., and Adamsons, I. (2002), “The European glaucoma prevention study design and baseline description of the participants,” *Ophthalmology*, 109, 1612–1621.
- Miki, A. (2012), “Assessment of structural glaucoma progression,” *Journal of current glaucoma practice*, 6, 62.
- Mirzania, D., Thompson, A. C., and Muir, K. W. (2021), “Applications of deep learning in detection of glaucoma: a systematic review,” *European Journal of Ophthalmology*, 31, 1618–1642.
- Mohammadzadeh, V., Rabiolo, A., Fu, Q., Morales, E., Coleman, A. L., Law, S. K., Caprioli, J., and Nouri-Mahdavi, K. (2020), “Longitudinal macular structure–function relationships in glaucoma,” *Ophthalmology*, 127, 888–900.
- Mohammadzadeh, V., Su, E., Zadeh, S. H., Law, S. K., Coleman, A. L., Caprioli, J., Weiss, R. E., and Nouri-Mahdavi, K. (2021), “Estimating ganglion cell complex rates of change with Bayesian hierarchical models,” *Translational vision science & technology*, 10, 15–15.

- Mohammadzadeh, V., Moghimi, S., Liang, Y., Xie, P., Nishida, T., Kamalipour, A., Christopher, M., Zangwill, L., Javidi, T., and Weinreb, R. N. (2022), “Detection of Glaucoma Progression on Longitudinal Series of Macular Optical Coherence Tomography Angiography Maps with a Deep Learning Model,” *Investigative Ophthalmology & Visual Science*, 63, 2919–F0072.
- Montesano, G., Garway-Heath, D. F., Ometto, G., and Crabb, D. P. (2021), “Hierarchical censored Bayesian analysis of visual field progression,” *Translational Vision Science & Technology*, 10, 4–4.
- Morrison, J. C. and Pollack, I. P. (2003), *Glaucoma: science and practice*, Thieme Medical Publishers.
- Mousavi, S. and Afghah, F. (2019), “Inter-and intra-patient ecg heartbeat classification for arrhythmia detection: a sequence to sequence deep learning approach,” in *ICASSP 2019-2019 IEEE international conference on acoustics, speech and signal processing (ICASSP)*, pp. 1308–1312, IEEE.
- Mowatt, G., Burr, J. M., Cook, J. A., Siddiqui, M. R., Ramsay, C., Fraser, C., Azuara-Blanco, A., and Deeks, J. J. (2008), “Screening tests for detecting open-angle glaucoma: systematic review and meta-analysis,” *Investigative ophthalmology & visual science*, 49, 5373–5385.
- Murata, H., Araie, M., and Asaoka, R. (2014), “A new approach to measure visual field progression in glaucoma patients using variational Bayes linear regression,” *Investigative ophthalmology & visual science*, 55, 8386–8392.
- Musch, D. C., Lichter, P. R., Guire, K. E., and Standardi, C. L. (1999), “The Collaborative Initial Glaucoma Treatment Study: study design, methods, and baseline characteristics of enrolled patients,” *Ophthalmology*, 106, 653–662.
- Musch, D. C., Gillespie, B. W., Lichter, P. R., Niziol, L. M., Janz, N. K., and Investigators, C. S. (2009), “Visual field progression in the Collaborative Initial Glaucoma Treatment Study: the impact of treatment and other baseline factors,” *Ophthalmology*, 116, 200–207.
- Nagesh, S., Moreno, A., Ishikawa, H., Wollstein, G., Shuman, J. S., and Rehg, J. M. (2019), “A spatiotemporal approach to predicting glaucoma progression using a ct-hmm,” in *Machine Learning for Healthcare Conference*, pp. 140–159, PMLR.
- Natarajan, N., Dhillon, I. S., Ravikumar, P. K., and Tewari, A. (2013), “Learning with noisy labels,” *Advances in neural information processing systems*, 26.
- Nguyen, A. T., Greenfield, D. S., Bhakta, A. S., Lee, J., and Feuer, W. J. (2019), “Detecting glaucoma progression using guided progression analysis with OCT and visual field assessment in eyes classified by international classification of disease severity codes,” *Ophthalmology Glaucoma*, 2, 36–46.

- Nouri-Mahdavi, K., Hoffman, D., Gaasterland, D., and Caprioli, J. (2004a), “Prediction of visual field progression in glaucoma,” *Investigative ophthalmology & visual science*, 45, 4346–4351.
- Nouri-Mahdavi, K., Hoffman, D., Coleman, A. L., Liu, G., Li, G., Gaasterland, D., and Caprioli, J. (2004b), “Predictive factors for glaucomatous visual field progression in the Advanced Glaucoma Intervention Study,” *Ophthalmology*, 111, 1627–1635.
- Nouri-Mahdavi, K., Mohammadzadeh, V., Rabiolo, A., Edalati, K., Caprioli, J., and Yousefi, S. (2021), “Prediction of visual field progression from OCT structural measures in moderate to advanced glaucoma,” *American journal of ophthalmology*, 226, 172–181.
- Öhnell, H., Heijl, A., Brenner, L., Anderson, H., and Bengtsson, B. (2016), “Structural and functional progression in the early manifest glaucoma trial,” *Ophthalmology*, 123, 1173–1180.
- O’Leary, N., Chauhan, B. C., and Artes, P. H. (2012), “Visual field progression in glaucoma: estimating the overall significance of deterioration with permutation analyses of pointwise linear regression (PoPLR),” *Investigative ophthalmology & visual science*, 53, 6776–6784.
- Omodaka, K., Kikawa, T., Kabakura, S., Himori, N., Tsuda, S., Ninomiya, T., Takahashi, N., Pak, K., Takeda, N., Akiba, M., et al. (2022), “Clinical characteristics of glaucoma patients with various risk factors,” *BMC ophthalmology*, 22, 1–20.
- O’Leary, N., Crabb, D. P., Mansberger, S. L., Fortune, B., Twa, M. D., Lloyd, M. J., Kotecha, A., Garway-Heath, D. F., Cioffi, G. A., and Johnson, C. A. (2010), “Glaucomatous progression in series of stereoscopic photographs and Heidelberg retina tomograph images,” *Archives of ophthalmology*, 128, 560–568.
- Parmar, H., Nutter, B., Long, R., Antani, S., and Mitra, S. (2020), “Spatiotemporal feature extraction and classification of Alzheimer’s disease using deep learning 3D-CNN for fMRI data,” *Journal of Medical Imaging*, 7, 056001–056001.
- Pascolini, D. and Mariotti, S. P. (2012), “Global estimates of visual impairment: 2010,” *British Journal of Ophthalmology*, 96, 614–618.
- Pham, Q. T., Han, J. C., Shin, J., et al. (2023), “Multimodal Deep Learning Model of Predicting Future Visual Field for Glaucoma Patients,” *IEEE Access*, 11, 19049–19058.
- Prum, B. E., Rosenberg, L. F., Gedde, S. J., Mansberger, S. L., Stein, J. D., Moroi, S. E., Herndon, L. W., Lim, M. C., and Williams, R. D. (2016), “Primary open-angle glaucoma preferred practice pattern® guidelines,” *Ophthalmology*, 123, P41–P111.

- Quigley, H. A. and Broman, A. T. (2006), “The number of people with glaucoma worldwide in 2010 and 2020,” *British journal of ophthalmology*, 90, 262–267.
- Quigley, H. A., Tielsch, J. M., Katz, J., and Sommer, A. (1996), “Rate of progression in open-angle glaucoma estimated from cross-sectional prevalence of visual field damage,” *American journal of ophthalmology*, 122, 355–363.
- Rabiolo, A., Morales, E., Mohamed, L., Capistrano, V., Kim, J. H., Affi, A., Yu, F., Coleman, A. L., Nouri-Mahdavi, K., and Caprioli, J. (2019), “Comparison of methods to detect and measure glaucomatous visual field progression,” *Translational vision science & technology*, 8, 2–2.
- Racette, L., Boden, C., Kleinhandler, S. L., Girkin, C. A., Liebmann, J. M., Zangwill, L. M., Medeiros, F. A., Bowd, C., Weinreb, R. N., Wilson, M. R., et al. (2005), “Differences in visual function and optic nerve structure between healthy eyes of blacks and whites,” *Archives of ophthalmology*, 123, 1547–1553.
- Ramdas, W. D., Wolfs, R. C., Hofman, A., de Jong, P. T., Vingerling, J. R., and Jansonijs, N. M. (2011), “Ocular perfusion pressure and the incidence of glaucoma: real effect or artifact?: the Rotterdam study,” *Investigative ophthalmology & visual science*, 52, 6875–6881.
- Ramrattan, R. S., van der Schaft, T. L., Mooy, C. M., De Bruijn, W., Mulder, P., and De Jong, P. (1994), “Morphometric analysis of Bruch’s membrane, the choriocapillaris, and the choroid in aging.” *Investigative ophthalmology & visual science*, 35, 2857–2864.
- Roberti, G., Michelessi, M., Tanga, L., Belfonte, L., Del Grande, L. M., Bruno, M., and Oddone, F. (2022), “Glaucoma Progression Diagnosis: The Agreement between Clinical Judgment and Statistical Software,” *Journal of Clinical Medicine*, 11, 5508.
- Rui, C., Montesano, G., Crabb, D. P., Brusini, P., Chauhan, B. C., Rossetti, L. M., Fogagnolo, P., Giraud, J.-M., Fenolland, J.-R., and Oddone, F. (2021), “Improving event-based progression analysis in glaucomatous visual fields,” *Scientific reports*, 11, 1–9.
- Russell, R. A., Malik, R., Chauhan, B. C., Crabb, D. P., and Garway-Heath, D. F. (2012), “Improved estimates of visual field progression using bayesian linear regression to integrate structural information in patients with ocular hypertension,” *Investigative ophthalmology & visual science*, 53, 2760–2769.
- Sabharwal, J., Hou, K., Herbert, P., Bradley, C., Johnson, C. A., Wall, M., Ramulu, P. Y., Unberath, M., and Yohannan, J. (2023), “A deep learning model incorporating spatial and temporal information successfully detects visual field worsening using a consensus based approach,” *Scientific reports*, 13, 1041.

- Saeedi, O., Boland, M. V., D'Acunto, L., Swamy, R., Hegde, V., Gupta, S., Venjara, A., Tsai, J., Myers, J. S., Wellik, S. R., et al. (2021), "Development and comparison of machine learning algorithms to determine visual field progression," *Translational vision science & technology*, 10, 27–27.
- Salim, S., Brown, E. N., Aref, A. A., Ramulu, P., and Kitchen, D. (2022), "Eye-Wiki: Standard Automated Perimetry," https://eyewiki.aao.org/Standard_Automated_Perimetry, Last accessed on 2023-09-29.
- Sampani, K., Abdulaal, M., Peiris, T., Lin, M. M., Pitoc, C., Ledesma, M., Lammer, J., Silva, P. S., Aiello, L. P., and Sun, J. K. (2020), "Comparison of SDOCT scan types for grading disorganization of retinal inner layers and other morphologic features of diabetic macular edema," *Translational Vision Science & Technology*, 9, 45–45.
- Sample, P. A., Boden, C., Zhang, Z., Pascual, J., Lee, T.-W., Zangwill, L. M., Weinreb, R. N., Crowston, J. G., Hoffmann, E. M., Medeiros, F. A., et al. (2005), "Unsupervised machine learning with independent component analysis to identify areas of progression in glaucomatous visual fields," *Investigative ophthalmology & visual science*, 46, 3684–3692.
- Schuster, A. K., Erb, C., Hoffmann, E. M., Dietlein, T., and Pfeiffer, N. (2020), "The diagnosis and treatment of glaucoma," *Deutsches Ärzteblatt International*, 117, 225.
- Sedai, S., Antony, B., Ishikawa, H., Wollstein, G., Schuman, J. S., and Garnavi, R. (2020), "Forecasting retinal nerve fiber layer thickness from multimodal temporal data incorporating OCT volumes," *Ophthalmology Glaucoma*, 3, 14–24.
- Shigueoka, L. S., Mariottoni, E. B., Thompson, A. C., Jammal, A. A., Costa, V. P., and Medeiros, F. A. (2021), "Predicting age from optical coherence tomography scans with deep learning," *Translational Vision Science & Technology*, 10, 12–12.
- Shuldiner, S. R., Boland, M. V., Ramulu, P. Y., De Moraes, C. G., Elze, T., Myers, J., Pasquale, L., Wellik, S., and Yohannan, J. (2021), "Predicting eyes at risk for rapid glaucoma progression based on an initial visual field test using machine learning," *PloS one*, 16, e0249856.
- Singh, S. P., Wang, L., Gupta, S., Goli, H., Padmanabhan, P., and Gulyás, B. (2020), "3D deep learning on medical images: a review," *Sensors*, 20, 5097.
- Strouthidis, N. G., Grimm, J., Williams, G. A., Cull, G. A., Wilson, D. J., and Burgoyne, C. F. (2010), "A comparison of optic nerve head morphology viewed by spectral domain optical coherence tomography and by serial histology," *Investigative ophthalmology & visual science*, 51, 1464–1474.

- Strouthidis, N. G., Fortune, B., Yang, H., Sigal, I. A., and Burgoyne, C. F. (2011), “Longitudinal change detected by spectral domain optical coherence tomography in the optic nerve head and peripapillary retina in experimental glaucoma,” *Investigative ophthalmology & visual science*, 52, 1206–1219.
- Su, E., Weiss, R. E., Nouri-Mahdavi, K., and Holbrook, A. J. (2023), “A Spatially Varying Hierarchical Random Effects Model for Longitudinal Macular Structural Data in Glaucoma Patients,” *arXiv preprint arXiv:2303.09018*.
- Su, G., Chen, W., and Xu, M. (2021), “Positive-Unlabeled Learning from Imbalanced Data.” in *IJCAI*, pp. 2995–3001.
- Suda, K., Akagi, T., Nakanishi, H., Noma, H., Ikeda, H. O., Kameda, T., Hasegawa, T., and Tsujikawa, A. (2018), “Evaluation of structure-function relationships in longitudinal changes of glaucoma using the spectralis OCT follow-up mode,” *Scientific reports*, 8, 17158.
- Sugiyama, M., Nakajima, S., Kashima, H., Buenau, P., and Kawanabe, M. (2007), “Direct importance estimation with model selection and its application to covariate shift adaptation,” *Advances in neural information processing systems*, 20.
- Sung, K. R., Wollstein, G., Bilonick, R. A., Townsend, K. A., Ishikawa, H., Kagemann, L., Noecker, R. J., Fujimoto, J. G., and Schuman, J. S. (2009), “Effects of age on optical coherence tomography measurements of healthy retinal nerve fiber layer, macula, and optic nerve head,” *Ophthalmology*, 116, 1119–1124.
- Susanna Jr, R. (2009), “Unpredictability of glaucoma progression,” *Current medical research and opinion*, 25, 2167–2177.
- Swaminathan, S. S., Jammal, A. A., Berchuck, S. I., and Medeiros, F. A. (2021), “Rapid initial OCT RNFL thinning is predictive of faster visual field loss during extended follow-up in glaucoma,” *American journal of ophthalmology*, 229, 100–107.
- Swaminathan, S. S., Berchuck, S. I., Jammal, A. A., Rao, J. S., and Medeiros, F. A. (2022), “Rates of glaucoma progression derived from linear mixed models using varied random effect distributions,” *Translational vision science & technology*, 11, 16–16.
- Tanna, A. P., Budenz, D. L., Bandi, J., Feuer, W. J., Feldman, R. M., Hennon, L. W., Rhee, D. J., Whiteside-de Vos, J., Huang, J., and Anderson, D. R. (2012), “Glaucoma Progression Analysis Software Compared with Expert Consensus Opinion in the Detection of Visual Field Progression in Glaucoma,” *Ophthalmology*, 119, 468–473.

- Tao, S., Ravindranath, R., and Wang, S. Y. (2023), “Predicting Glaucoma Progression to Surgery with Artificial Intelligence Survival Models,” *Ophthalmology Science*, 3, 100336.
- Tatham, A. J. and Medeiros, F. A. (2017), “Detecting structural progression in glaucoma with optical coherence tomography,” *Ophthalmology*, 124, S57–S65.
- Termote, K. and Zeyen, T. (2010), “The challenges of monitoring glaucoma progression,” *Bull Soc Belge Ophtalmol*, 314, 25–32.
- Texas, G. C. (2007), “Understanding Glaucoma: Types of Glaucoma?” <https://www.gcot.net/types-of-glaucoma.html>, Last accessed on 2023-09-27.
- Thakur, S., Le Dinh, L., Lavanya, R., Liu, Y., Cheng, C.-Y., et al. (2023), “Use of artificial intelligence in forecasting glaucoma progression,” *Taiwan Journal of Ophthalmology*, 13, 168.
- Tham, Y.-C., Li, X., Wong, T. Y., Quigley, H. A., Aung, T., and Cheng, C.-Y. (2014), “Global prevalence of glaucoma and projections of glaucoma burden through 2040: a systematic review and meta-analysis,” *Ophthalmology*, 121, 2081–2090.
- Thenappan, A., Tsamis, E., Zemborain, Z. Z., La Bruna, S., Eguia, M., Joiner, D., De Moraes, C. G., and Hood, D. C. (2021), “Detecting Progression in Advanced Glaucoma: Are OCT Global Metrics Viable Measures?” *Optometry and vision science: official publication of the American Academy of Optometry*, 98, 518.
- Thompson, A. C., Jammal, A. A., and Medeiros, F. A. (2020), “A review of deep learning for screening, diagnosis, and detection of glaucoma progression,” *Translational Vision Science & Technology*, 9, 42–42.
- Thompson, A. C., Li, A., and Asrani, S. (2021), “Agreement between trend-based and qualitative analysis of the retinal nerve fiber layer thickness for glaucoma progression on spectral-domain optical coherence tomography,” *Ophthalmology and Therapy*, 10, 629–642.
- Tsatsos, M. and Broadway, D. (2007), “Controversies in the history of glaucoma: is it all a load of old Greek?” *British Journal of Ophthalmology*, 91, 1561–1562.
- U.S. Census Bureau. (2022), “QuickFacts North Carolina, Population Estimates, July 1, 2022, (V2022),” <https://www.census.gov/quickfacts/fact/table/NC#>, Last accessed on 2023-09-27.
- v. Graefe, A. (1856), “Ueber die Untersuchung des Gesichtsfeldes bei amblyopischen Affectionen,” *Archiv für Ophthalmologie*, 2, 258–298.

- Vesti, E., Johnson, C. A., and Chauhan, B. C. (2003), “Comparison of different methods for detecting glaucomatous visual field progression,” *Investigative ophthalmology & visual science*, 44, 3873–3879.
- Vianna, J. R. and Chauhan, B. C. (2015), “How to detect progression in glaucoma,” *Progress in brain research*, 221, 135–158.
- Vianna, J. R., Danthurebandara, V. M., Sharpe, G. P., Hutchison, D. M., Belliveau, A. C., Shuba, L. M., Nicolela, M. T., and Chauhan, B. C. (2015), “Importance of normal aging in estimating the rate of glaucomatous neuroretinal rim and retinal nerve fiber layer loss,” *Ophthalmology*, 122, 2392–2398.
- Viswanathan, A. C., Fitzke, F. W., and Hitchings, R. A. (1997), “Early detection of visual field progression in glaucoma: a comparison of PROGRESSOR and STAT-PAC 2,” *British Journal of Ophthalmology*, 81, 1037–1042.
- Walber (2014), “Precision and recall,” https://en.wikipedia.org/wiki/Precision_and_recall, Last accessed on 2023-09-30.
- Wang, C., Pu, J., Xu, Z., and Zhang, J. (2021), “Asymmetric Loss for Positive-Unlabeled Learning,” in *2021 IEEE International Conference on Multimedia and Expo (ICME)*, pp. 1–6, IEEE.
- Wang, M., Shen, L. Q., Pasquale, L. R., Petrakos, P., Formica, S., Boland, M. V., Wellik, S. R., De Moraes, C. G., Myers, J. S., Saeedi, O., et al. (2019), “An artificial intelligence approach to detect visual field progression in glaucoma based on spatial pattern analysis,” *Investigative ophthalmology & visual science*, 60, 365–375.
- Wang, S. Y. and Stein, J. D. (2023), “Machine learning approaches for predicting glaucoma progression in a large multicenter electronic health records consortium: the Sight Outcomes Research Collaborative (SOURCE),” *Investigative Ophthalmology & Visual Science*, 64, 357–357.
- Wang, S. Y., Tseng, B., and Hernandez-Boussard, T. (2022), “Deep learning approaches for predicting glaucoma progression using electronic health records and natural language processing,” *Ophthalmology Science*, 2, 100127.
- Wang, X. and Qi, G.-J. (2022), “Contrastive learning with stronger augmentations,” *IEEE transactions on pattern analysis and machine intelligence*, 45, 5549–5560.
- Warren, J. L., Mwanza, J.-C., Tanna, A. P., and Budenz, D. L. (2016), “A statistical model to analyze clinician expert consensus on glaucoma progression using spatially correlated visual field data,” *Translational Vision Science & Technology*, 5, 14–14.

- Weinreb, R. N. and Kaufman, P. L. (2011), “Glaucoma research community and FDA look to the future, II: NEI/FDA Glaucoma Clinical Trial Design and Endpoints Symposium: measures of structural change and visual function,” *Investigative ophthalmology & visual science*, 52, 7842–7851.
- Wen, J. C., Lee, C. S., Keane, P. A., Xiao, S., Rokem, A. S., Chen, P. P., Wu, Y., and Lee, A. Y. (2019), “Forecasting future Humphrey visual fields using deep learning,” *PloS one*, 14, e0214875.
- Wolf, D., Regnery, S., Tarnawski, R., Bobek-Billewicz, B., Polańska, J., and Götz, M. (2022), “Weakly Supervised Learning with Positive and Unlabeled Data for Automatic Brain Tumor Segmentation,” *Applied Sciences*, 12, 10763.
- Wu, K., Lin, C., Lam, A. K.-N., Chan, L., and Leung, C. K.-S. (2020), “Wide-field trend-based progression analysis of combined retinal nerve fiber layer and ganglion cell inner plexiform layer thickness: a new paradigm to improve glaucoma progression detection,” *Ophthalmology*, 127, 1322–1330.
- Wu, Z. and Medeiros, F. A. (2018), “Comparison of Visual Field Point-Wise Event-Based and Global Trend-Based Analysis for Detecting Glaucomatous Progression,” *Translational Vision Science & Technology*, 7, 20–20.
- Wu, Z. and Medeiros, F. A. (2021), “A simplified combined index of structure and function for detecting and staging glaucomatous damage,” *Scientific Reports*, 11, 3172.
- Wu, Z., Saunders, L. J., Zangwill, L. M., Daga, F. B., Crowston, J. G., and Medeiros, F. A. (2017), “Impact of normal aging and progression definitions on the specificity of detecting retinal nerve fiber layer thinning,” *American journal of ophthalmology*, 181, 106–113.
- Xue, Y., Whitecross, K., and Mirzasoleiman, B. (2022), “Investigating why contrastive learning benefits robustness against label noise,” in *International Conference on Machine Learning*, pp. 24851–24871, PMLR.
- Yang, P., Li, X.-L., Mei, J.-P., Kwok, C.-K., and Ng, S.-K. (2012), “Positive-unlabeled learning for disease gene identification,” *Bioinformatics*, 28, 2640–2647.
- Yaqoob, Z., Wu, J., and Yang, C. (2005), “Spectral domain optical coherence tomography: a better OCT imaging strategy,” *Biotechniques*, 39, S6–S13.
- Yohannan, J., Wang, J., Brown, J., Chauhan, B. C., Boland, M. V., Friedman, D. S., and Ramulu, P. Y. (2017), “Evidence-based criteria for assessment of visual field reliability,” *Ophthalmology*, 124, 1612–1620.

- Yousefi, S., Goldbaum, M. H., Balasubramanian, M., Jung, T.-P., Weinreb, R. N., Medeiros, F. A., Zangwill, L. M., Liebmann, J. M., Girkin, C. A., and Bowd, C. (2013), “Glaucoma progression detection using structural retinal nerve fiber layer measurements and functional visual field points,” *IEEE Transactions on Biomedical Engineering*, 61, 1143–1154.
- Yousefi, S., Goldbaum, M. H., Balasubramanian, M., Medeiros, F. A., Zangwill, L. M., Liebmann, J. M., Girkin, C. A., Weinreb, R. N., and Bowd, C. (2014), “Learning from data: recognizing glaucomatous defect patterns and detecting progression from visual field measurements,” *IEEE Transactions on Biomedical Engineering*, 61, 2112–2124.
- Yousefi, S., Goldbaum, M. H., Shahrian, E. V., Zangwill, L. M., Weinreb, R. N., Medeiros, F. A., Girkin, C. A., Liebmann, J. M., and Bowd, C. (2015), “Unsupervised machine learning to recognize glaucoma defect patterns and detect progression in RNFL thickness measurements,” *Investigative Ophthalmology & Visual Science*, 56, 4564–4564.
- Yousefi, S., Balasubramanian, M., Goldbaum, M. H., Medeiros, F. A., Zangwill, L. M., Weinreb, R. N., Liebmann, J. M., Girkin, C. A., and Bowd, C. (2016), “Unsupervised Gaussian mixture-model with expectation maximization for detecting glaucomatous progression in standard automated perimetry visual fields,” *Translational vision science & technology*, 5, 2–2.
- Yousefi, S., Kiwaki, T., Zheng, Y., Sugiura, H., Asaoka, R., Murata, H., Lemij, H., and Yamanishi, K. (2018), “Detection of longitudinal visual field progression in glaucoma using machine learning,” *American journal of ophthalmology*, 193, 71–79.
- Yousefi, S., Pasquale, L. R., Boland, M. V., and Johnson, C. A. (2022), “Machine-identified patterns of visual field loss and an association with rapid progression in the ocular hypertension treatment study,” *Ophthalmology*, 129, 1402–1411.
- Yu, M., Lin, C., Weinreb, R. N., Lai, G., Chiu, V., and Leung, C. K.-S. (2016), “Risk of visual field progression in glaucoma patients with progressive retinal nerve fiber layer thinning: a 5-year prospective study,” *Ophthalmology*, 123, 1201–1210.
- Zemborain, Z. Z., Jarukasetphon, R., Tsamis, E., De Moraes, C. G., Ritch, R., and Hood, D. C. (2020), “Optical coherence tomography can be used to assess glaucomatous optic nerve damage in most eyes with high myopia,” *Journal of glaucoma*, 29, 833–845.
- Zhalechian, M., Van Oyen, M. P., Lavieri, M. S., De Moraes, C. G., Girkin, C. A., Fazio, M. A., Weinreb, R. N., Bowd, C., Liebmann, J. M., Zangwill, L. M., et al. (2022), “Augmenting Kalman Filter Machine Learning Models with Data from

- OCT to Predict Future Visual Field Loss: An Analysis Using Data from the African Descent and Glaucoma Evaluation Study and the Diagnostic Innovation in Glaucoma Study,” *Ophthalmology Science*, 2, 100097.
- Zhang, P., Luo, D., Li, P., Sharpsten, L., and Medeiros, F. A. (2015), “Log-gamma linear-mixed effects models for multiple outcomes with application to a longitudinal glaucoma study,” *Biometrical Journal*, 57, 766–776.
- Zhang, X., Dastiridou, A., Francis, B. A., Tan, O., Varma, R., Greenfield, D. S., Schuman, J. S., Huang, D., for Glaucoma Study Group, A. I., et al. (2017), “Comparison of glaucoma progression detection by optical coherence tomography and visual field,” *American journal of ophthalmology*, 184, 63–74.
- Zhu, H., Russell, R. A., Saunders, L. J., Ceccon, S., Garway-Heath, D. F., and Crabb, D. P. (2014), “Detecting changes in retinal function: analysis with non-stationary Weibull error regression and spatial enhancement (ANSWERS),” *PloS one*, 9, e85654.

Biography

Sayan Mandal was born in West Bengal, India. His high school years were primarily spent in Jharkhand and Karnataka. Academically driven, Sayan secured the top position in his class at the Atomic Energy Central School in Jaduguda during the All India Senior School Certificate Examination (AISSCE). This foundation set the stage for his later accomplishments, including the achievement of the Kishore Vaigyanik Protsahan Yojana (KVPY) scholarship in 2015.

Subsequently, Sayan attended the Indian Institute of Technology (IIT) Kharagpur, completing a Bachelor in Technology (Honors) in Aerospace Engineering in April 2019. At IIT, he developed a deep interest in Control Systems and Machine Learning. This inclination led to an internship during his third year at Duke University's Humans and Autonomy Lab, resulting in published research (Mandal et al. (2020); Alaparthi et al. (2021)).

Continuing his academic journey, Sayan enrolled in the Doctorate program at Duke University in Durham, focusing on Electrical and Computer Engineering with a specialization in Computer Engineering. His research interests revolved around the application of deep learning in medical image analysis. By December 2022, Sayan had completed his Master of Science in Electrical and Computer Engineering from Duke University. He is currently working towards his PhD degree.